Single-Electron Transfer and Single-Electron Transfer Degenerative Chain Transfer Living Radical Polymerization

Brad M. Rosen and Virgil Percec*

Roy & Diana Vagelos Laboratories, Department of Chemistry, University of Pennsylvania, Philadelphia, Pennsylvania 19104-6323

Contents

1. Introduction
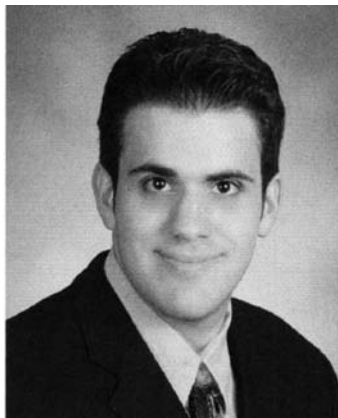
As we move forward through the 21st century, a major challenge for polymer chemistry will be to approach the complexity and fidelity of biological macromolecules via synthetic processes. The structural perfection of biological

* Corresponding author e-mail: percec@sas.upenn.edu.

Brad M. Rosen was born in Philadelphia, Pennsylvania. He received his A.B. and A.M. in Chemistry from Harvard University in 2005, where he worked on the synthesis of cyclic enediyne antibiotics under the direction of Professor Andrew G. Myers. He will receive his Ph.D. in 2009 from the University of Pennsylvania. Under the direction of Professor Virgil Percec, his doctoral studies focused on the development of Ni-catalyzed cross-coupling and borylation, synthesis and retrostructural analysis of self-assembling dendrons, and the elaboration of single-electron transfer living radical polymerization. He is the recipient of a Rohm and Haas Graduate Research Fellowship, an NSF Graduate Research Fellowship (2005−2008), an ACS Division of Organic Chemistry Graduate Fellowship (2008−2009, Sponsored by Roche, Inc.), and a University of Pennsylvania Dissertation Fellowship (2009). In 2009, he joined DuPont Central Research and Development in Wilmington, Delaware.
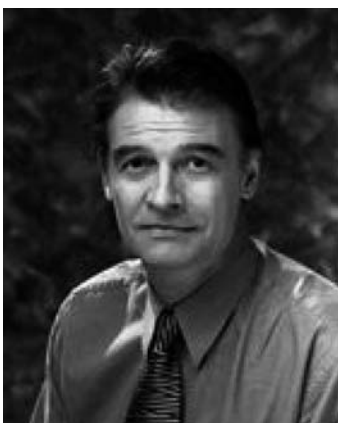
Virgil Percec was born and educated in Romania (Ph.D., 1976). He defected from his native country in 1981 and after short postdoctoral appointments at the University of Freiberg, Germany, and the University of Akron, U.S.A., he joined the Department of Macromolecular Science at Case Western Reserve University in Cleveland (1982) as an Assistant Professor. He was promoted to Associate Professor in 1984, to Professor in 1986, and to Leonard Case Jr. Chair in 1993. In 1999 he moved to the University of Pennsylvania as P. Roy Vagelos Professor of Chemistry. Percec's research interests lies at the interface between organic, bioorganic, supramolecular, polymer chemistry, and liquid crystals, where he contributed over 620 refereed publications, 50 patents, and over 1000 endowed and invited lectures. His list of awards includes Honorary Foreign Member to the Romanian Academy (1993), Humboldt Award (1997), NSF Research Award for Creativity in Research (1990, 1995, 2000), PTN Polymer Award from The Netherlands (2002), the ACS Award in Polymer Chemistry (2004), the Staudinger−Durrer Medal from ETH (2005), the International Award of the Society of Polymer Science from Japan (2007), and the H. F. Mark Medal from the Austrian Research Institute for Chemistry and Technology (2008). He is a Fellow of IUPAC (2001), PMSE Division of ACS (2003), AAAS (2004), and RSC (2008). He is the editor of the *Journal of Polymer Science, Part A: Polymer Chemistry* (since 1996) and of the book series *Liquid Crystals* and serves on the Editorial Boards of 20 international journals.

macromolecules is the result of enzymatically controlled and templated condensation polymerizations.[1] Some progress has

been made in harnessing biological polymerization for materials applications.[2] However, it is free-radical polymerization, not condensation polymerization, that currently dominates in industrial applications and also in academic research, largely due to the broad array of compatible unsaturated monomers and relatively mild reaction conditions.[3] As radical polymerization is typically kinetically controlled, precise tailoring of the monomer sequence at the level of biological polymerization is not necessarily feasible. Getting closer to this goal will first require the development of polymerization techniques that can achieve precise molecular weight and molecular weight distribution and provide polymers with perfect structural fidelity.[4]

1.1. Living Radical Polymerization (LRP). Definitions and Brief History

Significant progress has been made in the precise synthesis of polymers, most notably via living polymerization. Living polymerization occurs when all side reactions that lead to termination have been suppressed. By eliminating termination, chains can be extended indefinitely and grow more uniformly, leading to polymers with precisely tailored molecular weight and molecular weight distribution. Living polymerization[5] was first discovered by Szwarc in 1956 for the anionic polymerization of styrene initiated with sodium napthalenide.[6,7] As defined by Szwarc in one of his last publications,[7] "[Living Polymers are those] that retain their ability to propagate for a long time and grow to a desired maximum size while their degree of termination or chain transfer is still negligible."

Living polymerization has since been elaborated into several classes of powerful techniques, including living anionic polymerization, living cationic polymerization,[8] living ring-opening polymerization (ROP),[9] ring-opening metathesis polymerization (ROMP),[10] group-transfer polymerization (GTP),[11,12] and living radical polymerization (LRP). Each of these methods is restricted to limited classes of monomers and functional groups. Recently, much interest has been devoted to LRP, as it provides greater monomer diversity and less stringent reaction conditions specifically in regard to monomer purification. Since the discovery of living radical polymerization by Otsu in 1982,[13] a plethora of powerful LRP techniques have been developed, including but not limited to nitroxide-mediated LRP (NMP),[14,15] reversible addition/fragmentation transfer polymerization (RAFT),[16] macromolecular design via the interchange of xanthates (MADIX),[17,18] organotellurium-mediated LRP (TERP), organobismuthine-mediated LRP (BIRP), organostibine-mediated LRP (SBRP),[19] the Iniferter[20] method, and metal-catalyzed living radical polymerization,[21] pioneered by Otsu in 1990,[22] including cobalt-mediated LRP,[23,24] atom-transfer radical polymerization (ATRP),[25] single-electron transfer degenerative chain transfer mediated LRP (SET-DTLRP),[26] and single-electron transfer mediated LRP (SET-LRP).[27] In the latter two techniques, activation of dormant chains into propagating radicals is proposed to proceed through a heterogeneous outer-sphere electron-transfer (OSET) process. In this process, electron-transfer to the organic halide precedes the decomposition of the alkyl halide into a carbon-centered radical and a halide anion. OSET has been shown to be less sensitive to the bond dissociation energy of R−X species[28] than inner-sphere electron-transfer (ISET).[29] In all LRP techniques, reversible deactivation of propagating macroradicals is needed to ensure a low radical concentration,

thereby reducing bimolecular termination and other side reactions. However, a low concentration of radicals alone is insufficient for an LRP without the internal suppression of fast reactions[30,31] via the *persistent radical effect* or an alternative method to mediate the equilibrium between dormant and active species. As stated by Fischer, "Whenever in a chemical system transient and persistent radicals are formed with equal or similar rates, be it from the same or different precursors, their cross-reaction products are produced with a surprisingly high selectivity, and the otherwise prominent self-termination products of the transient radicals are virtually absent. This is not because the self-termination reaction does not take place at all. Quite on the contrary, this reaction combined with the reluctance of persistent species to undergo any self-termination causes a buildup of a considerable excess of the persistent over the transient species, and this excess then steers the reaction system toward the cross-reaction channel. Hence, the system orders itself in time, and the self-termination reaction of the transient radicals is important but it causes its own suppression."[31] In the context of LRP, the transient radicals are those that propagate or terminate through dimerization, while the persistent radical is the dormant chain end from which the transient radicals are derived. Depending upon the approach utilized to achieve regulation, different LRP processes will exhibit varying degrees of complexity.[32,33] As suggested by Ottino,[32] "Complex systems cannot be understood by studying parts in isolation. The very essence of the system lies in the interaction between parts and the overall behavior that emerges from the interactions. The system must be analyzed as a whole." Accordingly, the LRP processes described here will be addressed mechanistically from the perspective of complexity where no one component can be truly viewed on its own, but only in context of its effect on other parts of the system.

1.2. Scope of the Review

Non metal-catalyzed LRP can be very effective for the synthesis of tailored polymers. The balance between propagating macroradicals and the dormant species is typically maintained by a thermally reversible addition of a capping group that does not itself initiate polymerization. In many cases, this process cannot proceed under ambient conditions and isolated polymer cannot be used as a macroinitiator for block-copolymerization due to end-group loss. Metal-catalyzed LRP, can mediate rapid polymerization and retain chain-end functionality necessary for reinitiation in block copolymerization.

In this review, we aim to cover recent progress in two related polymerization methodologies that rely on single-electron transfer (SET): single-electron transfer degenerative chain transfer living radical polymerization (SET-DTLRP) and single-electron transfer living radical polymerization (SET-LRP). SET-DTLRP proceeds via SET initiation and competition of SET activation/deactivation and degenerative transfer (DT). SET-LRP proceeds exclusively through a SET initiation, activation, and deactivation. Both techniques arose from investigations into Cu-catalyzed LRP initiated with sulfonyl halides. The historical development, mechanism, present uses, and future perspective of both techniques will be discussed.

2. Path to SET-LRP and SET-DTLRP: Sulfonyl Halides as "Universal" Initiators for Cu-Catalyzed LRP

2.1. Cuprous Halide Catalysts for LRP Initiated with Sulfonyl Halides

The first metal-catalyzed LRP was developed in 1990 by Otsu.[22] A very successful cobalt-mediated LRP was reported by Wayland in 1994.[23] In 1994, Sawamoto described the first metal-catalyzed LRP of methyl methacrylate (MMA) initiated with CCl_4 using $Ru^{II}Cl_2(PPh_3)_3$[34,35] as a catalyst; later, Matyjaszewski applied the $Cu^ICl/2,2'$-bipyridine (bpy) system, which was previously well-established for radical reactions,[36] to the LRP of styrene (Sty) initiated with 1-phenylethyl chloride and coined the term atom-transfer radical polymerization (ATRP),[37] as it was believed that the polymerization was based on an atom-transfer radical addition (ATRA) mechanism.[38−40] That same year our laboratory reported the first CuCl/bpy-catalyzed LRP of Sty initiated with arenesulfonyl chlorides.[41] Arenesulfonyl halides were known to undergo efficient ATRA to olefins in the presence of $Cu^ICl/Cu^{II}Cl_2$[42−45] and $Ru^{II}Cl_2(PPh_3)_2$[46] catalysts. Using a variety of *para*-substituted arenesulfonyl chlorides (*p*-RBSC, R = {NO_2, H, F, Cl, CH_3, OCH_3}), a diverse array of chain-end functionalized polystyrenes (PS) with acceptable polydispersities (M_w/M_n = 1.48−1.80) were produced in bulk. In this bulk polymerization of Sty, regardless of the ratio between Cu^ICl and bpy employed, the catalyst is only partially solubilized and, thus, the activation and deactivation processes are heterogeneous. The predictability of molecular weight evolution and distribution and the overall conversion in the Cu^ICl/bpy-catalyzed LRP of Sty initiated with *p*-methoxybenzenesulfonyl chloride (MBSC) was greatly improved ($M_w/M_n ≈ 1.3−1.5$) through the use of solvents (e.g., anisole, dioxane, and xylenes) that better solvated the Cu^ICl/bpy and $Cu^{II}Cl_2$/bpy complexes and with more soluble derivitized bpy ligands, thereby providing a homogeneous LRP process.[47] With more complete kinetics accessible via the homogeneous polymerization, it was first observed that the rate of initiation of arenesulfonyl chlorides was significantly faster than the rate of propagation of Sty. A more precise study with multiple monomers including Sty, MMA, butyl methacrylate (BMA), and butyl acrylate (BA) demonstrated that, depending upon the monomer structure, the rate of initiation of arenesulfonyl chlorides is 3−5 orders of magnitude faster than the rate of propagation.[48] This dramatic difference in rates allowed for complete separation of these two processes via temperature (Table 1).[49−51] An expanded library of arenesulfonyl chloride,[51,52] arenedisulfonyl chloride,[48,51] and alkylsulfonyl chloride[52] initiators was synthesized and tested in the Cu^ICl/bpy-catalyzed LRP of Sty, MMA, and BMA (Figure 1). In all cases, a complete separation of initiation and propagation was observed and initiator efficiency (I_{eff}) was 100%. This phenomenon allowed us to establish arenesulfonyl chlorides and arenedisulfonyl chlorides as the first "universal" class of functional initiators for the metal-catalyzed LRP of Sty, methacrylates, and acrylates, wherein initiation is quantitative and significantly faster than propagation regardless of the substitution pattern of the initiator or monomer.

Table 1. Comparison of Rate Constants of Initiation and Propagation for the Cu^{I}Cl/bpy9 Catalyzed LRP of Various Monomers and Initiators from Figure 1 (Adapted with Permission from Ref 51; Copyright 1998 American Chemical Society)

monomer	initiator	solvent	k_i^{app} at 43 °C (s^{-1} M^{-1})	k_i^{app}/T °C (s^{-1} M^{-1})	k_p^{app}/T °C (s^{-1} M^{-1})
MMA	MBSC	p-xylene	116.0×10^{-3}	103.8×10^{-1}/80 °C	6.19×10^{-4}/80 °C
MMA	MM11	p-xylene	0	0.0062×10^{-1}/80 °C	6.21×10^{-4}/80 °C
BMA	MBSC	PhOPh	23.0×10^{-3}		27.54×10^{-4}/90 °C
MA	MBSC	p-xylene	8.66×10^{-3}	6.62×10^{-1}/90 °C	10.2×10^{-4}/90 °C
BA	MBSC	PhOPh	2.65×10^{-3}	30.7×10^{-1}/140 °C	6.97×10^{-4}/140 °C
Sty	MBSC	p-xylene	479.1×10^{-3}	631.6×10^{-1}/130 °C	12.10×10^{-4}/130 °C
Sty	MBSC	PhOPh	479.1×10^{-3}	400.2×10^{-1}/120 °C	19.60×10^{-4}/120 °C
Sty	CH$_3$CHPhCl	PhOPh	0	0.0064×10^{-1}/120 °C	6.33×10^{-4}/120 °C

2.2. Cu^0 and Cu$_2$O Catalysts for LRP Initiated with Sulfonyl Chlorides

Inspired by a review by Minisci,[53,54] which mentioned that the FeCl$_2$-catalyzed Karasch addition of alkyl halides was accidentally discovered during the polymerization of acrylonitrile in CHCl$_3$ and CCl$_4$ in a steel autoclave, and also by a series of publications[55−58] from Hájek and Silhavy from 1974−1992 detailing the role of zerovalent metals and metal oxides as redox catalysts for radical additions to olefins, we began investigating their use in metal-catalyzed LRP. In 1998, we discovered that Cu^0/bpy (powder, wire, films, coins), Cu$_2$O/bpy, and mixtures thereof could be utilized in a self-regulated phase-transfer catalyzed (PTC) LRP of BMA and Sty initiated by arenesulfonyl chlorides and alkylsulfonyl chlorides and mediated by multidentate acyclic neutral ligands (Figure 2), including octopus-like compounds (STA2, STA3, STA4, TBZ, TDA), poly(ethylene glycol) (PEG), and ethylene glycol.[59] Control of molecular weight evolution and distribution in the heterogeneous PTC systems typically exceeded those observed in Cu^{I}Cl/bpy catalyzed LRP initiated with arenesulfonyl chlorides ($M_w/M_n = 1.07−1.44$). In

Cu^{I}Cl, Cu^0, and Cu$_2$O catalyzed LRP of BMA initiated with MBSC, k_p^{app} could be enhanced through the addition of carboxylate salts via modification of the active species to a metal carboxylate.[60]

In the heterogeneous PTC LRP of BMA, Cu^0 provided the greatest rates of polymerization. At the time, it was suggested that Cu^0 and Cu$_2$O mediated LRP of BMA and Sty initiated with arenesulfonyl chlorides and alkylsulfonyl chlorides proceeded at early stages by initiation via bulk metal or metal oxide, but that, at later stages, reactivity was dominated by Cu^{I}Cl/bpy generated in situ. The relatively fast apparent rate constants of propagation, k_p^{app}, were thought to be due to the reduction of Cu^{II}Cl$_2$/bpy levels via reaction with Cu^0, a hypothesis that was also noted by those pursuing Cu^{I}Cl catalysts for ATRP.[61] In retrospect, it is now evident that all initiations of sulfonyl halides with Cu^0 or Cu$_2$O are likely to proceed through a heterogeneous outer-sphere SET process. The extremely high rate of initiation with sulfonyl halides coupled with their high electron affinity and their experimentally observed ability to form radical-anion intermediates,[62] suggests an outer-sphere SET process even for
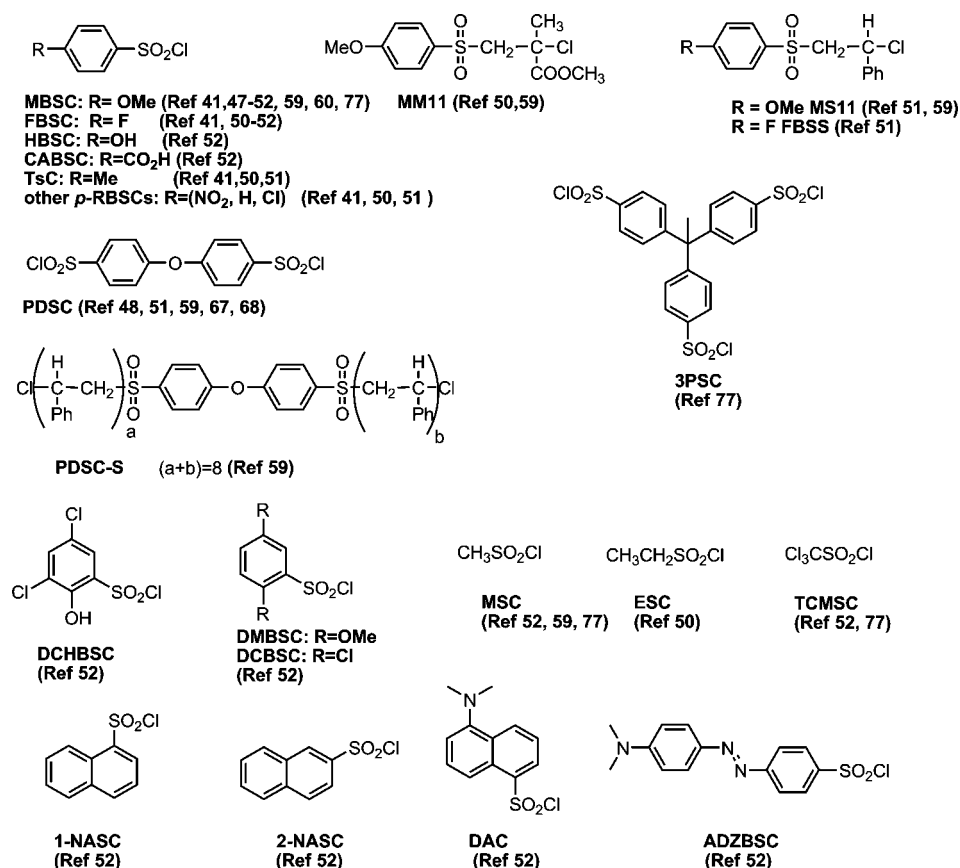

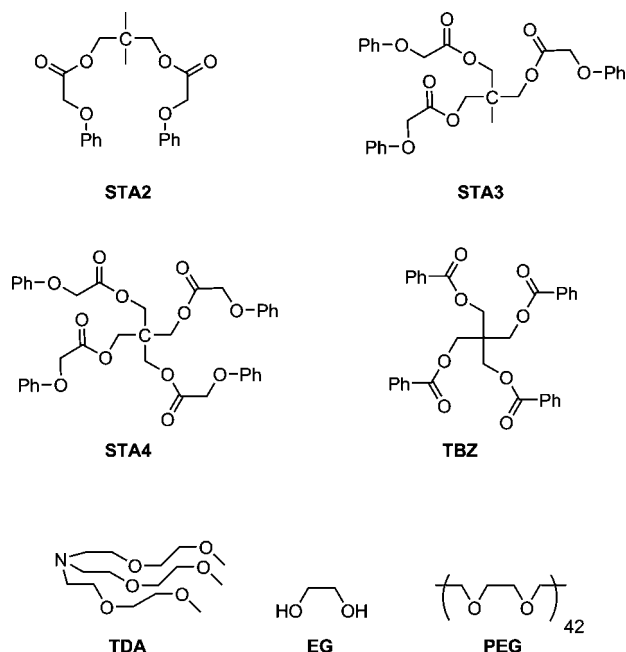**Figure 1.** Structures of sulfonyl chlorides used as initiators in the Cu^{I}Cl, Cu^0, and Cu$_2$O/bpy-catalyzed LRP.

Figure 2. Multidentate phase-transfer catalysts (PTCs) used in the Cu^0/Cu$_2$O-catalyzed LRP of Sty and BA initiated with sulfonyl halides.

homogeneous donors and presumably inner-sphere donors such as Cu^{I}Cl/bpy. Given the large excess of Cu^0 and Cu$_2$O relative to the levels of Cu^{I}Cl/bpy generated in situ as well as the possibility of disproportion of Cu^{I}Cl in the presence of polar phase-transfer catalysts, it is also likely that activation of dormant halides could proceed via competitive pathways, with one being homogeneous Cu^{I}Cl/bpy activation and the other being heterogeneous Cu^0 or Cu$_2$O activation. Early experiments with Cu^0 and Cu$_2$O, which were later verified in greater depth (vida infra), demonstrated that the surface area of the catalyst was the most important factor for the control of the rate of polymerization.[59,63]

While Cu^0 and copper oxides were previously known to participate in ATRA reactions and their use was able to be expanded to metal-catalyzed LRP, less was known about other Cu^I and Cu^{II} salts. CuS[64] and CuSe[65,66] were known to participate in some radical reactions, but the use of CuY and Cu$_2$Y (where Y = S, Se, or Te) in radical polymerizations was not reported. To achieve greater understanding of the heterogeneous activation process, the catalytic activity of a complete series of known Cu^I and Cu^{II} salts in the LRP of MMA initiated with phenoxybenzene-2,2′-disulfonyl chloride

(PDSC) in Ph$_2$O at 90 °C was examined.[67] For CuY compounds, the rates decreased monotonically in the order Y = Se > S > O. Likewise for Cu$_2$Y compounds, the rates decreased in the order Y = Te > Se > S > O. For all cases except for CuO, which had a negligible rate, poor I_{eff}, and low conversion, the control of molecular weight distribution was excellent (M_w/M_n = 1.11−1.13). An identical series of experiments using organocopper species CuSBu, CuSPh, and CuC≡CPh also demonstrated compatibility with an LRP process, achieving very good control of molecular weight distribution (M_w/M_n = 1.10−1.32).[68] The rates were comparable with copper salts and decreased in the order CuSBu > CuSPh > CuC≡CPh. As before, the original assumption was that both Cu^I and Cu^{II} salts as well as organocopper species mediate LRP via the in situ production of Cu^{I}Cl active catalyst. However, it is now believed that all initiation events to the sulfonyl chlorides proceed through a SET process and that the mechanism at later stages of polymerization is complex (vida infra).

2.3. Arenesulfonyl Bromides, Arenesulfonyl Iodides, and N-Centered Initiators

Following the development of arenesulfonyl chlorides and alkylsulfonyl chlorides as the first universal class of functional initiators for Cu-catalyzed LRP, we explored the possibility of other arenesulfonyl halides, specifically arenesulfonyl bromides. Inspired by literature procedures,[54,69−72] two arenesulfonyl bromides, p-toluenesulfonyl bromide (TsB) and phenoxybenzene-2,2′-disulfonyl bromide (PDSB) (Scheme 1), were synthesized by converting the corresponding arenesulfonyl chlorides to arenesulfonyl hydrazides followed by oxidative bromination with molecular bromine.[73] These arenesulfonyl bromides could be used as initiators in the LRP of MMA, BA, and Sty in Ph$_2$O catalyzed by Cu^{I}Br/bpy, Cu$_2$O/bpy, Cu$_2$S/bpy, Cu$_2$Se/bpy, and Cu$_2$Te/bpy. Like their arenesulfonyl chloride analogues, they provided perfect I_{eff} and polymers with excellent control of molecular weight distribution (M_w/M_n = 1.10−1.37). Further, arenesulfonyl bromides had a diminished induction time and allowed for polymerization under milder conditions (60 °C, as opposed to 90 °C for arenesulfonyl chlorides). Thus, arenesulfonyl bromides serve as the second "universal" class of functional initiators for Cu-catalyzed LRP.

In a similar fashion, p-toluenesulfonyl chloride (TsC) was converted to the corresponding arenesulfonyl hydrazide and oxidatively iodinated with molecular iodine[70] to form p-toluenesulfonyl iodide (TsI) (Scheme 1). Like TsB, TsI

Scheme 1. Synthesis and Structures of Arylsulfonyl Bromides and Iodide Initiators Used in Cu-Catalyzed LRP
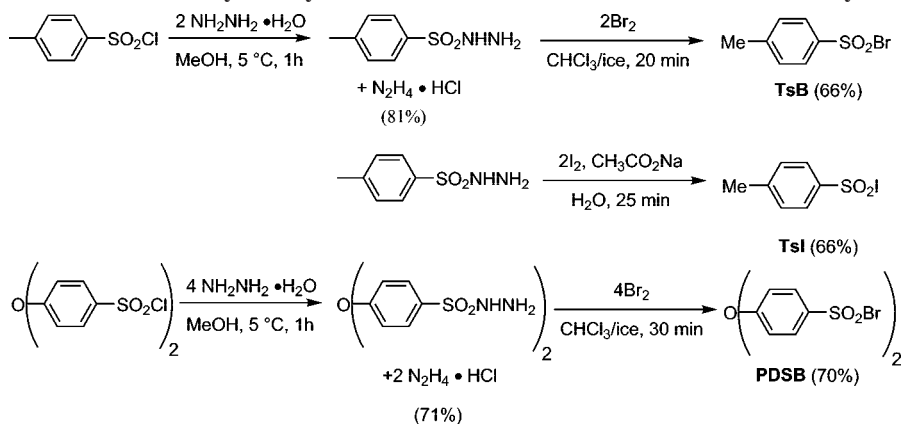
Scheme 2. Synthesis of *N*-Chloro Amides, Lactams, Carbamates, and Imides
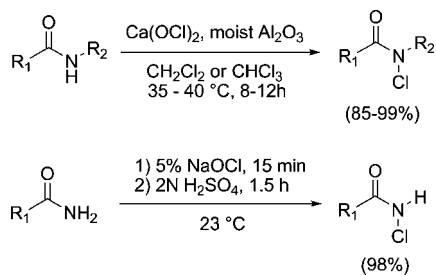
provides access to PMMA and PS with good control of molecular weight evolution and distribution (M_w/M_n = 1.19−1.52) via a mild (70 °C) Cu-catalyzed LRP process, providing the third "universal" class of functional initiators for Cu-catalyzed LRP.[74] The narrow molecular weight distribution observed with TsI indicates that the activation and deactivation in this LRP is faster than chain transfer. As with TsB, various Cu catalysts are practical such as Cu^0/bpy, Cu_2O/bpy, Cu_2S/bpy, Cu_2Se/bpy, Cu_2Te/bpy, CuCl/bpy, CuBr/bpy, and CuI/bpy. Moreover, if CuCl/bpy or CuBr/bpy is employed as the catalyst, halogen exchange is observed, resulting in polymers with chloride or bromide functional chain ends, respectively. Thus, through variation of the catalyst polymers with either Cl, Br, or I, chain ends can be synthesized using a single initiator.

While the major impact of sulfonyl halides as initiators for Cu-catalyzed LRP is their "universality," the original motivation for their development was to provide a greater diversity of end-group functionality. Along similar lines,

N-chloro initiators were pursued to expand the breadth of functional initiators and to provide the opportunity for graft polymerization from *N*-chloro proteins. A variety of *N*-chloro initiators were synthesized from their precursor amides, lactams, and carbamates via chlorination with calcium hypochloride $Ca(OCl)_2$ or sodium hypochloride NaOCl[75] (Scheme 2 and Figure 3).

In clear contrast to sulfonyl halide initiators, *N*-chloro initiators are not "universal" with initiator efficiencies that are highly dependent on their structure. Specifically, *N*-chloro lactams and *N*-chloro benzamides appear to have the highest initiator efficiencies (83−93%), while *N*-chloro imides exhibit the lowest. Despite the variability in initiator efficiency, all polymerizations using *N*-chloro initiators exhibit excellent molecular weight evolution and distribution (M_w/M_n = 1.16−1.38) and possess intact chain-end functionality.

2.4. TERMINI. The First Iterative Method Based on LRP

In 1996, we reported the first LRP of acrylonitrile (AN) initiated with alkyl halides and catalyzed by Cu^IBr/bpy in ethylene carbonate.[76] Later, we improved upon this technique through the use of Cu^IBr/bpy, Cu^ICl/bpy, Cu_2O/bpy, and CuO/bpy catalysts in conjunction with arenesulfonyl chloride and alkylsulfonyl chloride initiators.[77] In that report, we began exploring the use of multifunctional initiators for the synthesis of branched polymers, specifically the use of 1,1,1-tris(4-chlorosulfonylphenyl)ethane (3PSC) to produce a three-armed star polyacrylonitrile (PAN).
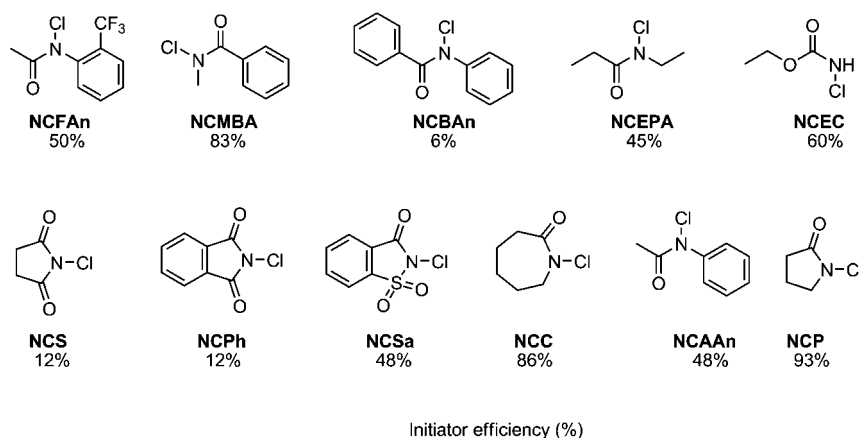
Figure 3. Structures of *N*-chloro initiators used in Cu-catalyzed LRP and their I_{eff}. Adapted with permission from ref 75. Copyright 2005 John Wiley & Sons.
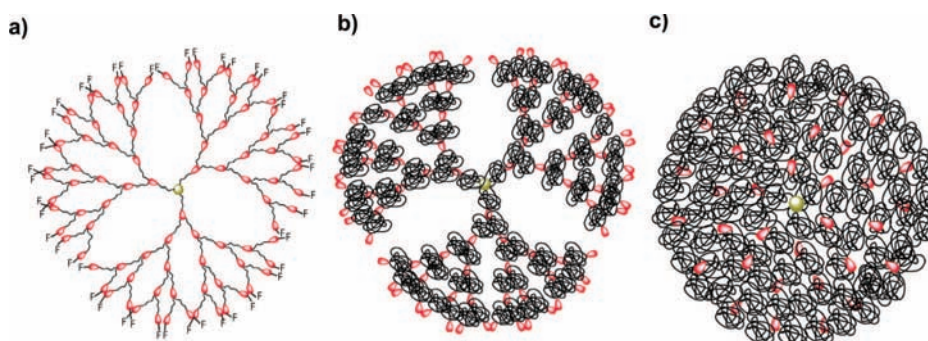
Figure 4. Dendritic macromolecules with tailored polymer spacers between the branching points of (a) low DP, (b) medium DP, and (c) high DP. Red ellipsoids are TERMINI branches, and F represents functional chain ends. Reprinted with permission from ref 86. Copyright 2003 American Chemical Society.
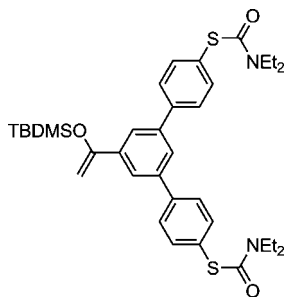
Figure 5. TERMINI molecule.

Our laboratory is also involved in the development of dendrimers and related routes to complex molecular architectures.[78−83] Thus, we became interested in utilizing the self-regulated Cu₂O/bpy LRP initiated with arenesulfonyl chlorides for the production of dendritic macromolecules from commercial monomers by using for the first time LRP in an iterative synthesis. Each branch in this dendritic architecture would be separated by a tailored polymeric arm with different degrees of polymerization (DPs). This technique provides a diversity of dendritic architectures that are not accessible via conventional iterative methods (Figure 4). Low DP spacers are rigid (Figure 4a), while increasing DP results in flexible random-coil spacers (Figure 4b), and ultimately spacers that exhibit chain−chain entanglement (Figure 4c).

Arenesulfonyl chlorides have perfect I_{eff} and thermally separable initiation and propagation steps. Thus, a branched arenesulfonyl halide initiator, such as 3PSC, could be perfectly extended into a three-armed star polymer. However,

in order to produce dendritic macromolecules, an efficient method was needed to convert the chain ends into branched initiation sites. One possibility that emerged was to introduce into the reaction mixture at a specified conversion a more reactive monomer as an irreversible chain terminator that contained a branching point and two "masked" initiator sites. We developed a "masked" sulfonyl halide[84] (Figure 5) that could terminate the polymerization, via loss of TBDMSCl (*tert*-butylchlorodimethylsilane), and in a subsequent step be unmasked to reveal two new arenesulfonyl chloride initiator sites. A library of other TERMINI molecules was prepared and investigated in order to select the most efficient TERMINI (Figure 6).[85]

Thus, this molecule would serve as a terminator multi-functional initiator (TERMINI).[86] Through the TERMINI concept, an array of complex dendritic architectures were synthesized, allowing us to move toward self-assembly and complex architectures with dendritic polymers generated from conventional, commercial monomers (Scheme 3, Figures 4 and 7).[86,87] The TERMINI strategy demonstrated the ability to use LRP in iterative chemical synthesis.

3. SET-DTLRP

3.1. Toward the LRP of Vinyl Chloride (VC)

3.1.1. Cu⁰ Overcomes the Challenge of Reactivation Required for the Living Radical Polymerization of VC

Poly(vinyl chloride) (PVC) is one of the most important thermoplastic materials.[88] The only method available for the production of PVC is free-radical polymerization in

Figure 6. Library of TERMINI molecules investigated.[85]

Scheme 3. Synthesis of Dendritic Macromolecules via the TERMINI Concept and LRP (Adapted with Permission from Ref 86; Copyright 2003 American Chemical Society)

i. MMA, Cu₂O, bpy, *p*-xylene, 90 °C
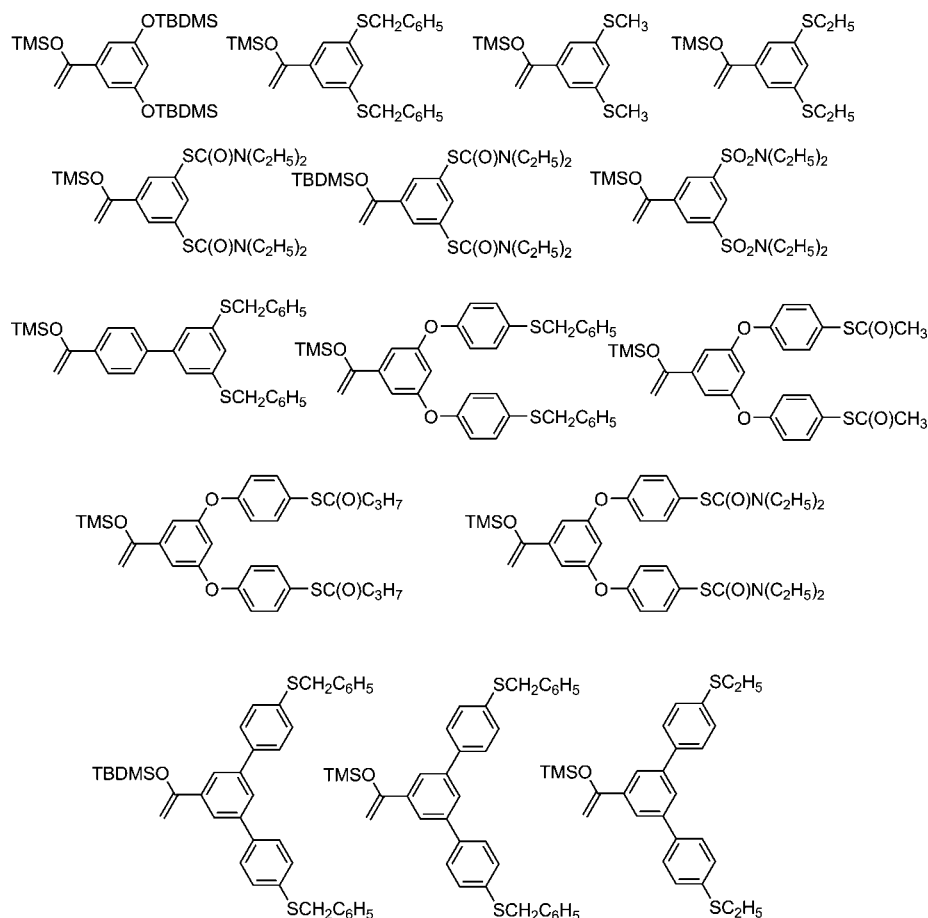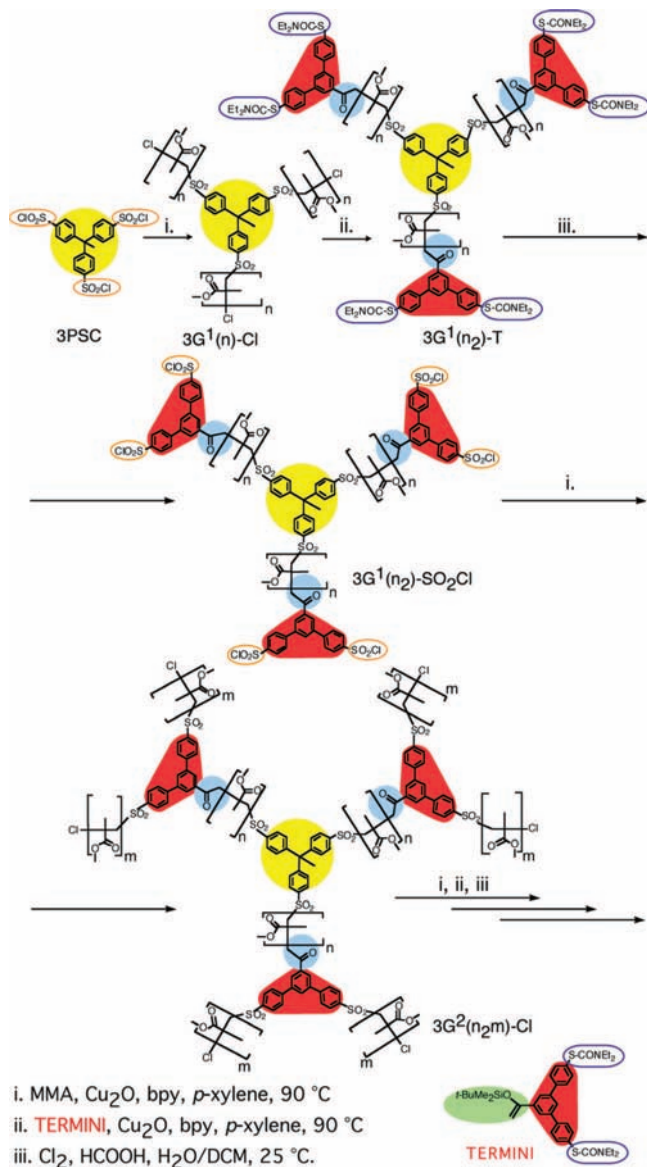ii. TERMINI, Cu₂O, bpy, *p*-xylene, 90 °C
iii. Cl₂, HCOOH, H₂O/DCM, 25 °C.

suspension, emulsion, and bulk. In the absence of additives, PVC is brittle, has a broad molecular weight distribution, contains relatively few intact chain ends, and possesses tertiary chloride and allyl chloride structural defects[89–110] that lead to zipperlike dehydrochlorination reactions when the temperature is elevated above T_g. To combat these deficiencies, PVC is stabilized with organometallic compounds that are added to inhibit decomposition. Other PVC topologies such as telechelics, macromonomers, stars, and block-copolymers were not accessible via conventional radical polymerization. An LRP of VC would provide precise molecular weight and molecular weight distribution, provide perfect chain-end functionality allowing for the use of PVC as a macroinitiator in block-copolymerization, likely suppress the formation of structural defects known to limit performance, and allow access to other, even more complex topologies.[89] Further, PVC is a widely used polymer in medical applications, and potential health concerns have been raised regarding the release of plasticizers such as di(2-ethylhexyl)phthalate (DEHP) from PVC containing devices.

As an LRP process would provide access to effective PVC/elastomer copolymers, plasticizers would no longer be needed to produce flexible PVC based tubing and other medical applications. An LRP of VC could herald a new era of commercial PVC and allow for the production of tailored PVC homopolymers, block-copolymers, or polymers with complex architecture.

As late as 2001, the LRP of VC remained a challenge to us as well as to the entire polymer community. Metal catalysis has been shown to provide access to LRP processes, granting improved control of molecular weight evolution and distribution, retention of end-group functionality, and suppression of defect-causing side reactions in polyacrylates, polymethacrylates, polystyrenes, and even polyacrylonitriles. Unfortunately, the application of such techniques to the synthesis of PVC presents a unique challenge. Even the most active Cu^IX complexes pursued for ATRP have failed to reactivate the relatively inert ∼CHClX end groups.[111] It was suggested that the development of more powerful ATRP catalysts might allow for the polymerization of monomers that form highly stable end groups: "Future catalysts may provide sufficient reactivity for other monomers that cannot be polymerized using current ATRP catalysts. For example, a monomer that would generate a more stable halogen end group, such as vinyl acetate (chloroacetoxy ethane), vinyl chloride (dichloroalkane), or ethylene (bromoalkane), does not polymerize using the current catalysts due to its low K_{eq}."[111] However, to date no such ATRP catalyst has been developed for the polymerization of VC. Continuing our concurrent investigations that began with the development of Cu^IX, Cu_2X, and Cu^0 catalysts for use in sulfonyl halide initiated LRP, we began to screen Cu and other metal catalysts for the LRP of VC. While low-oxidation-state metal complexes such as Cu^IX/bpy (where X = Cl, Br, I) and organocopper species CuSPh/bpy and CuC≡C-Ph/bpy were found to be capable of mediating initiation and primary radical generation in the polymerization of VC, subsequent reactivation of stable ∼CHClX end-groups was negligible, and therefore, $Cu^{II}Cl_2$/bpy generated in situ via initiation serves as an irreversible chain terminator. Our experience with sulfonyl halide initiated polymerization taught us to look beyond Cu^ICl and related catalysts. Somewhat surprisingly, it was found that zero-oxidation state metals including Fe^0/*o*-phenanthroline and Cu^0/bpy were particularly apt at mediating reactivation of dormant ∼CHClI chain ends of PVC derived from iodine-containing initiators in *ortho*-dichlorobenzene (*o*-DCB).[112]

3.1.2. Cu⁰ Catalyzed SET-DTLRP of VC via the Disproportionation of Cuⁱ

While the superior activity of Cu^0 toward reactivation in VC was a definitive breakthrough, it did not immediately lead to an LRP process. In ATRP and many other metal-mediated LRP processes, the living behavior is achieved through the reversible termination of propagating radicals. By reducing the concentration of active radicals, deleterious side reactions such as bimolecular termination are suppressed. The ratio between active and dormant chains is shifted to dormant species through bimolecular termination at the early stages of the reaction that irreversibly builds up levels of higher oxidation state deactivators, mediating the so-called persistent radical effect (PRE) that provides an internal suppression of fast reactions (Scheme 4).[30,113–120]
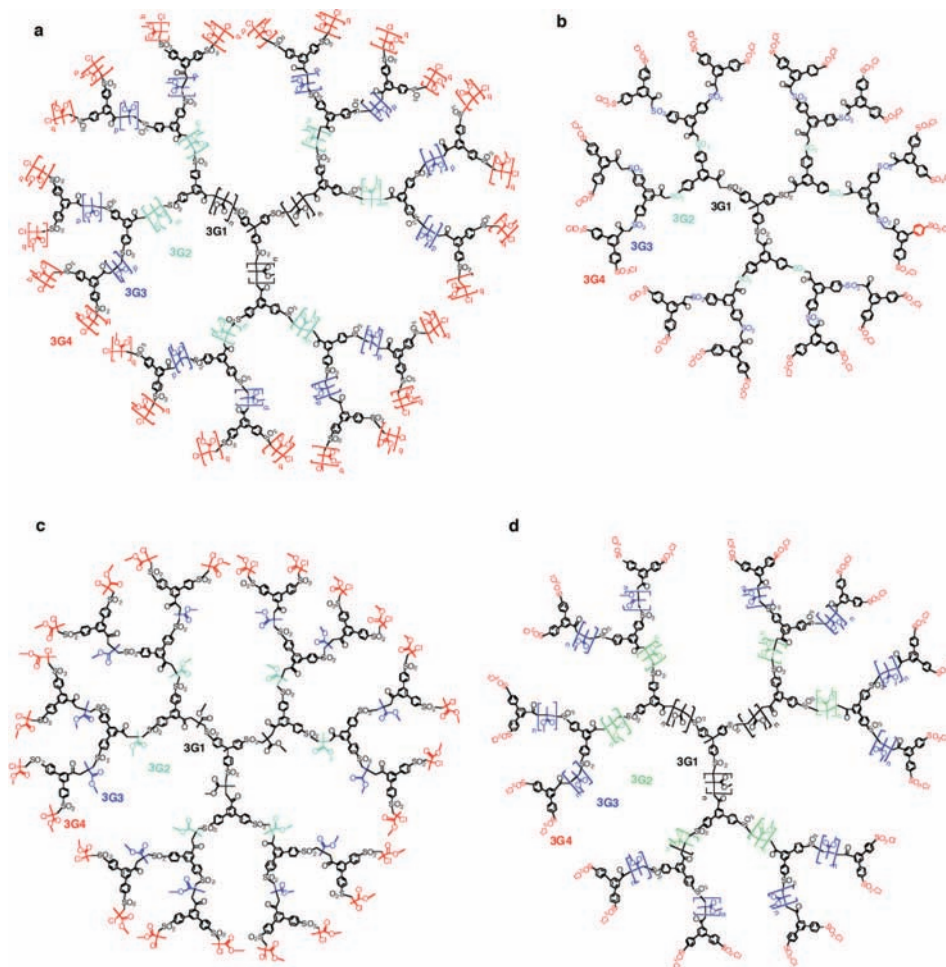
Figure 7. Examples of dendritic macromolecules prepared via TERMINI and LRP. Adapted with permission from ref 86. Copyright 2003 American Chemical Society.

Scheme 4. Establishment of the Persistent Radical Effect (PRE) in ATRP[30]
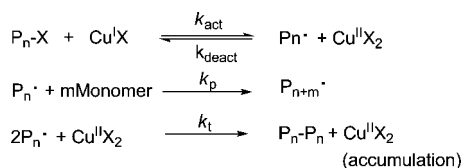
If bimolecular termination were the predominant side-reaction of propagating macroradicals in PVC, a PRE-based method to shift the equilibrium of dormant and active species toward the dormant species would be possible. However, the free-radical polymerization of VC is plagued by one of the largest values of chain-transfer constant to monomer (C_{VC} = 1.08×10^{-3} to 1.28×10^{-3}).[121] Thus, even though Cu^0 is capable of mediating reactivation, chain transfer to monomer (Scheme 5, lines 4 and 5) dominates over bimolecular termination (Scheme 5, Line 3), preventing the establishment of the PRE through buildup of $M^{n+1}XY$ levels.

The seemingly intractable problem of control in metal-catalyzed polymerization of VC caused by the inability of achieving requisite levels of higher oxidation state metal through bimolecular termination was eventually circumvented through an alternative means of deactivator generation. Cu^IX/N-Ligand, the noted activator in ATRP, can be generated in situ via initiation or activation with Cu^0, Cu_2O,

and other Cu^I salts (vida supra). However, Cu^IX/N-Ligand is known to be extremely unstable to disproportionation in water (eqs 1 and 2).[122−129]

$$2Cu^IX \underset{}{\overset{K_{dis}}{\rightleftharpoons}} Cu^0 + Cu^{II}X_2 \qquad (1)$$

$$K_{dis} = [Cu^{II}X_2][Cu^IX]^{-2} = 0.54 \times 10^6 \text{ to } 5.8 \times 10^7 \text{ M}^{-1} \qquad (2)$$

While disproportion of Cu^IX has been regarded as an unwanted side reaction in ATRP,[130] it can be harnessed for useful purposes. Given the extremely high K_{dis} and the low total Cu^IX concentrations in a typical Cu-catalyzed polymerization, if such a reaction were to be carried out in the aqueous phase, at steady state only a negligible amount of Cu^IX would remain, with the bulk being spontaneously converted to Cu^0 and $Cu^{II}X_2$. For every equivalent of Cu^0 that is used in an activation process, an equivalent of Cu^IX will be produced, rapidly regenerating 1/2 equiv of Cu^0 and generating 1/2 equiv of $Cu^{II}X_2$ via disproportionation. Likewise for every equivalent of $Cu^{II}X_2$ involved in a deactivation process, an equivalent of Cu^IX will be produced, rapidly regenerating 1/2 equiv of $Cu^{II}X_2$ and generating 1/2 equiv of Cu^0 via disproportionation. Thus, in a heterogeneous polymerization performed with Cu^0, Cu_2O, or a related Cu_2Y salt, disproportionation would serve as a feedback process wherein reactive Cu^0 activator is maintained throughout the

Scheme 5. Side Reactions in the Radical Polymerization of VC
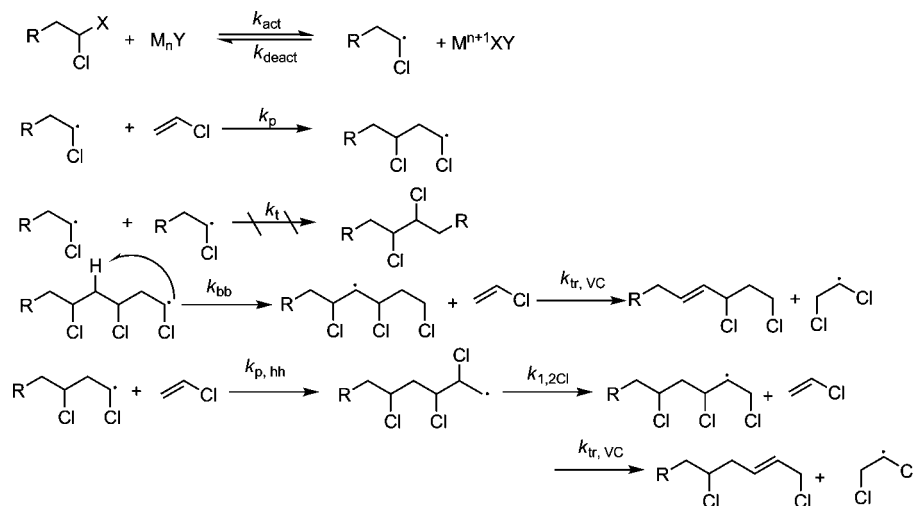
Scheme 6. SET Mechanism of Cu⁰-Catalyzed LRP of VC in Aqueous Media at Room Temperature (RT)
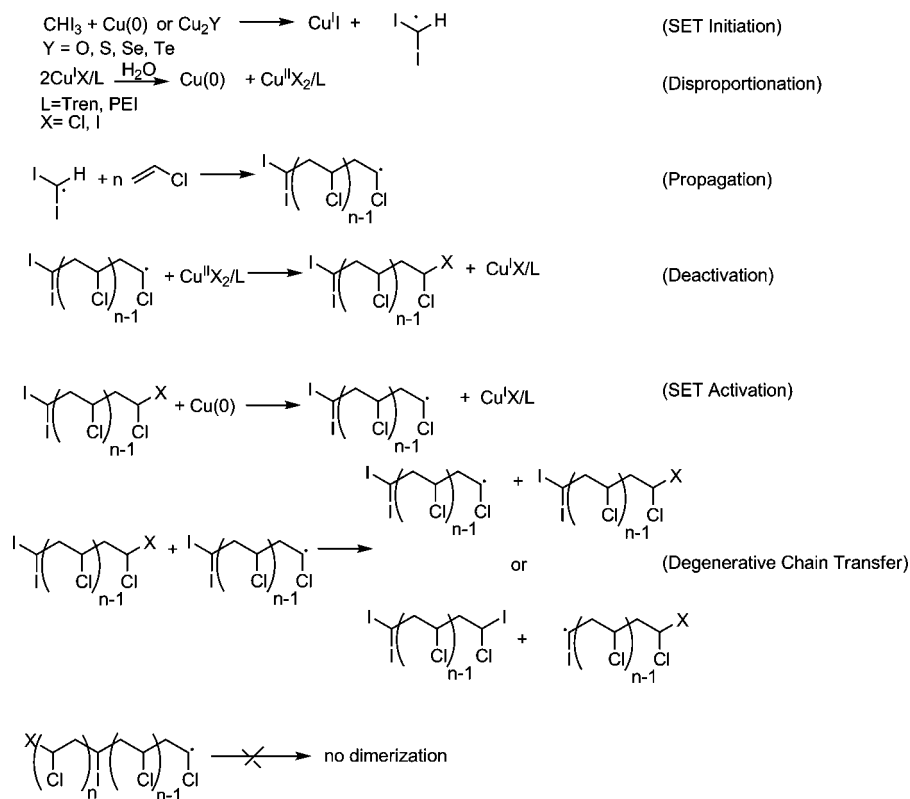
reaction and far more pertinent $Cu^{II}X_2$ deactivator is regulated at a relatively constant level *without* the need for either bimolecular termination or external addition of $Cu^{II}X_2$.

This hypothetical method to regulate the equilibrium of the reaction via disproportionation was made into reality, allowing for the first LRP of VC, later renamed SET-DTLRP as it combines SET and DT processes.[131] Remarkably, Cu^0, Cu_2O, and Cu_2Te in conjunction with certain *N*-ligands that strongly bind $Cu^{II}X_2$, namely, tris(2-aminoethyl)amine (TREN) or polyethyleneimine (PEI), mediate the LRP of VC initiated with iodoform (CHI_3) in 1:1 H_2O/THF at 25 °C. PVC obtained in this fashion exhibited predictable molecular weight evolution and distribution ($M_w/M_n \approx 1.5-1.6$) and perfect chain-end functionality as confirmed by NMR and reinitiation experiments. The perfect chain-end functionality allowed for the first time the possibility of performing block

copolymerization using a PVC macroinitiator. Cu^ICl/TREN, Cu^IBr/TREN, and Cu^II/TREN were able to mediate a similar LRP process, through the disproportionation of the Cu^IX/TREN complex prior to polymerization. When Cu^ICl/TREN and Cu^IBr/TREN are used as catalysts, halogen exchange is expected, resulting in extremely unreactive $-CH_2CHCl_2$ and $-CH_2CHClBr$ end groups, further highlighting the remarkable activity of bulk Cu^0 and "nascent" Cu^0 produced via disproportionation. The kinetic plots of the Cu^0 catalyzed LRP of VC exhibit two distinct domains. The first kinetic domain with relatively faster k_p^{app} corresponds to a liquid−liquid emulsion polymerization. The second kinetic domain with a relatively slower k_p^{app} corresponds to a visually identifiable solid−liquid dispersion polymerization process. Later studies clarified the mechanism of the Cu^0-catalyzed LRP of VC as

Scheme 7. Proposed Mechanism of SET-DTLRP of VC in H₂O
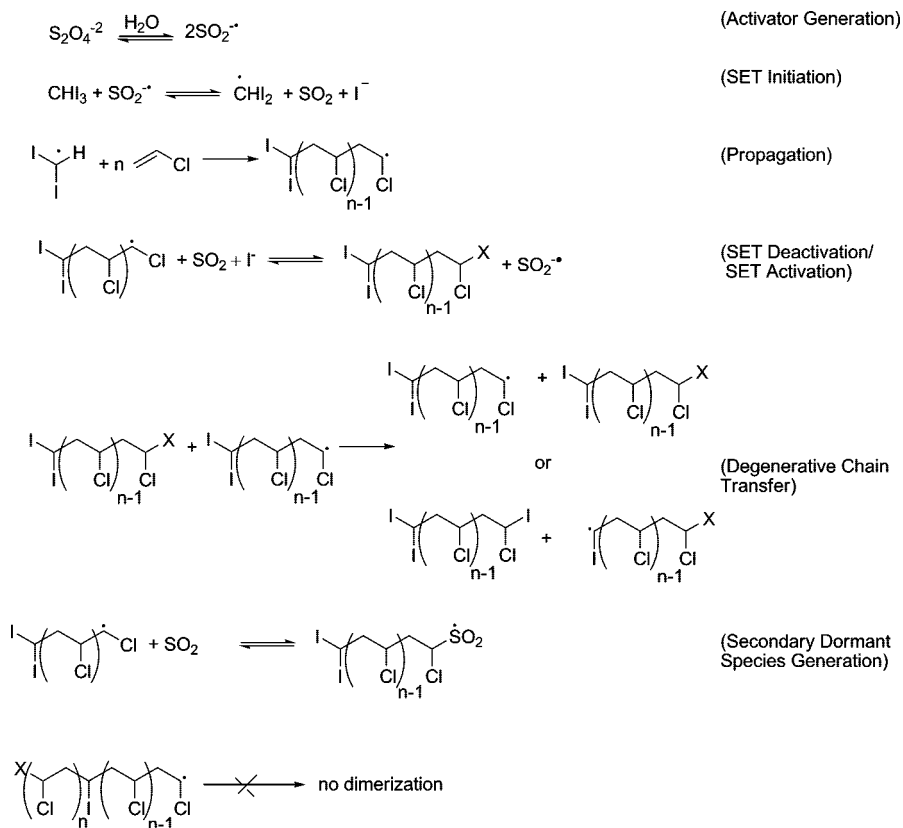
a competition between SET activation/deactivation and degenerative chain transfer (Scheme 6).[26]

The inability to achieve extremely narrow polydispersities can be attributed to the heterogeneity of the polymerization vis-à-vis the growing polymer chain and chain transfer to tetrahydrofuran (THF). The use of anionic surfactant such as sodium dodecyl sulfate (SDS) allows for the LRP process to be conducted without the addition of an organic cosolvent such as THF. The Cu^0/PEI-catalyzed LRP of VC in H_2O using sodium dodecyl sulfate (SDS) as surfactant proceeds with only one kinetic domain (solid–liquid dispersion polymerization), as PVC is not soluble in VC alone. Detailed ^{1}H NMR, ^{13}C NMR,[132] and multidimensional COSY and HMQC NMR experiments revealed that, in Cu^0 catalyzed LRP of VC in aqueous media, CHI_3 serves as a bifunctional initiator forming telechelic α,ω-di(iodo)PVC with perfect chain end-functionality useful for ABA block copolymerization or additional chain-end functionalization. Further, it was found that the polymer was free of branching or unsaturated structural defects[89] and that the resulting PVC has a higher syndiotacticity (62%) than that obtained by a free-radical process at the same temperature (56%).[133−135]

3.1.3. Non-Transition Metal Mediated SET-DTLRP

The compatibility of Cu^0 catalyzed LRP of VC with an aqueous reaction makes the reaction more environmentally benign than those conducted in organic media. The process could be made even more eco-friendly via the replacement of Cu^0 with a nontransition metal catalyst. While, PVC prepared via Cu^0 is typically a white powder, indicating a low-metal content, it would nevertheless still be beneficial to completely eliminate any metallic impurities. The Cu^0 catalyzed LRP of VC in aqueous media is dominated by

competitive SET activation/deactivation and degenerative chain transfer. It seemed reasonable that Cu^0 could be replaced with an environmentally benign water-soluble reductant, such as sodium dithionite ($Na_2S_2O_4$).[136−138] Rewardingly, $Na_2S_2O_4$/$NaHCO_3$ was able to mediate the "green" LRP of VC initiated with CHI_3 in water at 25 °C with the aid of various suspension agents including hydroxypropyl methyl cellulose (Methocel F50), 72.5% hydrolyzed poly(vinyl acetate) (Alcotex 72.5), and poly(vinyl alcohol) containing 11−13% acetate groups (PVA 88) as well as in the presence of electron-transfer cocatalysts 1,1′-dialkyl-4,4′-bipyridinium dihalides and alkyl viologens.[139,140] The resulting PVC exhibited predictable molecular weight evolution and distribution as compared to the Cu^0-catalyzed LRP process. Likewise, it is free of structural defects, exhibits perfect telechelic chain-end functionality, and has higher thermal stability[141] and syndiotacticity than commercially available PVC.

The similarities of the PVC obtained by Cu^0-catalyzed and $Na_2S_2O_4$-catalyzed SET-DTLRP suggest a similar mechanism. Specifically, the $S_2O_4^{2-}$ dianion has a small but definitive dissociation constant in water, $K_d \approx 10^{-6}$ mM.[142] Dissociation of $S_2O_4^{2-}$ results in the formation of $2SO_2^{-\bullet}$. $SO_2^{-\bullet}$ serves as an electron donor to mediate the SET activation of the initiator and dormant polymer chains. $Na_2S_2O_4$ also serves in a second role, scavenging oxygen, a strong inhibitor of radical polymerization process.[143,144] $NaHCO_3$ buffer maintains the basic pH, shown to be helpful in aqueous VC polymerization,[145] prevents decomposition of $Na_2S_2O_4$,[136] and consumes SO_2 liberated after SET reduction via $SO_2^{-\bullet}$. Absence of $NaHCO_3$ and excess SO_2 has been shown to inhibit the $Na_2S_2O_4$ mediated LRP of VC. Thus, it is possible that low residual levels of SO_2 that are not eliminated by $NaHCO_3$ can also reversibly add to

propagating radicals to form an alternative dormant species, as is the case with perfluoroalkyl radicals[137,146] and in the copolymerization[147,148] of VC with SO_2. As the LRP of VC catalyzed by $Na_2S_2O_4/NaHCO_3$ in water combines SET activation with degenerative chain transfer (DT), the resulting polymerization was also classified as SET-DTLRP (Scheme 7). Though the name was coined for $Na_2S_2O_4/NaHCO_3$ catalyzed LRP in water, Cu^0/TREN or PEI and Cu_2X/TREN or PEI catalyzed LRP of VC in THF/H_2O mixtures is also a SET-DTLRP process.

3.2. Applications of SET-DTLRP

Prior to the development of SET-DTLRP, conventional free-radical polymerization was only able to produce VC up to a maximum $M_n = 113\,000$. Sodium dithionite mediated SET-DTLRP has been used to prepare ultrahigh molecular weight PVC, $M_n = 200\,000$ ($M_w/M_n = 1.70$).[149] The resulting polymer is defect free and has a higher T_g (93 °C) than commercial PVC. Recent work, has shown that PVC-*b*-poly(isonorbornyl acrylate)-*b*-PVC prepared via SET-DTLRP exhibits even higher T_g (100−133 °C).[150] SET-DTLRP is not restricted to the synthesis of PVC. SET-DTLRP mediated by $Na_2S_2O_4/NaHCO_3$ initiated with CHI_3 in water has been applied to the polymerization of a variety of acrylate monomers including ethyl acrylate (EA),[151] *n*-butyl acrylate (BA),[152,153] *i*-butyl acrylate (*i*BA),[153] *t*-butyl acrylate (*t*BA),[153,154] lauryl acrylate (LA),[155] 2-ethylhexyl acrylate (2EHA),[154] and 2-methoxy ethyl acrylate (MEA).[156] The SET-DTLRP of EA was effectively scaled up for use in a pilot plant.[151] The SET-DTLRP of MEA provided for the first power relationship between M_w and η or R_g.[156] The SET-DTLRP of *t*BA allowed for the ultrafast synthesis of ultrahigh molecular weight α,ω-di(iodo)P*t*BA with excellent control of polydispersity ($M_n^{GPC} = 823\,150$, $M_w/M_n = 1.15$).[154] SET-DTLRP of VC initiated with CHI_3 results in a telechelic polymer with identical chain ends, forming a polymer with the structure **I**(ClCHCH2)$_m$CHI(CH$_2$CHCl)$_n$**I**. A unique telechelic polymer with asymmetric functional chain ends can be achieved via SET-DTLRP of VC initiated with methylene iodide (CH_2I_2), to form a polymer with the structure **ICH$_2$**(CH$_2$CHCl)$_{n-1}$CH$_2$CHCl**I**.[157] CHI_3 serves as a bifunctional initiator in SET-DTLRP and is suitable for the synthesis of macroinitiators for ABA block-copolymerization, whereas CH_2I_2 serves as a monofunctional initiator and is suitable for the synthesis of macroinitiators for AB block copolymerization. Other α,ω-di(iodo)PVC samples were prepared via SET-DTLRP initiated by bis(2-iodopropionyloxy)ethane (BIPE), 2,5-diiodohexanediothoate (DMDIH), and bis(2-methoxyethyl) 2,5-diiodohexanedioate (BMEDIH).[158] Similarly, four-armed star PVC and PBA were synthesized via SET-DTLRP initiated with Pentaerythritol tetrakis(2-iodopropionate) (4IPr).[158] SET-DTLRP of PVC initiated with α,ω-di(iodo)-PBA and four-armed star PBA macroinitiator provided PVC-*b*-PBA-*b*-PVC[159−161] and four-armed star block-co-polymer [PVC-*b*-PBA-CH(CH$_3$)−CO−O−CH$_2$]$_4$C,[162] respectively. Perhaps most significantly, the use of Cu^0/TREN catalyzed SET-DTLRP provided the first general approach for the synthesis of ABA block copolymers with PVC in the B block.[163] Cu^0/TREN catalyzed SET-DTLRP provided α,ω-di(iodo)PVC macroinitiators with M_n's of 2 100−29 800 ($M_w/M_n = 1.66−2.16$). These macroinitiators were subse-

quently used in the CuCl/bpy-catalyzed polymerization of MMA at 90 °C to provide PMMA-*b*-PVC-*b*-PMMA block copolymers with M_n up to 95 700 with excellent control of molecular weight distribution ($M_w/M_n = 1.21$).

3.3. Perspective on SET-DTLRP

SET-DTLRP has opened the doorway to the LRP of VC and the synthesis of complex molecular architectures with PVC blocks. While control of molecular weight distribution is better in SET-LRP (vida infra), especially in the case of acrylates, SET-DTLRP variants utilizing nontransition metal catalysts and aqueous media provide for "green chemistry".

4. Single-Electron Transfer Living Radical Polymerization

SET-LRP is the direct descendent of SET-DTLRP, wherein the DT process has been suppressed through appropriate reaction conditions.[27] SET-LRP is a robust methodology that allows for the ultrafast synthesis of linear polyacrylates, polymethacrylates, and poly(vinyl chloride) with ultrahigh molecular weight at room temperature or below.[164] Polymers produced via SET-LRP exhibit predictable molecular weight evolution and distribution, perfect retention of chain-functionality, and no detectable structural defects, and they are colorless without any purification. In SET-LRP the balance between dormant and active chains is mediated by an outer-sphere heterolytic SET[165,166] activation process via Cu^0 surfaces and deactivation with $Cu^{II}X_2$/*N*-ligand. Cu^0 activator and $Cu^{II}X_2$/*N*-Ligand deactivator are maintained at requisite levels through the rapid disproportionation of in situ produced Cu^IX mediated by the appropriate choice of *N*-ligand and solvent.

4.1. Preparative Characteristics of SET-LRP

4.1.1. Ultrafast Polymerization at Room Temperature

Compared to other metal-catalyzed LRP processes, SET-LRP is significantly more rapid. A typical SET-LRP of MA initiated with methyl 2-bromopropionate (MBP) in dimethyl sulfoxide (DMSO) at 25 °C ([MA]/[MBP]/[Cu^0]/[Me$_6$-TREN] = 222/1/0.1/0.1 can achieve complete conversion in maximum 50 min, to achieve PMA with $M_n \approx 20\,000$. The kinetics of SET-LRP for a given monomer-to-initiator ratio can be tuned by solvent concentration, ligand loading level, a change in the mass or surface area of the homogeneous catalyst, a change in the initiator structure, supplementary addition of $Cu^{II}X_2$/*N*-ligand deactivator, or a change in temperature. The external rate order of [DMSO]$_0$ was calculated to be roughly ∼0.6−1.2.[27] Increasing the ratio of monomer to polar solvent such as DMSO tends to increase the rate of SET-LRP in concentrated mixtures. The role of ligand is more complex. Increasing ligand levels have been observed to increase k_p^{app} until a maximum value is reached, while the absence of ligand results in no polymerization (vida infra). Studies where the total surface area of Cu^0 was increased through variation of Cu^0 particle size,[167] or through the use of extended Cu^0 wire sources[168] in the SET-LRP of MA, have shown that nearly complete conversion can be achieved in under 15 min, while maintaining similar levels of living character and
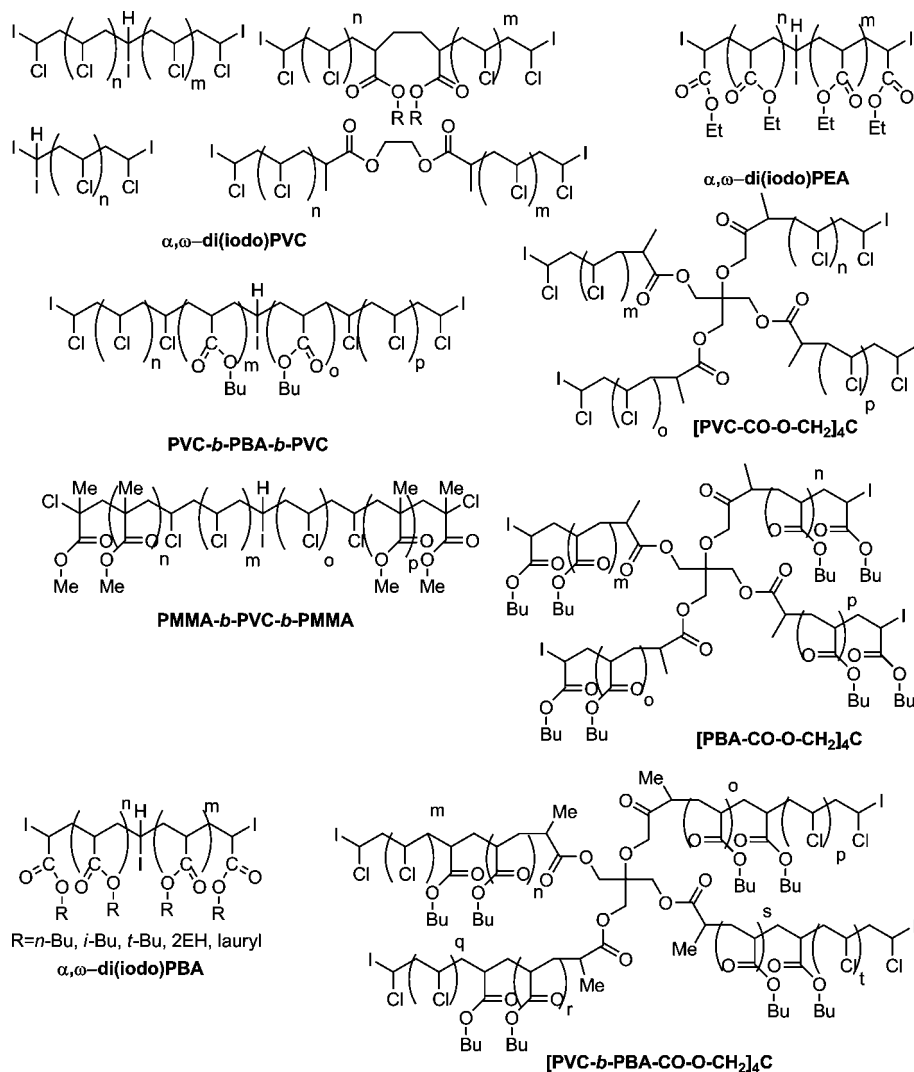
Figure 8. Diversity of PVC and combined PVC−polyacrylate structures produced via SET-DTLRP.

perfect chain-end functionality. While the external rate order of $[Cu^0]_0$ was originally calculated to be ~0.51,[174] the k_p^{app} in the SET-LRP of MA can be varied by approximately 1 order of magnitude through the manipulation of Cu^0 surface area. Other acrylate monomers proceed with similar k_p^{app} to MA, but monomers with lower inherent k_p such as MMA or with low k_{act} such as VC proceed slower.

4.1.2. Linear Polymers with Ultrahigh Molecular Weight

Prior to the development of SET-LRP, the highest molecular weight linear polymers produced via metal-catalyzed LRP processes were $M_n = 300\,000$ for PBMA,[48] $M_n = 367\,000$ for PMMA,[169] $M_n = 554\,000$ for PMA,[23,24] and $M_n = 823\,000$ for PtBA.[154] Unoptimized Cu^0/Me₆-TREN[170] catalyzed SET-LRP of MA initiated with MBP in DMSO was able to provide the ultrafast (<10 h) synthesis of ultrahigh molecular weight (UHMW) linear PMA of $M_n = 1\,420\,000$ with a very narrow molecular weight distribution ($M_w/M_n = 1.15$).[27] In the same report, an unoptimized Cu^0/PMDETA catalyzed SET-LRP of MMA initiated with 2,2-dichloroacetophenone (DCAP) in DMSO was able to provide very high molecular weight PMMA, $M_n \approx 150\,000$ ($M_w/M_n \approx 1.25$), in roughly 13 h. Unpublished results have also achieved UHMW PMMA via this method. The remarkable ability of

SET-LRP to achieve UHMW polymers is largely attributed to its near-complete suppression of termination reactions.

4.1.3. Predictable Molecular Weight Evolution and Distribution

In spite of the ultrafast kinetics observed in SET-LRP, predictable molecular weight evolution and distribution can be achieved. Unoptimized conditions for Cu^0 powder-catalyzed SET-LRP uniformly exhibit a linear dependence of M_n^{GPC} with conversion and in excellent agreement with M^{th} with I_{eff} 98+%. Cu^0 powder-catalyzed SET-LRP typically results in polymers with narrow polydispersity ($M_w/M_n \approx 1.20-1.45$ for monofunctional initiators and as low as 1.15 for bifunctional initiators). Cu_2X (where X = Te, Se, S, O) catalyzed SET-LRP achieves similar results. Cu^0-wire-catalyzed SET-LRP is more effective when monofunctional initiators are used, resulting in narrower polydispersities ($M_w/M_n < 1.15$). In addition to standard gel permeation chromatography (GPC) techniques, the monitoring of molecular weight evolution and distribution can be conducted in real-time via rapid chromatographic techniques such as Polymer Laboratories' Polymerization Monitoring and Control System (PL-PMC).[171]

Figure 9. Example MALDI-TOF-MS analysis of a PMA produced via Cu^0/Me_6-TREN catalyzed SET-LRP of MA initiated with BPE in methanol/water (95/5 v/v) at 25 °C. Reprinted with permission from ref 179. Copyright 2008 John Wiley & Sons, Inc.

4.1.4. Perfect Retention of Chain-End Functionality

The complete retention of chain-end functionality is necessary to achieve UHMW polymers and allows for the synthesis of macroinitiators for block-copolymerization. Preliminary NMR studies and the observa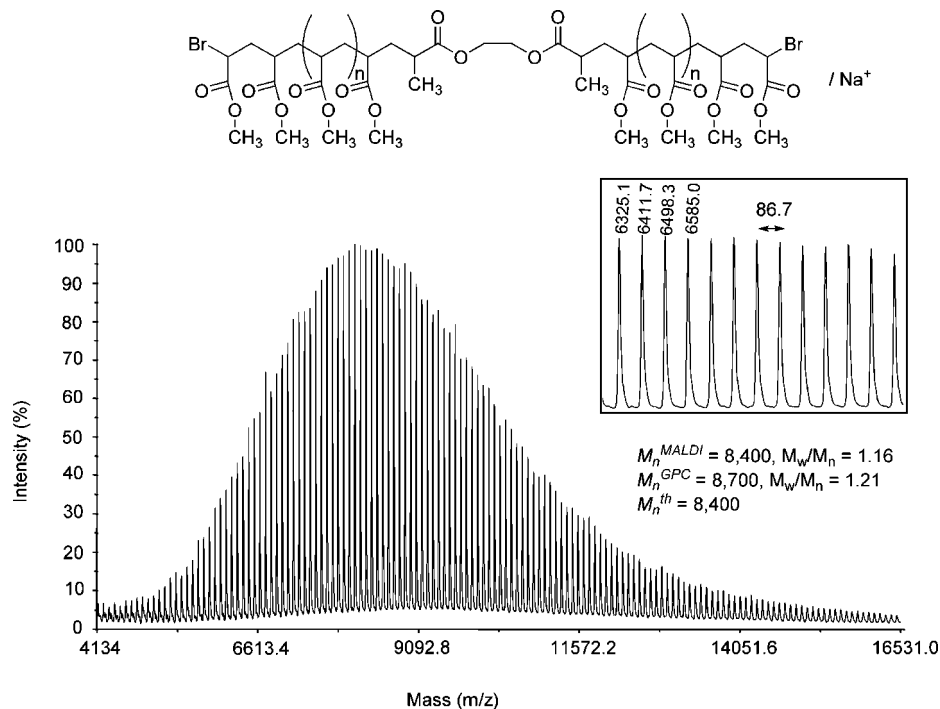tion that SET-LRP provides access to UHMW polymers supported the claim of perfect retention of chain-end functionality.[27] A contradictory report claimed imperfect chain ends in SET-LRP.[172]

Following these initial reports, a series of in depth NMR, MALDI-TOF, and reinitiation studies confirmed that indeed SET-LRP produces polymers with perfect chain-end functionality. Comparison of the ^{1}H NMR integrals of initiator and $\sim$CH(CO$_2$Me)Br chain-end protons demonstrates perfect retention of chain-end functionality throughout the entire course of the reaction for Cu^0/Me_6-TREN catalyzed SET-LRP of MA,[173−177] EA,[173] and BA[173] initiated with bis(2-bromopropionyloxy)ethane (BPE),[173,178] haloforms,[175−177] and MBP[168,175,176] in DMSO at 25 °C and for the Cu^0/Me_6-TREN catalyzed SET-LRP of MA initiated with BPE in 95:5 methanol/water[179] at 25 °C. Interestingly, Cu^0/Me_6-TREN catalyzed polymerization of MA initiated with MBP in solvents that do not mediate adequate disproportionation of Cu^IBr/Me_6-TREN such as toluene[175] and MeCN[176] exhibits a linear decrease in chain-end functionality with conversion. In the nondisproportionating solvents toluene and MeCN, the final chain-end functionality is as low as 80% (Figure 20).[175,176]

MALDI-TOF-MS experiments were also used to confirm the structure of PMA, PEA, and PBA samples produced via Cu^0/Me_6-TREN catalyzed SET-LRP in DMSO at 25 °C. All PMA samples showed a single set of peaks corresponding to the halogen functionalized chain end[173,174,177,178] (Figure 9). PEA and PBA samples showed predominantly one set of peaks corresponding to halogen functionalized chain but had a trace subset of peaks corresponding to HBr elimination. As signals corresponding to unsaturation were not evident in ^{1}H NMR, the HBr elimination in PEA and PBA was

suspected to be a result of in-source decay (ISD) or postsource decay (PSD) in the MALDI-TOF-MS experiment.[180] This suspicion was confirmed through the end-capping of the PEA and PBA samples with thiophenolate prior to MALDI-TOF-MS. Thiophenol capped PEA and PBA provided only a single set of peaks corresponding to thiophenol derivitized chain ends.[173]

^{1}H NMR and MALDI-TOF-MS experiments provided structural analysis in support of perfect retention of chain-end functionality. Reinitiation experiments were performed on a sample of telechelic α,ω-di(bromo)PMA produced via Cu^0/Me_6-TREN catalyzed SET-LRP of MA initiated with BPE in DMSO at 25 °C (Figure 10). The initial polymer $M_n^{GPC} = 34\ 861$ ($M_w/M_n = 1.23$) was extended via reinitiation and subsequent polymerization to $M_n^{GPC} = 498\ 053$. The resulting polymer exhibited a narrow polydispersity ($M_w/M_n = 1.10$) and a unimodal distribution, indicating a perfect I_{eff} of the macroinitiator and, consequently, perfect retention of chain-end functionality.

4.1.5. Colorless Reaction Mixtures and Colorless Polymers

SET-LRP performed with Cu^0 powder and Cu_2Y salts, even at catalyst loading levels in excess of 10% relative to initiator, resulted in colorless polymerization mixtures and colorless polymers. Even larger loading levels of Cu^0 wire can be accommodated without discoloration. The absence of color in the polymerization mixture and the resulting polymer is due to a combination of four factors. (1) Cu^0 as opposed to Cu^IX is used as the activator. (2) The atomic Cu^0 produced via disproportionation does not get used in activation agglomerates. However, this process might be nucleated by the Cu^0 wire powder or catalyst, and thus, it does not impurify the reaction mixture. (3) Only a small fraction of the total Cu^0 is consumed in the activation process, and the low levels of Cu^IX produced in situ are eliminated
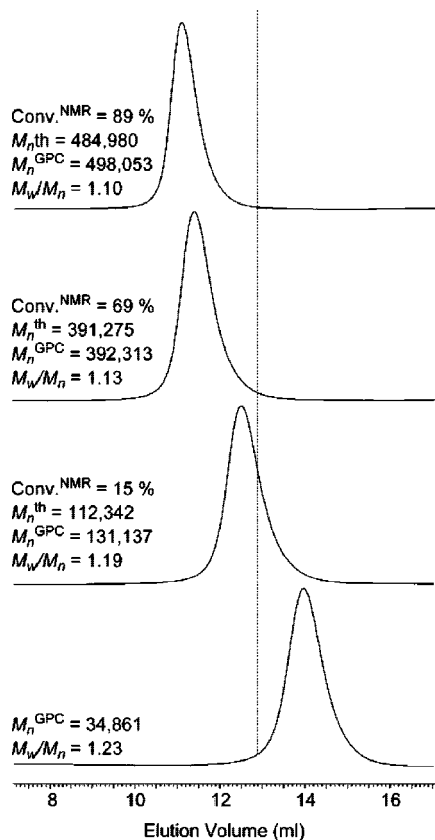
Figure 10. Reinitiation study of α,ω-di(bromo)PMA produced via Cu^0/Me$_6$-TREN catalyzed SET-LRP of MA in DMSO at 25 °C. Reprinted with permission from ref 173. Copyright 2007 John Wiley & and Sons, Inc.

via disproportion to regenerate Cu^0. (4) Cu^{II}X$_2$ is produced via a self-regulated disproportionation; therefore, large excesses of Cu^{II}X$_2$, which result in green discoloration, are not produced via the typical PRE process. Other Cu-catalyzed LRP processes such as ATRP require often tedious purification, such as column chromatography, of the polymer to remove discoloration and metal impurities.[181−183] SET-LRP provides a more efficient and economical route to colorless metal-free polymers. Even low MW PMA and PMMA can be prepared via SET-LRP so as to contain <1 ppm Cu as determined by inductively coupled plasma atomic emission spectroscopy (ICP-AES).[184]

A quick test for a SET-LRP process is to examine the color of the reaction mixture. Typical ATRP reactions using Cu^{I}X/bpy are darkly red or brown colored as a result of charge transfer interactions between *N*-ligands and the copper species (Figure 11c,d). The precise color is solvent and ligand dependent and can change somewhat during the course of the reaction due to changes in the relative abundance of Cu^I and Cu^{II} species, the latter of which often has a green color (e.g., Cu^{II}Br$_2$/Me$_6$-TREN). In SET-LRP, reactions are colorless throughout when typical levels of monomer, initiator, and catalyst are employed (Figure 11a). When very low DP polymers are prepared (i.e., low monomer-to-initiator ratio to catalyst ratios) or in the presence of a nondisproportion-ating solvent where bimolecular termination is prevalent, a light green color is sometimes observed due to the presence of higher levels of Cu(II)X$_2$/*N*-ligand. This same greenish color is observed in the Cu^{I}Br/Me$_6$-TREN catalyzed polymerization of MA in MeCN (Figure 11b).
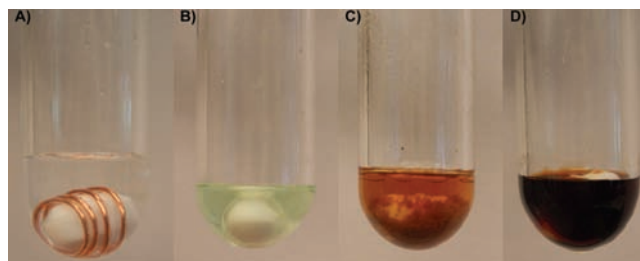
Figure 11. Representative colors of Cu-catalyzed LRP: (A) Cu(0)-wire catalyzed SET-LRP of MA (the 12.5 cm of 20 gauge wire is wrapped around the stirring bar); reaction conditions: [MA]$_o$/[MBP]$_o$/[Me$_6$-TREN]$_o$ = 222/1/0.1. (B) Cu^{I}Br/Me$_6$-TREN catalyzed polymerization of MA in MeCN; reaction conditions: [MA]$_o$/[MBP]$_o$/[Cu^{I}Br]$_o$/[Me$_6$-TREN]$_o$ = 222/1/0.1/0.1. (C) Cu^{I}Br/bpy catalyzed ATRP of MA in toluene [MA]$_o$/[MBP]$_o$/[Cu^{I}Br]$_o$/[bpy]$_o$ = 222/1/1/1. (D) Cu^{I}Br/bpy catalyzed ATRP of MA in MeCN [MA]$_o$/[MBP]$_o$/[Cu^{I}Br]$_o$/[bpy]$_o$ = 222/1/1/1.

4.1.6. Use of Commercial-Grade Reagents

In SET-LRP, monomer, solvent, catalyst, initiator, and most ligands can be used as purchased from chemical suppliers with no need for purification. SET-LRP is tolerant to radical inhibitors found in commercial monomers (vida infra). Even Me$_6$-TREN, typically made in-house from commercially available TREN,[170] can be used without purification.

4.1.7. Other Experimental Considerations

The detailed discussion of the reaction conditions employed for SET-LRP is beyond the scope of this review and can be found in any of the numerous references reported. However, some experimental details are of note. SET-LRP is tolerant of unpurified and inhibited monomer, solvent, ligand, and initiator. Additionally, in most cases, the addition or residual presence of H$_2$O is helpful rather than harmful. Even oxygen is tolerated by SET-LRP as Cu^0 will first react with oxygen to form copper oxide, which itself is an initiator for SET-LRP. However, in the presence of oxygen, an induction period is observed as copper oxide initiates and disproportionates far more slowly than Cu^0 and Cu^{I}X, respectively. On large scale, excess Cu^0 can remove oxygen more effectively than on small scale, and therefore, most laboratory experiments must be rigorously degassed through sequential freeze−pump−thaw processes. Special care in the process must be given when low melting point solvents are employed.

4.2. Monomer Compatibility

A variety of monomers have been used in SET-LRP (Figure 12). While the majority of the monomers tested thus far are acrylates, a larger diversity of vinyl monomers is expected to be compatible with SET-LRP.

4.2.1. Acrylates

SET-LRP has been used in conjunction with acrylates and acrylamides such as MA, EA, BA, *t*BA, solketal acrylate ((2,2-dimethyl-1,3-dioxolan-4-yl)methyl acrylate),[185] 2-meth-oxyethyl acrylate (MEA),[186] poly(ethylene glycol) methyl ether acrylate (PEGMEA),[187] 2-EHA,[188] and *N*-isopropy-lacrylamide (NIPAM).[188−190] With the latter three monomers, it was only realized recently that the reaction was proceeding by SET-LRP.[190] The compatibility of SET-LRP with func-
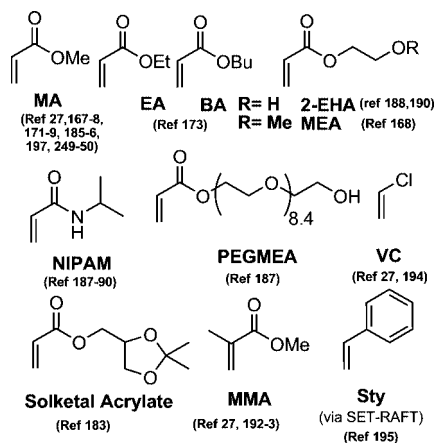
Figure 12. Monomers used in SET-LRP.

tional monomers such as 2-EHA, PEGMEA, NIPAM, and solketal suggests a broad scope of monomers is expected. Other acrylate monomers have been tested with the related polymerization SET-DTLRP including *I*BA and lauryl acrylate and, due to the mechanistic overlap with SET-LRP, are expected to be compatible. Among the acrylates tested for SET-LRP, k_p^{app} and molecular weight evolution and distribution are comparable.

4.2.2. Methacrylates

SET-LRP of MMA in DMSO as well as in ionic liquids[191] has been performed. Self-regulated Cu^0/bpy and Cu_2O/bpy catalyzed LRP has been shown to be compatible with other methacrylate monomers such as BMA. Because of the lower intrinsic k_p of methacrylates, SET-LRP of MMA is about 5−10 times slower than SET-LRP of MA under identical conditions. The SET-LRP of MMA is also feasible using 2-cyanoprop-2-yl 1-dithionaphthalate (CPDN), a typical RAFT agent, as an initiator. The syndiotacticity for MMA prepared in this fashion was 0.67, which is close to what is observed for free radical polymerization.[192] Cu^0/PMDETA-catalyzed SET-LRP of MMA initiated with ethyl 2-bromoisubutyrate in 1,1,1,3,3,3-hexafluoro-2-propanol (HFIP) was also reported.[193] Here, HFIP provided enhanced rate of polymerization even at low temperatures from 0 to −18 °C, improved molecular weight evolution, and also enhancing syndiotacticity to 0.77, compared to 0.56−0.66 for free radical polymerization.

4.2.3. Vinyl Halides

In the initial report of SET-LRP, compatibility with VC as a monomer was demonstrated to provide DP = 350−700 PVC with very narrow polydispersity.[27] In a later report, the combination Cu^0/$CuBr_2$/TREN catalyzed SET-LRP initiated with $CHBr_3$ provided access to the synthesis of PVC with DP as low as 100 and as high as 1400.[194] On the basis of calculations, other vinyl halides and fluorinated vinyl halides should be compatible with SET-LRP. However, in the cases of vinyl bromide, a degree of halogen exchange is expected with the use of chloro- or iodo-containing initiators.

4.2.4. Other Monomers

While acrylates, methacrylates, and vinyl halides provide a large scope of vinyl monomers in SET-LRP polymerization, there are still monomer classes to explore. Specifically,

the polymerization of acrylonitrile and styrenes has not been explored in any depth. Both acrylonitrile and styrene were polymerized via self-regulated Cu_2O/bpy catalyzed LRP initiated with sulfonyl halides, and computational studies have suggested similar bond dissociation energy (BDE) profiles[165] as with acrylates, methacrylates, and vinyl halides, suggesting their compatibility with SET-LRP.

One group has reported that Cu^0/PMDETA catalyzed SET-LRP of Sty initiated with 1-bromoethyl benzene (1-PEBr), ethyl 2-bromo isobutyrate (EBiB), or diethyl-2-bromo-2-methyl malonate (DEBMM) in DMSO at 25 °C is feasible, but with relatively broad polydispersity ($M_w/M_n > 1.4$).[195] They also suggest that the combination of SET-LRP and RAFT (SET-RAFT) can improve the living character of the reaction. They claim that Cu^0/PMDETA/(2-ethoxy carbonyl) prop-2-yl-pyrrole-1-carbodithioate (CTA) catalyzed SET-RAFT of Sty initiated with DEBMM or TsCl in DMSO at 25 °C provides PS with a lower final polydispersity (M_w/M_n ≈ 1.20−1.26).

More promising is a report that the Cu^0/Me_6-TREN catalyzed SET-LRP of MA can be performed in hydrophobic media such as toluene through the use of polar phenol additives.[196] By expanding the compatibility of SET-LRP to include hydrophobic media, monomers that are insoluble or for which their growing polar chains are insoluble in polar solvents can now be polymerized by SET-LRP. More recent results indicate that binary mixtures of organic solvents can be prepared wherein, through cooperative and synergistic effects, a suitable balance of polarity, extent of disproportionation, and ability to stabilize colloidal Cu^0 and regulate its size distribution can be achieved.[197] Binary mixtures of varied composition can also be used to create a solvent system capable of dissolving a larger array of monomers and their corresponding polymers.

4.2.5. Tolerance of Radical Inhibitors

Vinyl monomers are typically stabilized with 4-methoxyphenol (MEHQ) to prevent impurity-induced polymerization or autopolymerization. For example, commercial MA contains ∼10−100 ppm of MEHQ. Prior to the use of vinyl monomers in conventional radical polymerization and metal-catalyzed LRP such as ATRP and its variants, MEHQ and other inhibitors are typically removed by passing them through a basic Al_2O_3 chromatographic column, by washing with basic water, or through distillation.

SET-LRP is compatible with commercially available stabilized monomers. Most reports detailing the development of SET-LRP have used raw commercial monomers. The curious compatibility of SET-LRP with MEHQ stabilizer was investigated, by comparison of the kinetics of SET-LRP of uninhibited MA with the kinetics of SET-LRP of MA initiated with MBP or BPE in DMSO or methanol with varying levels of added MEHQ.[178] Regardless of MEHQ loading level, 1:0 initiator/MEHQ to 1:10 initiator/MEHQ, the polymerization proceeded to high conversion (>95%) with excellent predictability of molecular weight evolution and distribution (M_w/M_n ≈ 1.2). Only at the highest loading level, 1:10 initiator/MEHQ, was a small induction period detected, which could be attributable to trapped oxygen in the solid MEHQ. While the addition of MEHQ did retard the polymerization rate, even at the highest loading level (1:10 initiator/MEHQ) the rate decrease was not significant (∼10%). In this original study, MEHQ was added as a solid and may not in fact act as a homogeneous radical inhibitor.

Table 2. E_{HOMO} of Various Cu Catalysts Calculated Using HF/DFT Methods

E_{HOMO} (eV)	catalyst	method[a]
−7.00	Cu_2Te	HF/LACVP+*//B3LYP/LACVP*
−7.34	Cu_2Se	HF/6-31+G*//B3LYP/6-31+G*
−7.62	Cu(0)	HF/6-31+G*//B3LYP/6-31+G*
−7.67	Cu_2S	HF/6-31+G*//B3LYP/6-31+G*
−8.26	Cu_2O	HF/6-31+G*//B3LYP/6-31+G*
−8.84	CuI	HF/LACVP+*//B3LYP/LACVP*
−9.71	CuBr	HF/6-31+G*//B3LYP/6-31+G*
−10.24	CuCl	HF/6-31+G*//B3LYP/6-31+G*

[a] For Te or I containing molecules, LACVP* pseudopotential was implemented for heavy atoms in conjunction with the 6-31+G* basis set.

In a recent study, the SET-LRP of MA in various solvents and their binary mixtures with H_2O was investigated.[186] The kinetics of SET-LRP were investigated using both uninhibited monomer and monomer that contained ∼100 ppm of MEHQ inhibitor as supplied by Aldrich (Table 3). As with the study involving the addition of solid MEHQ to the polymerization, the homogeneous radical inhibitor in MA only slightly reduced the rate of polymerization.

The compatibility of SET-LRP with raw commercial monomers makes its use more economical. SET-LRP is of interest in the preparation of polymers with complex architecture. Most dendritic monomers are also stabilized with radical inhibitors.[198−206]

4.3. Catalyst Compatibility

Any Cu-containing electron donor that produces Cu(I)X in situ via SET activation should be capable of mediating a successful SET-LRP. The reactivity of a molecular or atomic species toward electron donation is related to its ionization potential (I_p). Low ionization potentials result in higher electron-donor activity. Ionization potential can be roughly correlated with E_{HOMO}.

Table 2 shows the results from crude calculations of various Cu sources. SET-LRP has been determined to be a surface-mediated reaction; the monomolecular or monatomic assumption of these calculations is probably too naïve and should incorporate the surface structure of the catalyst. However, the results are still rewarding. A relative order of electron-donating capability was established as Cu_2Te > Cu_2Se > Cu^0 > Cu_2S > Cu_2O > CuX (X = I, Br, Cl). Thus, Cu^0 and Cu_2Y (Y = Te, Se, S, O) are likely more efficient outer-sphere electron donors than CuX (X = I, Br, Cl) species, which are commonly implicated in ATRA and ATRP inner-sphere processes.

As expected, Cu^0 and Cu_2Y (Y = Te, Se, S, O) species have been successfully employed as catalysts for SET-LRP. Most studies employed Cu^0 in powder form. Recent results have confirmed that the catalytic activity of Cu^0 is dependent on the surface characteristics of the powder. Because of differences in surface area and structure of the Cu_2Y catalysts and the expectation that they produce Cu^0 in situ via disproportionation, direct comparison and establishment of experimental trends are complicated.

Early studies in the SET-mediated initiation of sulfonyl halides for LRP of Sty and BA indicated that nondispersed Cu catalysts, such as Cu coins, were also effective. Recently, this concept was expanded to the use of Cu wire as a simple catalyst with enhanced reaction performance.

4.3.1. Cu^0 Powder and Cu^0 Wire

Cu^0 powder has been used in the SET-LRP of MA, EA, BA, solketal acrylate, MMA, and VC initiated with chloro-, bromo-, and iodo-containing compounds. Cu^0 wire has been used in the SET-LRP of MA and MEA initiated with MBP and BPE and VC initiated with $CHBr_3$.[27,168] In the case of MA, Cu^0 wire provides PMA with greater predictability of molecular weight evolution and distribution and provides greater accuracy in the empirical prediction of k_p^{app} due to the "monodispersity" and greater uniformity of the catalyst surface. Further, the use of Cu^0 wire provides for a simpler experimental setup and easier recovery and recycling of catalyst and purification of the reaction mixture.[168]

4.3.2. Cu Salts

Cu_2Te/Me_6-TREN and Cu_2Se/Me_6-TREN have been utilized in the SET-LRP of MA initiated with chloroform in DMSO at 25 °C. Therein, k_p^{app} decreased according to Cu_2Te > Cu_2Se, while maintaining similar levels of living character. Cu_2Te/Me_6-TREN, Cu_2Se/Me_6-TREN, Cu_2O/Me_6-TREN, and Cu_2S/Me_6-TREN have also been used in the SET-LRP of MA initiated with bromoform in DMSO at 25 °C. Here k_p^{app} decreased according to Cu_2Te > Cu_2Se > Cu_2S > Cu_2O. Cu_2Te/Me_6-TREN, Cu_2Se/Me_6-TREN, Cu_2O/Me_6-TREN, and Cu_2S/Me_6-TREN have been utilized in the SET-LRP of MA initiated with iodoform in DMSO at 25 °C. In this case, k_p^{app} decreased according to Cu_2Te > Cu_2Se > Cu_2S > Cu_2O. Here too, differences in living character between catalysts were not remarkable. Cu_2Te/TREN, Cu_2Se/TREN, Cu_2O/TREN, and Cu_2S/TREN have been utilized in the SET-LRP of VC initiated with bromoform in DMSO at 25 °C. Here, k_p^{app} decreased according to Cu_2O > Cu_2Te > Cu_2Se > Cu_2S. While Cu_2O, Cu_2Te, and Cu_2Se catalysts produced polymers with narrow polydispersity, Cu_2S catalyzed polymerization produced polymers with broader polydispersity. In general, the reactivity of Cu_2Y salts where Y = Te, Se, S, or O was in correspondence with the crude electron donor capacity (E_{homo}) trend suggested above. The reason for the unusual acceleration of Cu_2O/TREN catalyzed SET-LRP of VC is not apparent. Cu_2O/bpy has also been used in the SET-LRP of MMA initiated with PDSC in ionic liquid $bmimPF_6$.[191] Cu^0 generated in situ from Cu^ICl/Me_6-TREN in DMF/H_2O or THF/H_2O solution has been used in the SET-LRP of 2-EHA, NIPAM, and PEGMEA.[187−190] Likewise, Cu^0 generated in situ from Cu^ICl/bpy in ionic liquid $bmimPF_6$ in the SET-LRP of MMA. In this polymerization, only "nascent" Cu^0 is present, and thus, the kinetics of the polymerization will be more sensitive to the size distribution and stabilization of this colloidal Cu^0.[207] It is necessary to consider the effect of solvent, ligand, and ligand concentration on the characteristics of the nascent Cu^0.

When Cu_2Y (Y = Te, Se, S, O) is used as the catalyst in SET-LRP, it is unclear what species is most responsible for activation. It is likely that Cu_2X activates initiator, thereby generating Cu^IX (X = Cl, Br, I) in situ. The Cu^IX will disproportionate into Cu^0 and $Cu^{II}X_2$. The nascent Cu^0 will then either react or agglomerate on the surface, creating a film of Cu^0 over the Cu_2Y. Thus, as the reaction progresses, activation on the surface may be a competition between dissimilar surface sites. We cannot also disregard the possibility of solvent/ligand-mediated disproportionation of Cu_2Y into $Cu^{II}X$ and Cu^0.
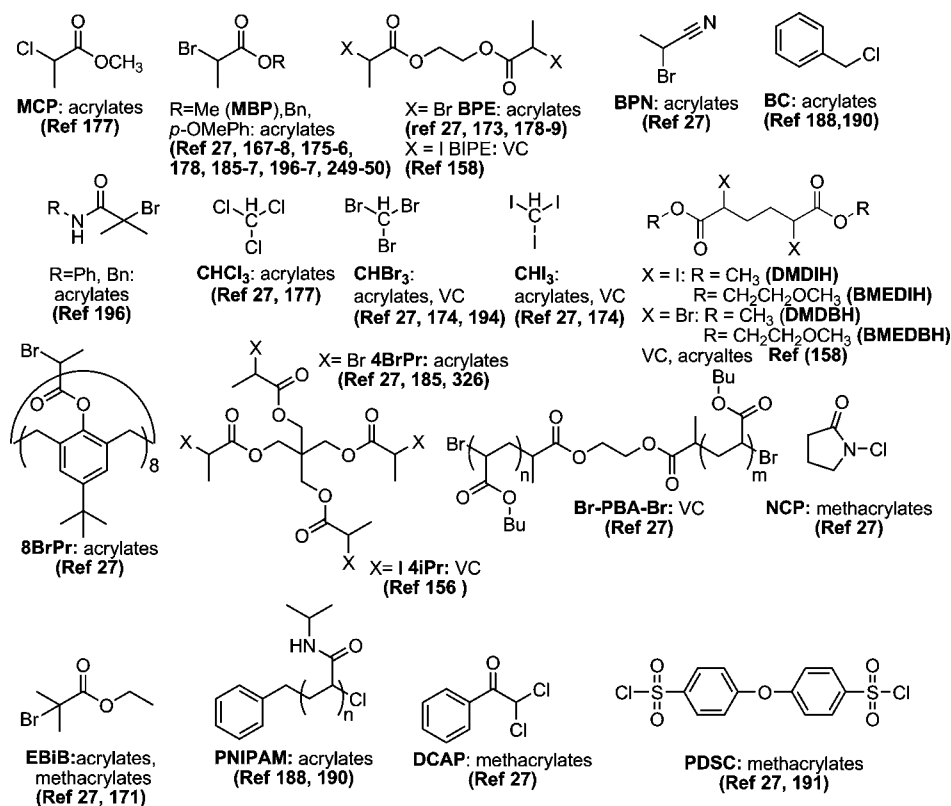
Figure 13. Initiators used in SET-LRP and their known compatible monomers.

4.4. Initiators

As with all metal-catalyzed LRP processes, the appropriate choice of initiator is critical. A variety of monofunctional initiators, bifunctional initiators, multifunctional initiators, and macroinitiators have been used in SET-LRP (Figure 13). Chloro-initiators are best suited for the polymerization of MMA and other methacrylates, while bromo- and iodo-initiators are best suited for acrylates and vinyl chloride. In SET-LRP there is little difference between the k_p^{app} for various halide initiators. While k_p^{app} is a complex rate constant, it nevertheless suggests a relatively small difference in k_{act}. This is in good agreement with an outer-sphere electron-transfer process where $k_{R-I}/k_{R-Br} \approx k_{R-Br}/k_{R-Cl} \approx 1-10$.[28] In ATRP, $k_{act}(R-Br)/k_{act}(R-Cl)$ is between 10^3 and 9×10^4.[208] This is in better agreement with an inner-sphere electron-transfer process where k_{R-Br}/k_{R-Cl} can be between 5×10^2 and 9×10^4.[29]

4.4.1. Haloforms

The haloforms $CHCl_3$,[27,177] $CHBr_3$,[27,174] and CHI_3[27,174] have been employed as initiators for the SET-LRP of MA in DMSO at 25 °C. $CHCl_3$ and $CHBr_3$ are monofunctional initiators for PMA. CHI_3 is monofunctional initiator for PMA at low conversion but transitions to a bifunctional initiator at high conversion. When $CHCl_3$ is used as an initiator, small levels of $CuCl_2$ are required to regulate the LRP. $CHBr_3$ has also been demonstrated as an effective initiator for the SET-LRP of VC in DMSO at 25 °C.[27,194]

4.4.2. α-Haloesters

The most typical initiator for the polymerization of monofunctional acrylates is MBP, which has also been used as an initiator in the CuCl/Me₆-TREN catalyzed SET-LRP of PEGMEA in DMF/H₂O.[187] Methyl 2-chloropropi-

onate (MCP) has also been used, though small levels of $Cu^{II}Cl_2$ were used to improve the LRP.[177] Ethyl 2-bromoisobutyrate (EBiB) has been used in the Cu⁰/bpy catalyzed LRP of MMA in DMSO[27] and the Cu⁰/PMDETA catalyzed SET-LRP of MMA in hexafluoroisopropanol (HFIP).[193] EBiB has also been used in the Cu⁰/Me₆-TREN catalyzed SET-LRP of MA in DMSO at 25 °C.[171] 2-Bromo-2-methylpropinoic acid benzyl ester and 2-bromo-2-methyl-propionic acid 4-methoxyphenol ester have also been utilized as an initiator in the Cu⁰/Me₆-TREN-catalyzed SET-LRP of MA in toluene/phenol mixtures.[196] BPE has been used as a bifunctional α-halo ester initiator for the preparation of telechelic PMA, PEA, and PBA. Pentaerythritol tetrakis(2-bromopropionate) (4BrPr) has been used as a multifunctional initiator to prepare 4-armed star PMA[27] and PMA-b-poly(solketal acrylate)[185] via Cu⁰ catalyzed SET-LRP. 5, 11,17,23,39,35,41,47-octa-tert-butyl-49,50,51,52,-53,54−55,56-octakis-(2-bromopropionyloxy) calyx[8]arene (Figure 13, 8BrPr) had been used as a multifunctional initiator to prepare 8-armed star PMA. α,ω-Di(bromo)-PBA has also been used as a macroinitiator for the SET-LRP of VC to form PVC-b-PBA-b-PVC.[162] A variety of α-bromo/iodo esters have been prepared and utilized for the SET-DTLRP of VC: 4IPr, DMDBH, DMDIH, BMEDBH, BMEDIH, and BIPE (Figure 13).[158] These compounds are also useful as bromo/iodo-initiators for SET-LRP.

4.4.3. Sulfonyl Halides

Sulfonyl halides have been demonstrated as effective initiators in the self-regulated Cu⁰ and Cu₂X catalyzed LRP of acrylates, methacrylates, and Sty. Unfortunately, sulfonyl halides are prone to side reactions in DMSO[209] and in the presence of aliphatic N-ligands.[210,211] While solvents other than DMSO can mediate disproportionation of Cu⁰X, multidentate aliphatic N-ligands are by far more effective than

bidentate aromatic N-ligands such as bpy. PDSC (Figure 13) was used as an initiator in conjunction with Cu^I/bpy catalyzed LRP of MMA in NMP. While bpy is not very effective at mediating disproportionation in DMSO, dramatic rate acceleration of the reaction was observed in NMP, suggesting SET activation. PDSC initiated SET-LRP catalyzed by Cu^I/bpy was also performed in ionic liquids, where disproportionation of Cu^I/bpy was feasible.[191] SET-LRP initiated with a broader range of sulfonyl halides should be possible in ionic liquids. Likewise, if aromatic N-ligands can be found that mediate disproportionation as effectively as multidentate aliphatic N-ligands, sulfonyl halides could be used as initiators in polar organic solvents.

4.4.4. Other Initiators

2-Bromopropionitrile (BPN) is an effective initiator for the SET-LRP of MA in DMSO at 25 °C. 2,2-Dichloroacetophenone (DCAP) is an effective initiator for the Cu^0/PMDETA catalyzed SET-LRP of MMA in DMSO at 25 °C. Additionally, PEG functionalized at one chain end with a 2,2-dichloroacetyl group was used as a macroinitiator for the synthesis of Y-shaped AB_2 PEG-b-$(PNIPAM)_2$ via Cu^ICl/Me_6-TREN catalyzed SET-LRP.[212] Benzyl chloride was used as an initiator in the CuCl/Me_6-TREN catalyzed block copolymerization of NIPAM and 2-EHA in DMF/H_2O.[188,189] As PNIPAM serves as a macroinitiator, α-haloamides are expected to be effective initiators in SET-LRP. It was subsequently determined that N-benzyl-2-bromo-2-methylpropionamide and N-phenyl-2-bromo-2-methylpropionamide are effective initiators for the Cu^0/Me_6-TREN catalyzed SET-LRP of MA in toluene/phenol mixtures.[196] N-chloro-2-pyrrolidinone (NCP) was used in the Cu^0/Me_6-TREN catalyzed LRP of MA in DMSO at 25 °C. 2-Cyanoprop-2-yl-1-dithionaphthalate (CPDN) has also been demonstrated as a compatible initiator for the Cu^0/PMDETA catalyzed SET-LRP of MMA.[192]

4.5. Solvents

4.5.1. DMSO

By far the most commonly used solvent thus far for SET-LRP is DMSO. DMSO enhances the polarity of the medium, thereby aiding electron transfer.[213,214] DMSO has been shown to be particularly adept at mediating electron transfer in $S_{RN}1$ reactions.[215] DMSO is also a coordinating solvent that stabilizes $Cu^{II}X_2$[213] and thereby shifts the K_{dis} further to the right. DMSO is also excellent at solubilizing a variety of monomers and polymers. While other solvents such as alcohols (vida supra) have similar properties, DMSO has the advantage of a particularly high freezing point (18 °C), which aids in the freeze–pump–thaw process, and therefore, it is the preferred solvent in academic research laboratories.

4.5.2. Alcohols

Alcohols including methanol, ethanol, 1-propanol, and $tert$-butanol have been shown to be effective solvents for the Cu^0-powder/Me_6-TREN catalyzed SET-LRP of MA initiated with BPE at 25 °C.[179] EtOH, MeOH, and methoxyethanol and their mixtures with water have been shown to be effective solvents for the Cu^0-wire/Me_6-TREN catalyzed SET-LRP of MA initiated with MBP at 25 °C.[186] Additionally, HFIP is a suitable solvent for the extremely rapid SET-LRP of MMA at very low temperature, providing dual

control of molecular weight distribution and the polymer tacticity.[193] Increasing the hydrophobic character of the alcohol decreases the k_p^{app} and also decreases the control of molecular weight distribution. Increasing hydrophobic character of the solvent decreases its polarity, diminishing the stabilization of charge separation, thereby reducing the rate of activation and also the extent and rate of disproportionation of Cu^I/N-ligand. The use of 95:5 mixtures of alcohol and water resulted in a 1.3–1.4-fold increase in the k_p^{app} while increasing the predictability of molecular weight evolution and distribution. Mixtures of water and polar organic solvents have been shown to decrease the stability of Cu^IX to disproportionation relative to the pure solvent (vida infra).[216–219] The enhancement of disproportionation offered by low levels of H_2O enhances the regeneration of active Cu^0 catalyst and $Cu^{II}X_2$ deactivator, increasing the rate and living character of the polymerization. Evidence of the chain-end functionality, narrow molecular weight distribution, and absence of side reactions are demonstrated through the MALDI-TOF chain-end analysis of PMA derived from Cu^0-Me_6-TREN-catalyzed SET-LRP in methanol/water (95/5 v/v) (Figure 9).

4.5.3. Ionic Liquids

The rapid Cu_2O/bpy, Cu^0/bpy, and Cu^ICl/bpy catalyzed LRP of MMA initiated with PDSC in ionic liquid 1-butyl-3-methylimidazolium hexafluorophosphate ($bmimPF_6$) at 70 °C was reported.[191] All polymerization in $bmimPF_6$ showed excellent predictability of molecular weight evolution and distribution ($M_w/M_n \approx 1.11$–1.26). Cu_2O and Cu^0 catalyzed SET-LRP in $bmimPF_6$ exhibited significant acceleration in comparison to the bulk polymerization, while CuCl/bpy catalyzed polymerization did not. In previous reports where rate acceleration was observed in metal-catalyzed LRP,[220–224] RAFT,[225,226] and NMP[227,228] in ionic liquids, a commensurate increase of the molecular weight distribution was observed. It was later determined that disproportionation of Cu^ICl/Me_6-TREN[27] and Cu^ICl/bpy was rapid and extensive in mixtures of $bmimPF_6$ and MMA. The rapid disproportionation of Cu^ICl allows for SET-LRP of MMA in $bmimPF_6$, wherein dramatic rate acceleration and narrow molecular weight distribution are not mutually exclusive.

4.5.4. Other Solvents and Binary Mixtures of Solvents

A variety of other solvents are known to mediate disproportionation of Cu^IBr in the presence of select N-ligands including dimethylformamide (DMF), dimethylacetamide (DMAC), H_2O, ethylene glycol, diethylene glycol, triethylene glycol, tetraethylene glycol, poly(ethylene glycol), 2-(2-ethoxyethoxy)ethanol, 1,2-dimethoxy ethane, ethylene carbonate, propylene carbonate, NMP, THF + 10% PhOH, toluene + phenols, glycerin, sugars, carbohydrates, and benzonitrile. These solvents are all therefore expected to be compatible with SET-LRP. In a recent report, the SET-LRP of MA initiated with 25 °C has been reported using acetone, DMAC, DMF, EC, methoxyethanol, NMP, PC, and a variety of previously reported solvents using uninhibited as well as MEHQ-inhibited monomer (Table 3).[186]

Interestingly, it was also shown that DMF/H_2O or THF/H_2O mixtures for the SET-LRP of hydrophilic monomers NIPAM, PEGMEA, and 2-EHA.[188–190] Additionally, toluene mixed with phenol additives for the SET-LRP of MA.[196] The latter case is extremely significant as the use of polar

Table 3. Comparison of SET-LRP of Inhibited vs Uninhibited MA Initiated with MBP in Various Solvents at 25 °C (Reprinted with Permission from Ref 186; Copyright 2009 John Wiley & Sons)

		uninhibited MA			inihibited MA (100 ppm MEHQ)		
no.	solvent	k_p^{app} (min^{-1})	M_w/M_n	I_{eff}	k_p^{app} (min^{-1})	M_w/M_n	I_{eff}
1	acetone	0.017	1.23	86	0.013	1.35	75
2	DMAC	0.020	1.39	92	0.022	1.20	79
3	DMF	0.034	1.21	91	0.030	1.18	95
4	DMSO	0.072	1.19	90	0.066	1.17	92
5	EC	0.053	1.23	89	0.056	1.19	81
6	EtOH	0.038	1.22	95	0.034	1.22	84
7	methoxyethanol	0.033	1.27	92	0.026	1.26	81
8	MeOH	0.036	1.14	83	0.033	1.14	83
9	NMP	0.021	1.35	97	0.018	1.78	83
10	PC	0.053	1.24	95	0.058	1.20	80

Table 4. SET-LRP of MA Initiated with MBP in Organic Solvents Containing Different Amounts of H$_2$O at 25 °C (Reprinted with Permission from Ref 186; Copyright 2009 John Wiley & Sons, Inc.)

no.	solvent	k_p^{1app} (min^{-1})	k_p^{2app} (min^{-1})	time (min)	conv (%)	M_n (GPC)	M_w/M_n	I_{eff}
1	acetone	0.017	0.004	230	83	18 605	1.23	86
2	acetone/5% H$_2$O	0.028	0.017	90	86	19 224	1.14	84
3	acetone/10% H$_2$O	0.053	0.027	45	85	18 585	1.15	85
4	DMAC	0.020	NA	100	86	17 672	1.39	92
5	DMAC/5% H$_2$O	0.047	0.018	75	86	18 066	1.24	93
6	DMAC/10% H$_2$O	0.068	0.019	60	87	19 396	1.19	87
7	DMF	0.034	NA	63	88	18 920	1.21	91
8	DMF/5% H$_2$O	0.046	NA	45	86	19 197	1.20	87
9	DMF/10% H$_2$O	0.071	NA	35	89	19 144	1.16	85
10	DMSO	0.071	NA	30	87	18 960	1.19	92
11	DMSO/5% H$_2$O	0.087	NA	27	88	19 372	1.14	86
12	DMSO/ 10% H$_2$O	0.102	NA	22	86	19 286	1.12	88
13	EtOH[a]	0.038	NA	50	84	17 553	1.22	95
14	EtOH/5% H$_2$O	0.046	NA	42	84	18 165	1.18	93
15	EtOH/10% H$_2$O	0.055	NA	42	89	19 393	1.22	89
16	EC	0.053	NA	45	90	20 328	1.23	89
17	NMP	0.021	NA	100	88	17 386	1.35	97
18	NMP/5% H$_2$O	0.034	NA	52	82	17 181	1.40	92
19	NMP/10% H$_2$O	0.052	NA	37	83	16 818	1.29	98
20	MeOH	0.036	NA	70	91	20 342	1.14	83
21	MeOH/5% H$_2$O	0.048	NA	55	91	19 751	1.16	84
22	MeOH/10% H$_2$O	0.054	NA	43	86	18 947	1.16	88
23	methoxyethanol	0.033	NA	75	88	19 453	1.27	92
24	methoxyethanol/5% H$_2$O	0.046	NA	50	89	18 133	1.23	97
25	methoxyethanol/10% H$_2$O	0.056	NA	42	87	18 797	1.23	90
26	PC	0.053	NA	45	89	18 534	1.24	95

[a] Polymer precipitates after indicated time.

additives allows for SET-LRP in hydrophobic media, which are otherwise unable to mediate requisite levels of disproportionation. Of the compounds investigated, phenol, *p*-methylphenol, and *o*-methylphenol provided a confluence of elevated k_p^{app}, higher conversion, and narrow molecular weight distribution. Polymerization using 2,5-dimethylphenol, 2,6-di-*tert*-butyl-4-methylphenol, *m*-methylphenol, and benzyl alcohol as additives resulted in diminished conversion. *p*-Nitrophenol resulted in no polymerization.[196]

Binary mixtures of organic solvents and water are generally effective for SET-LRP. SET-LRP of MA initiated with MBP in 5−10% H$_2$O mixtures with acetone, DMAC, DMF, DMSO, EC, ethanol methanol, methoxyethanol, NMP, and PC have been reported.[186] The addition of H$_2$O serves to increase the polarity of the medium and enhance the degree of disproportionation of Cu^{I}X, thereby enhancing the k_p^{app} and improving the predictability of molecular weight (Table 4 and Figure 22). Additionally, as previously demonstrated for the SET-LRP of NIPAM, PEGMEA, 2-EHA, and their block-copolymers, the binary mixtures of polar organic solvents and H$_2$O are extremely useful for the polymerization of hydrophilic monomers.

While the use of binary mixtures of organic solvents and water is a relatively common practice for the LRP of hydrophilic monomers, the use of binary mixtures of organic solvents to modulate reaction parameters such as rate and molecular weight predictability is not typically employed. While SET-LRP is tolerant to extrinsic factors such as material impurities and oxygen, causing only mild induction times, entrance into SET-LRP requires a proper balance of intrinsic reaction conditions. Extensive disproportionation of Cu^{I}X into Cu^0 and Cu^{II}X$_2$ mediated by appropriate ligand and solvent mixtures was originally thought to limit the range of compatible solvents for SET-LRP. However, it was found for the preparation of binary mixtures of organic solvents that each possesses unique monomer and polymer dissolution capacities, ability to mediate disproportionation, polarity, and ability to stabilize and regulate the size distribution of colloidal Cu^0, which allows for the cooperative and synergistic effects of SET-LRP in a broader spectrum of reaction media.[197] In this preliminary report, mixtures of acetone−DMSO, DMSO−MeOH, EC−DMAC, EC−DMF, EC−DMSO, and ethyl acetate−MeOH were reported as effective reaction media for the SET-LRP of MA (Table 5). The

Table 5. SET-LRP of MA Initiated with MBP in Binary Mixtures of Organic Solvents at 25 °C (Reprinted with Permission from Ref 197; Copyright 2009 John Wiely & Sons, Inc.)

solvent	k_p^{1app} (min^{-1})	k_p^{2app} (min^{-1})	time (min)	conv (%)	M_n (GPC)	M_w/M_n	I_{eff}
acetone	0.0166	0.0041	230	83.0	18 605	1.23	86
DMAC	0.0200	N/A	100	85.7	17 672	1.39	92
DMAC/10% EC	0.0281	0.0175	80	82.9	16 897	1.22	97
DMAC/30% EC	0.0450	0.0313	56	87.5	18 085	1.28	92
DMAC/50% EC	0.0655	0.0405	46	89.6	19 462	1.20	92
DMAC/70% EC	0.0713	0.0454	44	90.8	19 020	1.18	93
DMAC/80% EC	0.0702	N/A	38	86.5	17 785	1.20	94
DMAC/90% EC	0.0686	N/A	36	85.0	17 527	1.21	94
DMF	0.0338	N/A	63	88.0	18 920	1.21	85
DMF/10% EC	0.0410	0.0322	50	82.3	17 619	1.22	92
DMF/30% EC	0.0603	0.0302	50	88.8	18 385	1.21	93
DMF/50% EC	0.0686	0.0457	44	90.6	18 452	1.24	96
DMF/70% EC	0.0607	N/A	44	89.3	18 382	1.26	93
DMF/90% EC	0.0517	N/A	44	86.2	18 073	1.24	92
DMSO/5% acetone	0.0756	N/A	25	81.3	18 784	1.21	85
DMSO/10% acetone	0.0724	N/A	28	83.6	18 686	1.22	86
DMSO/20% acetone	0.0626	N/A	30	83.8	19 054	1.20	83
DMSO/40% acetone	0.0471	N/A	36	80.5	18 038	1.21	88
DMSO/60% acetone	0.0304	N/A	60	83.4	18 116	1.29	87
DMSO/80% acetone	0.0223	N/A	70	78.0	17 331	1.21	83
DMSO/10% EC	0.0767	N/A	30	86.0	17 911	1.21	93
DMSO/20% EC	0.0810	N/A	30	89.3	19 045	1.21	87
DMSO/30% EC	0.0763	N/A	32	84.4	17 836	1.24	91
DMSO/40% EC	0.0735	N/A	33	85.2	18 155	1.26	91
DMSO/60% EC	0.0682	N/A	35	83.4	19 026	1.22	86
DMSO/80% EC	0.0666	N/A	36	86.0	19 310	1.22	84
DMSO/10% MeOH	0.0710	N/A	30	81.2	18 700	1.24	88
DMSO/25% MeOH	0.0750	N/A	40	88.1	20 000	1.28	85
DMSO/50% MeOH	0.0820	N/A	40	90.0	19 200	1.20	85
DMSO/75% MeOH	0.0840	N/A	40	89.1	18 200	1.17	92
DMSO/90% MeOH	0.0680	N/A	40	87.1	19 000	1.16	85
DMSO	0.0719	NA	32	88.2	19 310	1.19	90
EC	0.0493	N/A	44	84.7	19 578	1.22	83
ethyl acetate	0.0140	N/A	120	72.6	15 700	1.31	92
Ethyl Acetate/10% MeOH	0.0310	NA	50	69.5	20 000	1.13	81
ethyl acetate/25% MeOH	0.0480	N/A	45	76.9	19 000	1.15	77
ethyl acetate/50% MeOH	0.0590	N/A	30	77.0	17 700	1.13	84
ethyl acetate/75% MeOH	0.0680	N/A	45	86.7	19 700	1.17	85
ethyl acetate/90% MeOH	0.0640	N/A	40	83.7	18 900	1.31	88
MeOH	0.0360	N/A	70	91.0	20 342	1.14	83

discovery of ethyl acetate−MeOH mixtures as effective solvents for SET-LRP is of particular interest for large-scale applications due to the low cost of ethyl acetate, as well as its distinct solubility profile as compared to the typical SET-LRP solvents. Effort will continue to exploit the approach of binary solvent mixtures for achieving better conditions for SET-LRP and expanding the monomer scope.

4.6. Mechanistic Aspects of SET-LRP

The synthetic utility of SET-LRP is readily apparent: simple and easily recoverable and recyclable Cu^0 catalysts, compatibility with a diverse array of solvents including "green" and aqueous solvents, colorless polymers without purification, extremely mild reaction conditions, and excellent predictability of molecular weight evolution and distribution. The desire to elucidate SET-LRP through the lens of ATRP is understandable as both utilize Cu catalysts and N-ligands. However, it is not uncommon in organic chemistry for subtle changes to reagent structure and experimental conditions to completely change the fundamental mechanism of a reaction. An example relevant to polymer synthesis is the change in the mechanism of aromatic polyetherification from S_NAr to $S_{RN}1'$ via minor changes in the structure of the reagents.[229−231] Here, by changing the active catalyst to Cu^0 and providing reaction conditions that favor electron transfer and dispro-portionation of in situ produced Cu^{I}X, a new mechanism of polymerization is achieved. As this mechanism does not
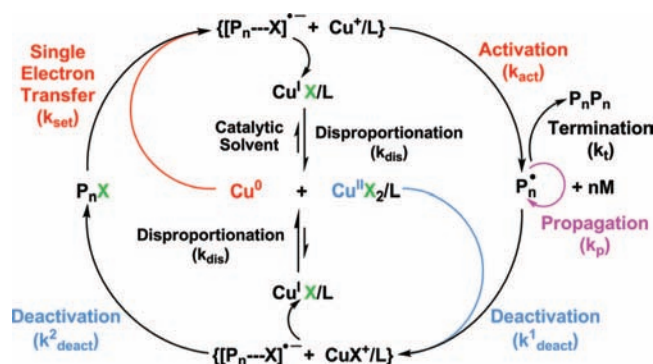

Figure 14. Mechanism of SET-LRP. Reprinted with permission from ref 166. Copyright 2007 John Wiley & Sons, Inc.

agree with the mechanism proposed for ATRP, this reaction that is mechanistically similar to SET-DTLRP was named SET-LRP.

SET-LRP can be divided into a few basic steps: (i) disproportionation of in situ produced or initially provided Cu^{I}X/N-ligand that provides self-regulated regeneration of Cu^0 and Cu^{II}X$_2$/N-ligand; (ii) activation of initiator and dormant polymer chains by heterogeneous SET from Cu^0 via a stepwise or concerted process; (iii) Homogenous deactivation of propagating macroradicals with Cu^{II}X$_2$/N-ligand; (iv) propagation of growing chains (Figure 14). Each of these steps, except propagation, will be discussed in detail,

Table 6. Values of K_{dis} Measured in the Absence of N-Ligands in Different Solvents at RT

solvent	K_{dis} (M^{-1})	log(K_{dis})
H$_2$O[122]	$0.054-5.8 \times 10^7$	$5.73-7.74$
DMF[217]	1.82×10^4	4.26
MeOH[122,232]	$4-6.3 \times 10^3$	$3.6-3.8$
EtOH[232]	3.6	0.56
DMSO[233,234]	$1.52-4.4$	$0.18-0.64$
acetone[235,236]	0.03	-1.5
CH$_3$CN[237]	6.3×10^{-21}	-20.2

providing both evidence for its mechanism and its relevance to preparative work.

4.6.1. Effects of Ligand and Solvent on the Disproportionation of Cu^I

SET has been utilized in other polymerizations to mediate activation of dormant chains. However, SET alone does not provide a LRP process. In order to achieve a successful SET-LRP process, Cu^{I}X produced in situ via activation and deactivation processes must rapidly disproportionate to Cu^0 and Cu^{II}X$_2$. Without disproportionation, there will be insufficient Cu^{II}X$_2$ to regulate the rapid SET-mediated polymerization. While Cu^{I}X will disproportionate spontaneously in water or predominately aqueous media, K_{dis} tapers off dramatically in other organic solvents or mixtures thereof (Table 6). It should also be noted that these values only reflect disproportionation at room temperature in the absence of coordinating ligand. Elevated temperature can provide for disproportionation even in solvents with otherwise low K_{dis}.

It is well-known that the presence of ligands can shift the equilibrium constant of disproportionation in either direction depending on its relative binding energy with Cu^I and Cu^{II} species.[238] However, it was serendipitously discovered that use of appropriate N-ligands can mediate rapid disproportion of Cu^{I}X in organic media.[27] The extent of disproportion of various N-ligands in different organic solvents has been tested by the preparation of various deoxygenated mixtures of N-ligand, solvent, and Cu^{I}X. Rapid disproportion is evident in certain cases through the rapid appearance of nascent Cu^0, which depending on the solvent will be stabilized as a colloid or agglomerate and precipitate,[207] and the apparent green or blue color of the reaction mixture is due to Cu^{II}X$_2$. A rough quantitative measure of disproportionation can be obtained through UV−vis analysis of a solution Cu^{I}X, N-ligand, and solvent and comparison with corresponding solutions of Cu^{II}X$_2$, N-ligand, and solvent. It should be noted that, while values of K_{dis} can be computed via UV−vis absorbances, they may not accurately reflect reaction conditions as both monomer and polymer can affect the aggregation kinetics and thermodynamics of nascent Cu^0, local heating via propagation can drive disproportionation, the difference between Cu^{I}X concentrations in the UV−vis experiments, and the concentrations derived in situ during polymerization, and a true equilibrium state may not be achieved due to competitive reactions with Cu^0 and Cu^{II}X$_2$. Additionally, in solvents that stabilize colloidal Cu^0, such as DMSO, the disproportionation through such methods will be underestimated due to the inability to precisely compensate for the contribution of colloidal Cu^0 absorption and scattering to the UV−vis spectrum.

While UV−vis measurements may not give a perfect picture of disproportionation in the polymerization flask, it does provide important general insight into ligand and
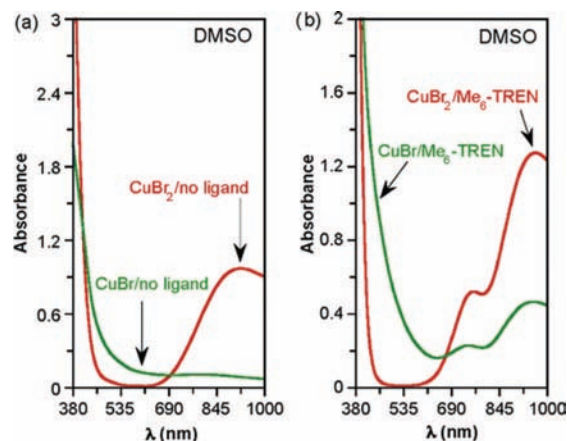

Figure 15. UV−vis analysis of disproportionation of CuBr in DMSO (a) with no ligand and (b) with Me$_6$-TREN. Reprinted with permission from ref 27. Copyright 2006 American Chemical Society.

solvent choice. In the absence of ligand, Cu^{I}X does not disproportionate in DMSO (Figure 15a).[27] Me$_6$-TREN (Figure 15b), TREN, N,N,N',N',N-pentamethyldiethylenetriamine (PMDETA), 1,1,4,7,10,10-hexamethyltriethylenetetraamine (HMTETA), and PEI have been shown through UV−vis studies to mediate the rapid disproportionation of CuBr in DMSO.[27] Me$_6$-TREN has been shown via UV−vis studies to mediate the disproportionation of CuBr in DMSO, DMF, diemethylacetamide (DMAC), H$_2$O, methanol, ethylene glycol, diethyleneglycol, tetraethylene glycol, 2-(2-ethoxyethoxy)ethanol, NMP, ethylene carbonate, propylene carbonate, glycerine, carbohydrates, 2-hydroxyethyl methacrylate, benzonitrile, N,N-dimethylacrylamide, and, to a lesser extent, poly(ethylene glycol) (M_n = 400). It is important to note that 2-hydroxyethyl methacrylate and N,N-dimethylacrylamide are monomers that disproportionate Cu^{I}X, providing the possibility for SET-LRP in bulk. DMF/H$_2$O and alcohol/H$_2$O mixtures exhibit enhanced Me$_6$-TREN disproportionation relative to the pure organic solvent. Me$_6$-TREN does not mediate the rapid disproportionation of CuBr in MeCN, THF, or toluene. However, in the presence of polar and potentially coordinating phenol additives, disproportion can be mediated in THF and toluene. Me$_6$-TREN and bpy mediate disproportionation of CuCl in ionic liquid bmimPF$_6$. Bpy does not mediate disproportionation of Cu^{I}X to a large extent in DMSO at room temperature, but it is more effective at elevated temperature. N-n-propyl-2-pyridylmethanimine (Pr-PMI/Haddleton's ligand),[239] which strongly binds Cu^{I}X, does not appear to mediate disproportionation at room temperature. However, at elevated temperature, Pr-PMI has also been shown to mediate disproportion of Cu^{I}X.[240] While every possible permutation of catalyst and ligand has not been studied via UV−vis analysis, it is apparent that Me$_6$-TREN, TREN, PMDETA, and PEI make the best ligands, and that DMSO, alcohols, ionic liquids, alkyl carbonates, DMF, and water are some of the best solvents for SET-LRP.

Historically, the disproportionation of Cu^{I}X into Cu^0 and Cu^{II}X$_2$ has been determined via electrochemical experiments (Table 6).[207] In these experiments, the equilibrium for disproportionation was described by eq 1 and did not account for the presence of N-ligand. Matyjaszewski made an effort to account for the role of ligand in disproportionation by using a corrected value for the disproportionation constant in the presence of stabilizing ligand.[130] However, in this case,
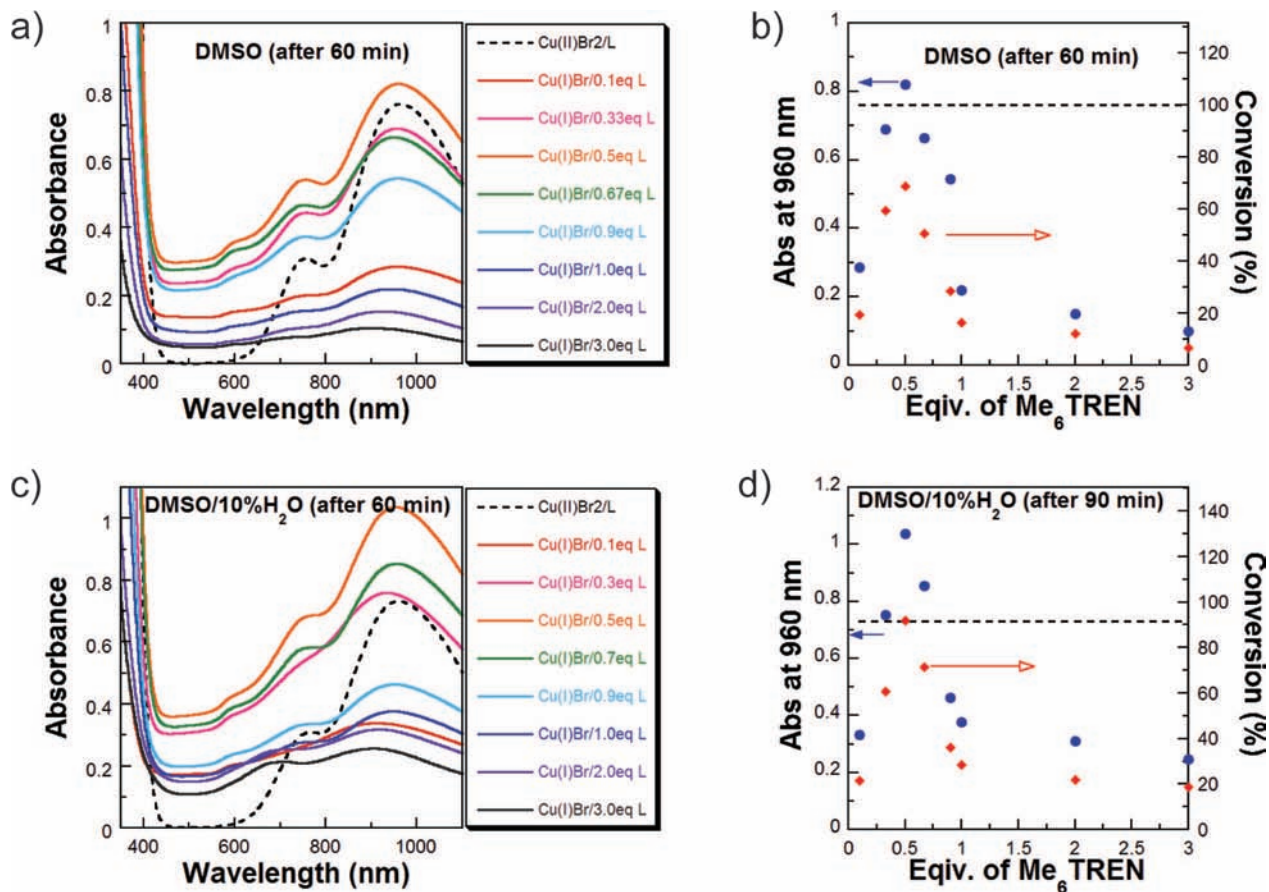
Figure 16. UV−vis spectra of the solution of Cu^IBr ($[Cu^IBr] = 0.00333$ M) in the presence of varying amounts of Me_6-TREN relative to Cu^IBr in DMSO (a) or 10% H_2O in DMSO (c) as solvent and the absorbance at the 960 nm maximum (blue dots) and the corresponding conversion of Cu^IBr into Cu^0 and Cu^{II} (red diamonds) in DMSO (b) or 10% H_2O in DMSO (d) as solvent. The dashed line represents either the UV−vis spectrum of $Cu^{II}Br_2$ at the concentration ($[Cu^{II}Br_2] = 0.00165$ M) expected if 100% disproportionation occurs or the absorbance intensity at the concentration of $Cu^{II}Br_2$ ($[Cu^{II}Br_2] = 0.00165$ M) expected from 100% disproportionation. Reprinted with permission from ref 207. Copyright 2009 John Wiley & Sons, Inc.

the concentration transfer of ligand should be incorporated into the equilibrium expression of disproportionation according to eqs 3 and 4.[207]

$$Cu^IX/L + Cu^IX/L \underset{}{\overset{K^*_{disp}}{\rightleftharpoons}} Cu^0 + Cu^{II}X_2/L + L \qquad (3)$$
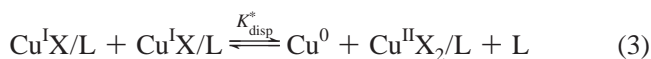
$$K^*_{disp} = [Cu^{II}X_2/L][L]/[Cu^IX/L]^2 \qquad (4)$$

Inspection of eqs 3 and 4 would suggest that, if the ligand strongly stabilizes Cu^{II} species versus Cu^I species, maximum disproportionation should occur when only 1/2 the amount of ligand is present relative to the initial amount of Cu^IX. Excess ligand would drive the reaction in the reverse direction, while less ligand would provide insufficient stabilization of the resultant $Cu^{II}X_2$. In the case of DMSO, disproportionation is indeed dependent on the concentration of ligand, and maximum disproportionation is indeed observed at 0.5 equiv of Me_6-TREN relative to Cu^IBr (Figure 16a,b).[207] The experimental extent of disproportionation of Cu^IBr in DMSO with varying concentrations of ligand was accurately modeled by numerical solutions to the equilibrium expression and a model of the disproportionation process via a series of differential equations. Visual inspection and DLS experiments demonstrated that, in DMSO, colloidal Cu^0 is stabilized and does not settle with time. The suspension of colloidal Cu^0 interferes with UV−vis experiments, causing a shift in the UV−vis baseline due to the absorption and

scattering of Cu^0 particles. While this shift is not uniform across the range of wavelengths, the exact contribution of Cu^0 colloids to the UV−vis spectra is not known; therefore, $Cu(II)Br_2/N$-ligand absorbance in the disproportionation experiments is conservatively underestimated by subtracting the absorbance at ~500 nm from the observed absorbance at ~960 nm. Even with this underestimation, the extent disproportionation is at least 1 order of magnitude greater than suggested by electrochemical experiments when $[Me_6$-$TREN]_o/[Cu^IBr]_o = 1$, and roughly 3 orders of magnitude greater when $[Me_6$-$TREN]_o/[Cu^IBr]_o = 0.5$. With the addition of as little as 10% H_2O to DMSO, the extent of disproportionation when $[Me_6$-$TREN]_o/[Cu^IBr]_o = 0.5$ is roughly 4 orders of magnitude greater than what is indicated by electrochemical experiments (Figure 16c,d). A maximum at $[Me_6$-$TREN]_o/[Cu^IBr]_o = 0.5$ is observed in many other solvents including acetone and DMF. In other solvents such as MeOH and EtOH, the location of the maximum is shifted somewhat, perhaps due to specific H-bonding with the ligand or specific solvent interaction with cuprous or cupric species. While in some cases the trends of disproportionation match those observed in electrochemical experiments, in many cases they do not, and in all cases the magnitudes of disproportionation differ dramatically. It is evident that electrochemical experiments do not accurately predict the disproportionation in the presence of ligand, and electrochemical data in general may not be applicable to the conditions of SET-LRP.
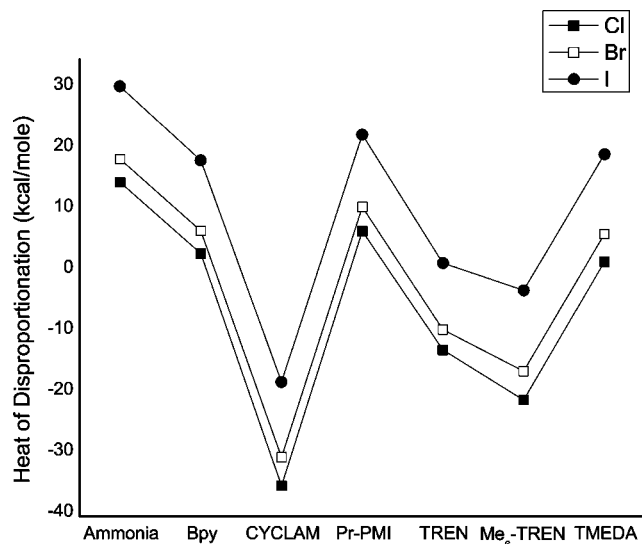
Figure 17. Preferential stabilization of Cu(II)X$_2$ by SET-LRP ligands. Reprinted with permission from ref 242. Copyright 2007 John Wiley & Sons, Inc.

Figure 18. Comparison of Cu^I/N-ligand and Cu^{II}Br/N-ligand structures for N-ligand = Me$_6$TREN and bpy. Adapted with permission from ref 242. Copyright 2007 John Wiley & Sons, Inc.

In addition to varying the extent of disproportionation, the concentration of ligand and the solvent composition have a noticeable effect on the size distribution of Cu^0 produced via disproportionation.[207] UV−vis and DLS experiments demonstrated that solvents such as acetone, DMAC, DMF, DMSO, NMP, and their mixtures with water stabilize small colloidal Cu^0 particles, while in ethanol, ethylene carbonate, methanol, propylene carbonate, and water result in larger agglomerated Cu^0 that precipitates. The ligand loading level also modulates the size distribution of the particles. In DMSO when [Me$_6$-TREN]$_o$/[Cu^{I}Br]$_o$ = 1.0 or 0.1 when the extent of disproportionation is lower, the size distribution of Cu(0) particles is bimodal. When [Me$_6$-TREN]$_o$/[Cu^{I}Br]$_o$ = 0.5, the size distribution is unimodal. While the exact effect of ligand concentration on particle size distribution varies from solvent to solvent and is not straightforward to predict, it is necessary to keep its role in mind, especially in Cu^{I}X/N-ligand mediated SET-LRP where the only Cu^0 in the system is the nascent Cu^0 prepared via disproportionation.

In a strongly polar or protic solvent, such as those known to mediate SET-LRP, cuprous ions and halide ions are expected to be highly solvated. In a polar environment such as DMSO, dissociation of Cu^{I}X and Cu^{II}X$_2$ salts are expected.[213,241] This dissociation is aided by the presence of strongly chelating ligands such as multidentate N-ligands, providing [Cu^I]$^+$/L and [Cu^{II}X]$^+$/L complexes. The structure of the N-ligand dictates the accessible geometries of the resulting complexes. A computational study comparing the energies of these complexes has shown that known SET-LRP ligands such as Me$_6$-TREN and TREN preferentially stabilize [Cu^{II}X]$^+$/L versus [Cu^I]$^+$/L, much more so than ATRP ligands such as bpy and Pr-PMI[242] (Figure 17). Preferential stabilization of [Cu^{II}X$^+$]/L, the halide dissociated form of Cu^{II}X$_2$/L, results in a more exergonic Cu^I → Cu^{II} half reaction and larger values for K_{dis}. A key feature of multidentate ligands such as the SET-LRP ligands Me$_6$-TREN and TREN is that they cannot adopt the preferred tetrahedral or distorted tetrahedral geometry for [Cu^I]$^+$/L that is accessible to bidentate ligands like bpy and Pr-PMI. Likewise, SET-LRP ligands Me$_6$-TREN and TREN also provide access to a relatively stable trigonal bipyramidal geometry for the [Cu^{II}X]$^+$/L complexes (Figure 18).

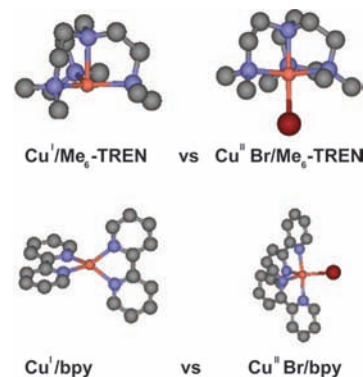The results obtained by UV−vis and computational studies suggest that multidentate and macrocyclic aliphatic N-ligands are particularly apt at mediating disproportionation relative to aromatic or bidentate ligands. These results agree with similar results for the activity of ligands in ATRP, where it was suggested that enhanced stability of the Cu^{II}X$_2$ species shifts the K_{ATRP} equilibrium in favor of activation.[243] If the solvent for the polymerization is not effective for mediating disproportionation (e.g., hydrophobic solvents or MeCN) and the source of Cu is Cu^{I}X, this is true and explains high k_p^{app} but somewhat diminished control under these conditions. However, when a solvent with relatively high K_{dis} is employed, especially in conjunction with a multidentate or macrocyclic N-ligand, disproportionation of Cu^{I}X/N-ligand is expected. Thus, the role of disproportion in waterborne ATRP[244−248] and the potential for an SET-LRP mechanism cannot be ignored, specifically now that it has been shown that even the addition of small levels of water can increase the extent of disproportionation by many orders of magnitude.[207]

Disproportionation is a fundamental step in SET-LRP. Without the regulated production of Cu^0 and Cu^{II}X$_2$ via disproportionation, a rapid LRP process cannot be achieved.[175,176] Cu^0/Me$_6$-TREN catalyzed SET-LRP of MA in DMSO, a solvent that mediates the rapid disproportionation of Cu^{I}X/Me$_6$-TREN, provides perfect first-order kinetics and polymers with perfect retention of chain-end functionality. Cu^0/Me$_6$-TREN catalyzed radical polymerization of MA in MeCN or toluene, solvents that do not mediate the rapid disproportionation of Cu^{I}X/Me$_6$-TREN, do not provide first-order kinetics, and the chain-end functionality of the PMA decreases linearly with conversion.[175,176] Kinetic studies of Cu^0/Me$_6$-TREN catalyzed radical polymerization in mixtures of DMSO and MeCN demonstrate that, as the solvent gradient is increased to favor a disproportionating solvent such as DMSO, a nonfirst-order (i.e., nonliving) process with poor retention of chain-end functionality is gradually transformed into a SET-LRP process with perfect retention of chain-end functionality and excellent control of the molecular weight evolution and distribution (Figure 19). Simple comparison of Cu^0/Me$_6$-TREN catalyzed SET-LRP in DMSO with Cu^0/Me$_6$-TREN catalyzed radical polymerization of MA in MeCN clearly delineates the differences in kinetics and polymer chain-end functionality (Figure 20). In spite of the poor retention of chain-end functionality in the Cu^0/Me$_6$-TREN catalyzed radical polymerization of MA in MeCN at 25 °C, polydispersities are not significantly
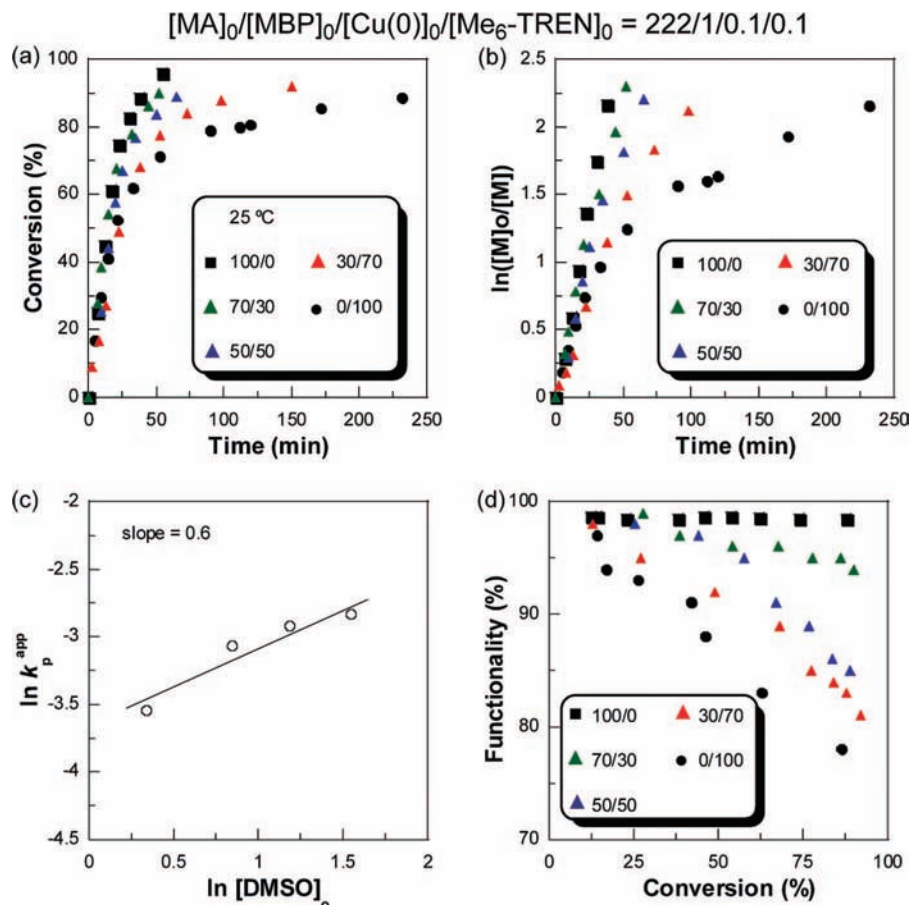
Figure 19. Kinetic experiments of Cu^0/Me_6-TREN catalyzed radical polymerization of MA in DMSO/MeCN mixtures at 25 °C. Kinetic plots (a, b), determination of external rate order of DMSO (c), and chain end-functionality vs conversion (d) in various DMSO/MeCN mixtures. Reprinted with permission from ref 176. Copyright 2008 American Chemical Society.
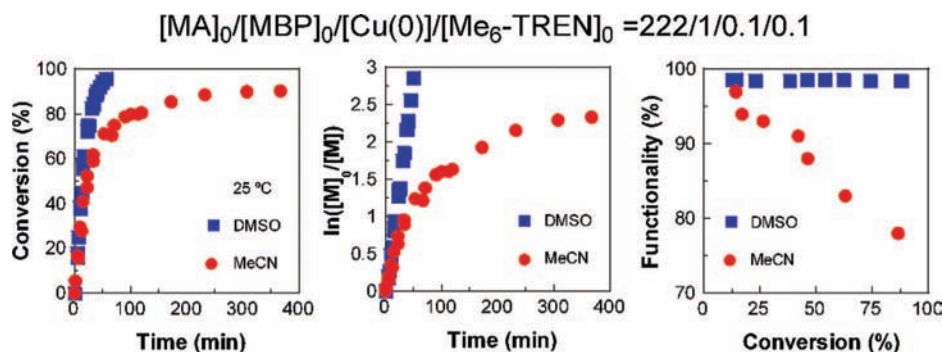

Figure 20. Comparison of SET-LRP in DMSO and Cu-catalyzed radical polymerization in MeCN. Reprinted with permission from ref 176. Copyright 2008 American Chemical Society.

elevated. The relative narrowness of molecular weight distribution present in nondisproportionating solvents can be attributed to continuous bimolecular termination throughout the reaction that produces excess $Cu^{II}X_2/Me_6$-TREN deactivator, though at the expense of $\sim 20\%$ chain-end functionality. These results are supported by kinetic modeling studies.[249] This PRE-type mechanism of control in nondisproportionating solvents is reinforced by a green reaction mixture as compared to the perfectly colorless reaction mixtures in SET-LRP.

In addition to the appropriate choice of solvent and ligand, it is also necessary to choose an appropriate initial concentration of ligand.[250] When too little ligand is added, the k_p^{app} is slow due to diminished surface activation consistent with a Langmuir−Hinshelwood mechanism (vida infra).[251] Additionally, in the case of low initial ligand concentration,

nonfirst-order kinetics are observed with poor predictability of molecular weight and broader molecular weight distribution. It appears that, when too little ligand is employed and, thus, the extent of disproportionation is low, resulting in insufficient $Cu^{II}X_2$ deactivator, bimolecular termination is prevalent, resulting in a bimodal distribution of the polymer molecular weight. Increasing the level of ligand results in an initially rapid increase in the rate of polymerization and degree of control. Eventually, the slope of this decreases to form a second linear domain and achieves a maximum. Above the maximum, increase in ligand loading level results in decreased rate. It has previously been shown that the ideal loading level of ligand to achieve the highest extent of disproportionation is generally 1/2 the molar equivalents of the amount of Cu^IX in the reaction mixture. The ligand-dependent maximum rate may correspond to this point of
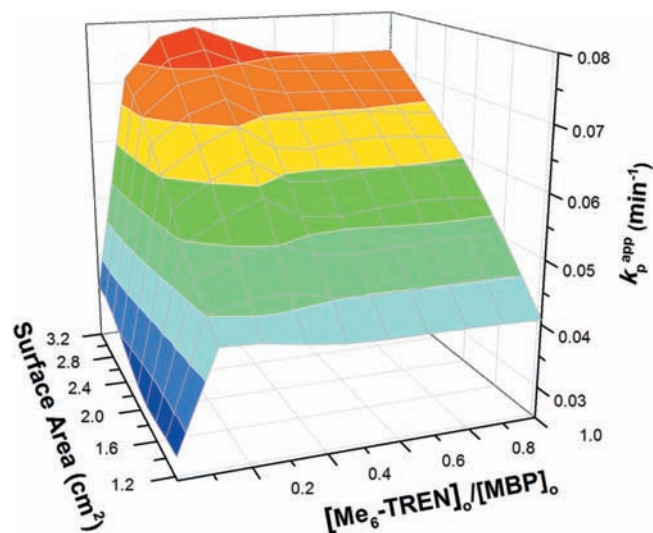
Figure 21. 3D plot of the dual effect of Cu^0 surface area (y-axis) and $[Me_6\text{-TREN}]_o/[MBP]_o$ (x-axis) on the k_p^{app} (z-axis). Reprinted with permission from ref 250. Copyright 2009 John Wiley & Sons, Inc.

maximum disproportionation or may be due to an optimum level of ligand for the surface-mediated activation process (vida infra). In any case, the position of the transition from rapid increase in rate and control (i.e., sufficient levels of disproportionation, but not necessarily maximum levels) to a region of slower increase, as well as the eventual maximum, varies according to the surface area of wire used and must be calibrated accordingly (Figure 21).

While solvents like THF and toluene do not mediate disproportion of Cu^IX on their own, it was observed that THF + 10% PhOH does mediate the rapid disproportionation of $Cu^IBr/Me_6\text{-TREN}$[27] and that SET-LRP tolerates the presence of phenol additives that are known to be radical inhibitors.[178] It was later observed by Haddleton that disproportionation in toluene could be mediated via the addition of a variety of phenol additives.[196] Using 20 mol % phenol, p-methylphenol, or o-methylphenol, excellent Cu^0/Me_6-TREN catalyzed SET-LRP of MA could be mediated in toluene. Other phenols and benzyl alcohols were somewhat less successful either due to enhanced aliphatic content, specific solvation interactions, or in one case competitive electron transfer to an electron-deficient phenol.

Recently, it was shown that addition of H_2O to organic solvents provides a linear increase in the k_p^{app} and generally improved control of molecular weight evolution and distribution (Table 4 and Figure 22).[186] The addition of water was particularly effective for solvents that did not mediate sufficient levels of disproportionation on their own, such as acetone. Narain has also reported the positive effect of H_2O on the ATRP of NIPAM in water-miscible organic solvents.[252] In some of these solvent mixtures, the authors suggested that Cu^I precipitated during the polymerization. Under these conditions, it is possible that Cu^I disproportionates and that the authors in fact observed the precipitated of agglomerated Cu^0. It was also shown that the addition of disproportionating organic solvents to less or nondisproportionating solvents to form binary organic mixtures also allowed for the achievement of suitable levels of control, for example, the addition of DMSO to EC or MeOH to ethyl acetate.[197] It is now evident that the kinetics and control of SET-LRP are cooperatively and synergistically controlled by a combination of factors including the extent of dispro-

portionation mediated by ligand and solvent and their ability to stabilize colloidal Cu^0 and control their size distribution.

4.6.2. Surface-Mediated Activation

The absorption and dissociation of gaseous organic halides on single crystal Cu surfaces is a well-known reaction.[253−256] At low temperatures, ~140 K, this process might occur via an atom-abstraction process of surface-absorbed alkyl halides.[253] At elevated temperatures, a thermally induced electron-transfer process becomes more feasible.[254] Rate enhancement of dissociation observed with branched alkyl halides[255] and alkyl halides bearing electron-withdrawing groups[256] support an electron-transfer model (vida infra). Here, the greater electron affinity E_a of the organic halide is responsible for mediating a more facile electron-transfer process. Degradation of electron-deficient organic halides via an expected electron-transfer mechanism has also been observed in organic solvents.[257−261] Here, Cu^0 surfaces catalyzed the C−X dissociation and subsequent radical recombination of benzyl halides, carbon tetrachloride. Langmuir−Hinshelwood[251] kinetics of the surface-mediated process were confirmed with the expected dependence on halide and solvent concentrations[257,259,260] of the process also confirmed. Dipolar aprotic solvents provided significant rate enhancements of the reaction, with a maximum rate being observed for DMSO.[260] A strong rate dependence on catalyst surface area was also observed.[261]

In studies of self-regulated Cu^0/bpy and Cu_2O/bpy catalyzed LRP initiated with sulfonyl chlorides, it was recognized that the surface composition and surface area played an important role in reaction kinetics. Another group suggested that the dependence of SET-LRP kinetics on the quality and type of Cu^0 source was evidence for Cu^IX mediated activation process, though a specific reason for this was not stated.[172]

Detailed studies on the relationship between Cu^0 catalyst surface area have been performed, providing strong evidence for a surface-mediated process. Cu^0/Me_6-TREN catalyzed SET-LRP of MA in DMSO at 25 °C was performed using various Cu^0 particle sizes: 425 μm, 75 μm, 45 μm, 3 μm, 100 nm, and 50 nm average diameter while maintaining equivalent $[Cu^0]_0$ (Table 7 and Figure 23).[167] All Cu^0 particle sizes provide polymerizations with first-order kinetics with good agreement between theoretical and observed molecular weights. The rate of the polymerization increased monotonically with decreasing particle diameter. Decreasing particle diameter results in an increased surface area (SA) to volume (V) ratio (SA/V), according to the equation SA/$V = 6/d$. Therefore, decreasing the particle diameter while maintaining the same $[Cu^0]_0$ results in an increased total surface of Cu^0.

The k_p^{app} was found to vary linearly with both $(SA/V)^{1/2}$ or $(SA)^{1/2}$ (Figure 24), in accord with the roughly 1/2-order external order of reaction previously calculated for Cu^0 in SET-LRP.[27] The same relationship between k_p^{app} and $(SA)^{1/2}$ was observed for the Cu^0/Me_6-TREN mediated radical polymerization of MA in MeCN at 25 °C. However, in this case, the kinetics were not first order in MA, indicating a nonliving process. The direct relationship between total surface area and k_p^{app} in both processes suggests a surface-mediated OSET process of activation regardless of solvent, as long as it is a solvent apt for mediating electron transfer. However, only in DMSO is disproportionation sufficient to regulate production of $Cu^{II}Br_2/Me_6$-TREN deactivator for an LRP process. In the Langmuir−Hinshelwood mechanism
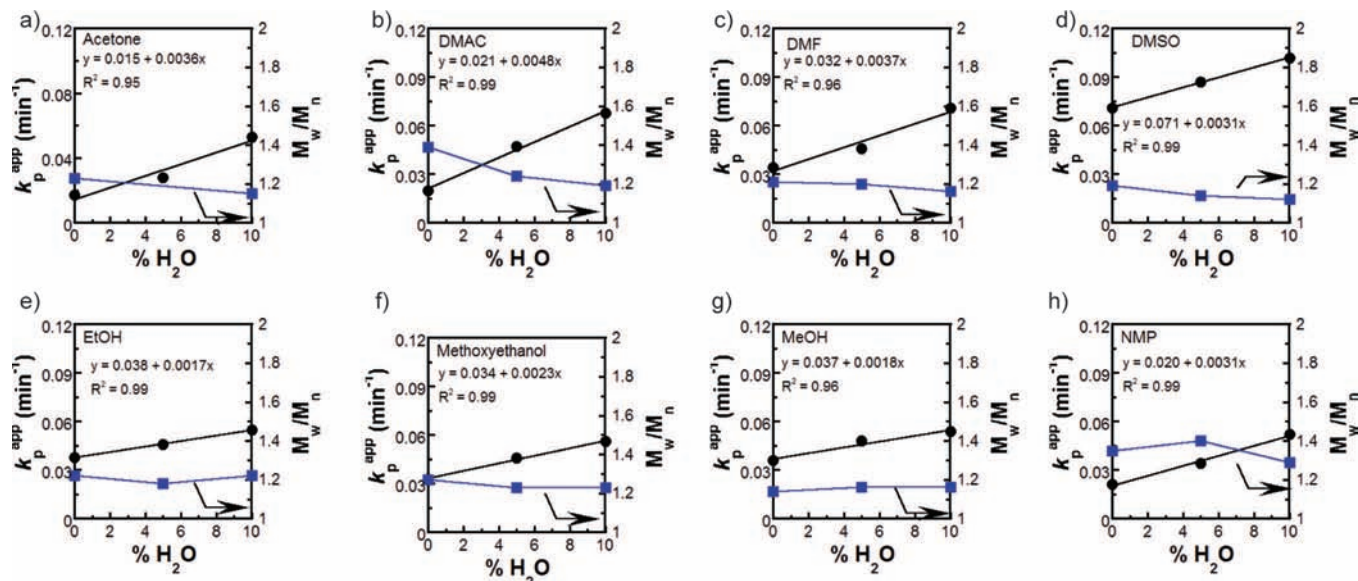
Figure 22. Effect of increasing % H_2O on the k_p^{app} and M_w/M_n in the SET-LRP of MA in (a) acetone, (b) DMAC, (c) DMF, (d) DMSO, (e) EtOH, (f) methoxyethanol, (g) MeOH, and (h) NMP. Reaction conditions: MA = 1.0 mL, solvent 0.5 mL, $[MA]_o$ = 7.4 mol/L, $[MA]_o/[MBP]_o/[Me_6\text{-}TREN]_o$ = 222/1/0.1, Cu^0 = 12.5 cm of 20 gauge wire. Reprinted with permission from ref 186. Copyright 2009 John Wiley & Sons, Inc.

$[MA]_0/[MBP]_0/[Cu(0)]_0/[Me_6TREN]_0 = 222/1/0.1/0.1$

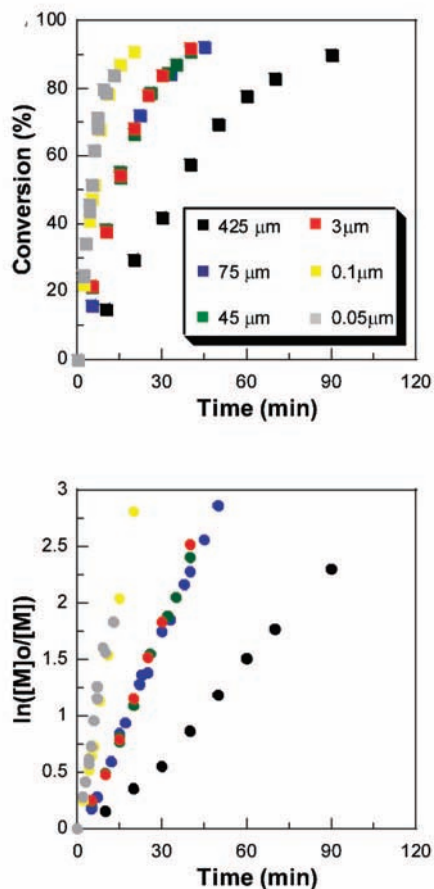**Figure 23.** Effect of Cu^0 particle size on the kinetics of Cu^0/Me$_6$-TREN catalyzed SET-LRP of MA in DMSO at 25 °C. Reprinted with permission from ref 167. Copyright 2008 American Chemical Society.

Table 7. Dependence of k_p^{app} on $SA^{1/2}$ for the Cu^0 Powder/Me$_6$-TREN-Catalyzed SET-LRP of MA in DMSO at 25 °C

particle diameter (μm)	$SA^{1/2}(cm^2)^{1/2}$	$k_p^{app}(min^{-1})$
425	0.071	0.028
75	0.169	0.059
45	0.218	0.060
3	0.845	0.063
0.1	4.63	0.142
0.05	6.54	0.162

a mechanism is consistent with surface-area dependent kinetics of SET-LRP and the ligand-concentration dependence (vida supra). A related mechanism, where only absorption of the ligand on the surface is required and activation of the dormant chains occurs via proximity but not binding to the surface, is also consistent with these observations.

The mechanism proposed in the first report on SET-LRP suggested that nascent or "atomic" Cu^0 formed via disproportionation of Cu^IX is responsible for the enhanced k_p^{app} in SET-LRP. To assess the role of "nascent" or "atomic" Cu^0 in SET-LRP, a simple experiment was devised (Figure 25).[167] A Schlenk tube containing Cu^0 catalyst (425 μm, powder),

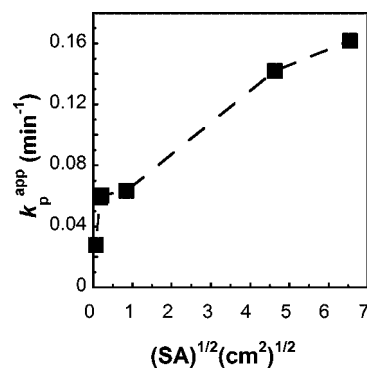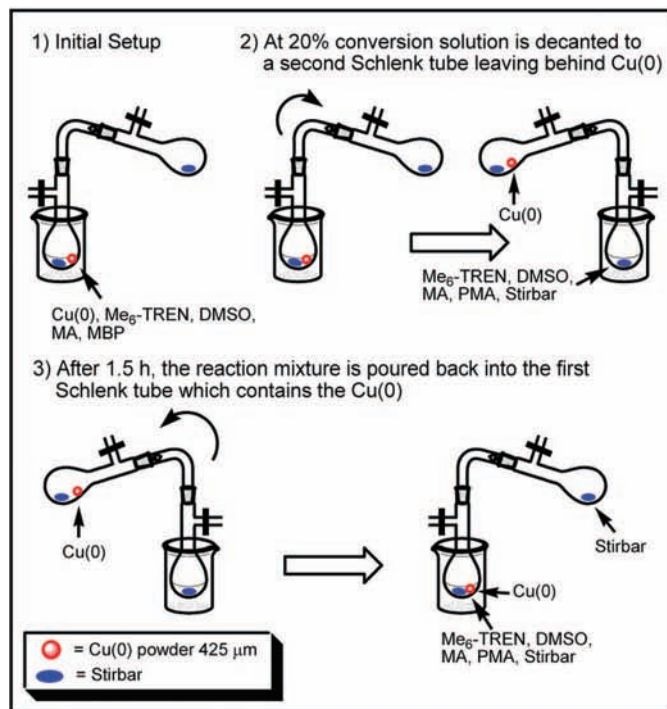**Figure 24.** Dependence of k_p^{app} vs $(SA)^{1/2}$ for the Cu^0/Me$_6$-TREN catalyzed SET-LRP of MA in DMSO at 25 °C. Reprinted with permission from ref 168. Copyright 2009 American Chemical Society.

proposed for oxidative dissolution of alkyl halides by Cu^0, activation requires coabsorption of organic halide and ligand/solvent on the Cu^0 surface, prior to the activation step. Such
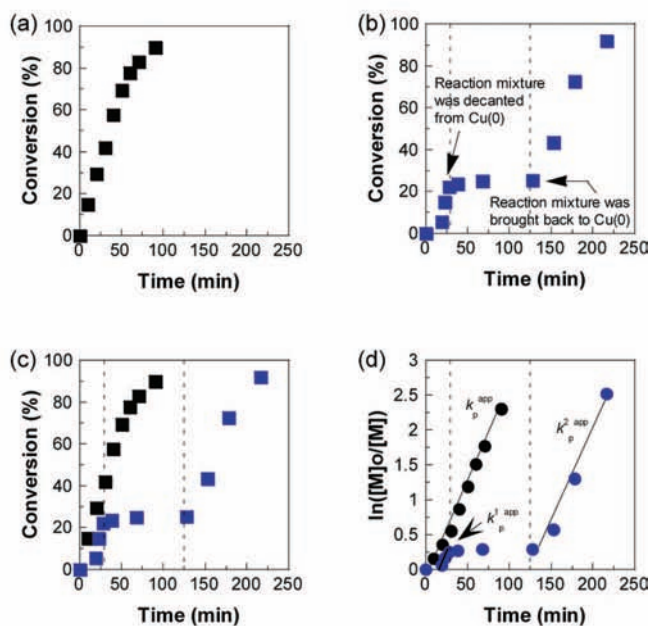
Figure 25. Cu[0] decantation experiment (left) and kinetic plots (right) for the Cu[0]/Me₆TREN-catalyzed SET-LRP of MA initiated with MBP in DMSO at 25 °C. (a) Monomer conversion vs time for a conventional kinetic experiment used as a control, (b) monomer conversion vs time for a kinetic experiment where reaction mixture was decanted from Cu[0] powder at approximately 20% conversion and brought back after 1.5 h, (c) overlapped monomer conversion from (a) and (b), and (d) ln([M]₀/[M]) vs time (k_p^{app} = 0.0277 min⁻¹, $k^1_p{}^{app}$ = 0.0253 min⁻¹, $k^2_p{}^{app}$ = 0.0261 min⁻¹) for both experiments. Polymerization conditions: MA = 2 mL, DMSO = 1 mL, [MA]₀ = 7.4 mol/L, [MA]₀/[MBP]₀/[Cu⁰]₀/[Me₆-TREN]₀ = 222/1/0.1/0.1, Cu⁰ = 425 μm. Reprinted with permission from ref 167. Copyright 2008 American Chemical Society.

monomer (MA), ligand (Me₆-TREN), solvent (DMSO), initiator (MBP), and a stir bar was connected to a second Schlenk tube containing only a stir bar. After three freeze−pump−thaw cycles, the polymerization was performed in the first flask at 25 °C. At this point, the setup was rotated and the reaction mixture was decanted from the first flask to the second flask, leaving behind the Cu⁰ powder in the first flask. No polymerization was observed while the reaction mixture was allowed to stir without the Cu⁰ powder. After 1.5 h, the reaction mixture was decanted back into the original flask that contained the Cu⁰ powder. At this point the reaction restarted without an induction period with the same k_p^{app}. Dynamic light scattering (DLS) studies[167] indicate agglomeration of nascent Cu⁰, which is highly dependent on experimental conditions. Thus, it is evident that the most active nascent catalyst derived via disproportionation is either rapidly consumed or it agglomerates via nucleation from the surface and is, therefore, not freely suspended in the reaction mixture. Huang has also shown that visible Cu⁰ prepared in situ via disproportionation from a mixture of DMF/H₂O and Me₆-TREN is rapidly consumed when treated with benzyl halide initiator.[262] Another group has suggested that secondary activation events in SET-LRP proceed via Cu[I]X produced in situ via initiation with Cu⁰.[172] As polymerization ceases entirely after Cu⁰ powder is removed from the reaction mixture, dissolved Cu(I)X/N-ligand *cannot* mediate polymerization under the conditions of SET-LRP at 25 °C.[167] Additionally, it could be argued that, when nascent Cu⁰ is treated with initiator, it is the residual Cu[I]X in solution that is being consumed, and the resulting Cu[II]X₂ is being reduced to Cu[I]X by Cu⁰. However, this assumes an unrealistically fast rate of comproportionation and does not explain the rapid formation of green coloration to the reaction mixture, which

if comproportionation were fast would not appear until all Cu⁰ was consumed.

Slight deviations in linearity in the plot of k_p^{app} vs (SA)^{1/2} and its failure to achieve a 0,0 intercept (0 reaction rate for 0 Cu surface area) were presumed to be the result of polydispersity of the Cu⁰ powder.[263] It had previously been shown that extremely small Cu⁰ such as Cu⁰ nanoparticles provide a discontinuous increase in C−X decomposition rates.[261] As larger Cu⁰ powders are typically only analyzed via mesh screening, smaller particle sizes are likely present and result in an elevation in the rate of polymerization.

Cu⁰ wire had been used in the SET-LRP of VC initiated with CHBr₃ in DMSO at 25 °C. Cu⁰ wire has practical advantages over Cu⁰ powder; the most obvious is that it is easily removed and recycled.[168] The use of Cu⁰ wire as a catalyst for SET-LRP also imparts greater precision in total surface area of Cu⁰ used. The surface of Cu⁰ wire is more uniform than Cu⁰ powder, it is a single "monodisperse" catalyst, and the total surface area can be easily modified by changing the thickness (as indicated by the American Wire Gauge system)[264] and length of wire used. Therefore, Cu⁰-wire-catalyzed SET-LRP can be used as a more careful probe of the surface-dependent kinetics of SET-LRP. A series of experiments using Cu⁰-wire/Me₆-TREN-catalyzed SET-LRP of MA initiated with MBP in DMSO at 25 °C, where the total surface of Cu⁰ wire in the experiment was modulated through the use of varying lengths and thicknesses of Cu⁰ wire (Table 8).

First, the external rate of order of Cu was re-examined through Cu⁰ wire experiments. Analysis via a semilogarithmic plot of ln[Cu⁰]₀ vs ln(k_p^{app}) indicated an external rate order of 0.329 was observed for [Cu⁰]₀ (Figure 26a). This plot contained notable deviations from linearity and, as a

Table 8. Surface Area vs k_p^{app} for the Cu^0-Wire/Me_6-TREN-Catalyzed SET-LRP of MA in DMSO at 25 °C[168]

no.	wire guage[a]	std. D^b(cm)	measured D^c(cm)	wire length (cm)	mass[d] (mg)	SA (cm²)	k_p^{app}(min⁻¹)	conv. (%)	time (min)	M_w/M_n
1	16	0.129	0.130	3.3	4.81	1.39	0.045	85.8	46	1.19
2	16	0.129	0.130	6.4	9.34	2.65	0.058	90.8	45	1.19
3	16	0.129	0.130	14.8	21.59	6.05	0.073	88.9	31	1.18
4	16	0.129	0.130	27.0	39.38	11.0	0.114	85.4	18	1.18
5	18	0.102	0.104	4.2	3.83	1.38	0.045	88.4	50	1.23
6	18	0.102	0.104	15.5	14.14	5.02	0.079	89.0	29	1.22
7	18	0.102	0.104	29.0	26.44	9.36	0.099	83.5	19	1.26
8	20	0.0812	0.0820	4.5	2.60	1.17	0.041	90.4	60	1.20
9	20	0.0812	0.0820	10.0	5.78	2.57	0.051	89.0	45	1.19
10	20	0.0812	0.0820	12.5	7.22	3.21	0.066	90.2	37	1.17
11	20	0.0812	0.0820	15.0	8.69	3.85	0.061	90.6	41	1.15
12	20	0.0812	0.0820	30.0	17.34	7.67	0.082	91.0	30	1.20
13	24	0.0511	0.0518	3.0	0.69	0.49	0.027	86.7	77	1.21
14	24	0.0511	0.0518	4.0	0.91	0.65	0.035	86.5	60	1.23
15	24	0.0511	0.0518	8.4	1.92	1.36	0.044	86.5	47	1.26
16	30	0.0255	0.0261	4.0	0.23	0.32	0.021	88.6	105	1.28
17	30	0.0255	0.0261	180.0	10.26	14.40	0.132	86.8	16	1.27

[a] American wire gauge, useful for purchasing in the U.S., and used hereafter as a substitute for wire D. [b] American Wire Gauge standard diameter, used in all calculations. [c] For verification only. [d] Calculated from dimensions and density.
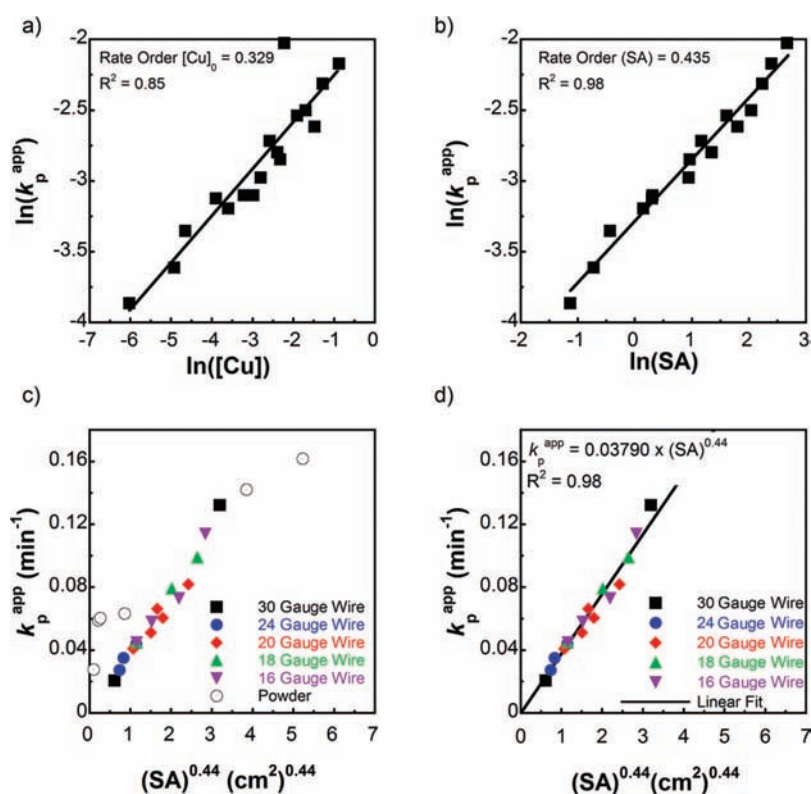

Figure 26. Effect of Cu^0-wire surface area on the k_p^{app} of SET-LRP of MA. Reprinted with permission from ref 168. Copyright 2009 American Chemical Society.

result, had an R^2 of only 0.85. As the reaction is presumed to be surface mediated, the total mass/concentration of Cu^0 should be less significant than the total surface area used. Semilogarithmic analysis of ln(SA) vs ln(k_p^{app}) provided an external surface area dependent rate order 0.44 (Figure 26b). The major deviations from linearity were corrected via transformation to surface area, and greater linearity was observed ($R^2 = 0.98$). A complex, less than unity external rate order with Cu^0 surface area is expected for heterogeneous reaction where the chemical step has a low activation barrier resulting in a mass-transfer limited process. However, the complex mechanism of SET-LRP cannot be ignored as a reason for the less than unity rate order.

Using the empirically derived external rate order of Cu^0 surface area, k_p^{app} was found to vary with near perfect linearity with $SA^{0.44}$ (Figure 26d). Cu^0 wire experiments were overlaid on the same scale (Figure 26c). Higher surface area/smaller diameter Cu^0 powder fit nicely with the previous data, while lower surface area/larger diameter powders were slightly faster than expected, likely a result of their polydispersity.

The surface-area dependence on k_p^{app} can be easily converted to a length dependence, and calibration curves for specific Cu^0 wire thickness were made (Figure 27). Using these calibration tables, the rate of a given SET-LRP polymerization can be easily tailored by choosing an appropriate wire thickness and length.

Cu^0-wire/Me_6-TREN catalyzed SET-LRP of MA in DMSO at 25 °C also provides better predictability of molecular weight evolution and distribution than powder-catalyzed
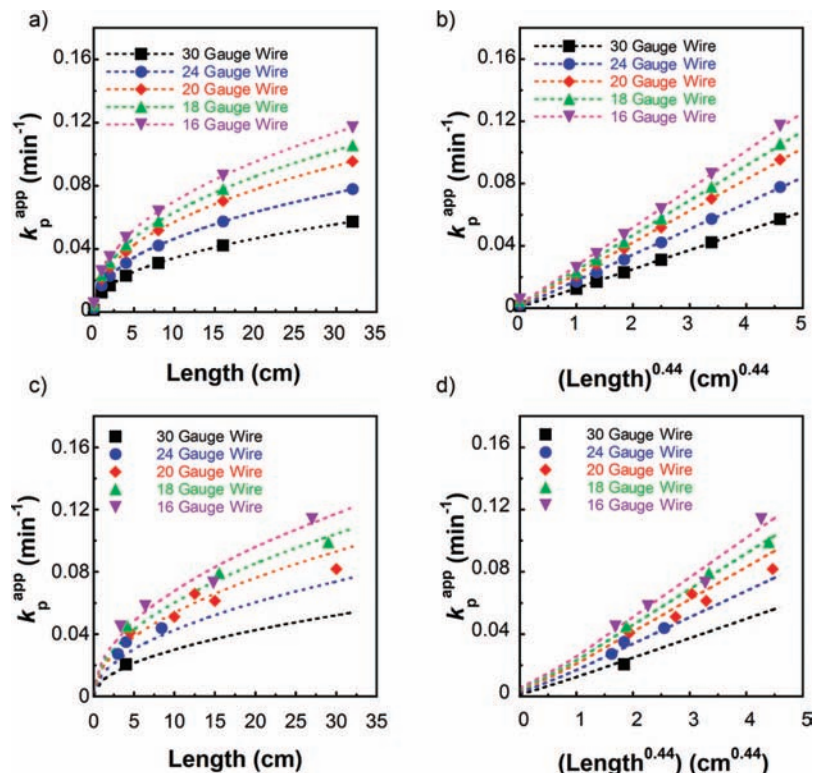
Figure 27. Calibration curves for k_p^{app}. (a) and (b) depict theoretical curves and computed data points, while (c) and (d) depict the fit of example experiments. Reprinted with permission from ref 168. Copyright 2009 American Chemical Society.

$[MA]_0/[MBP]_0/[Me_6\text{-}TREN]_0 = 222/1/0.1$ Cu(0) = 12.5 cm of 20 gauge wire

Figure 28. SET-LRP catalyzed by 12.5 cm of 20 gauge wire (diameter = 0. 0812 cm). Reprinted with permission from ref 168. Copyright 2009 American Chemical Society.

$[MA]_0/[MBP]_0/[Me_6\text{-}TREN]_0 = 222/1/0.1$ Cu(0) = 180.0 cm of 30 gauge wire

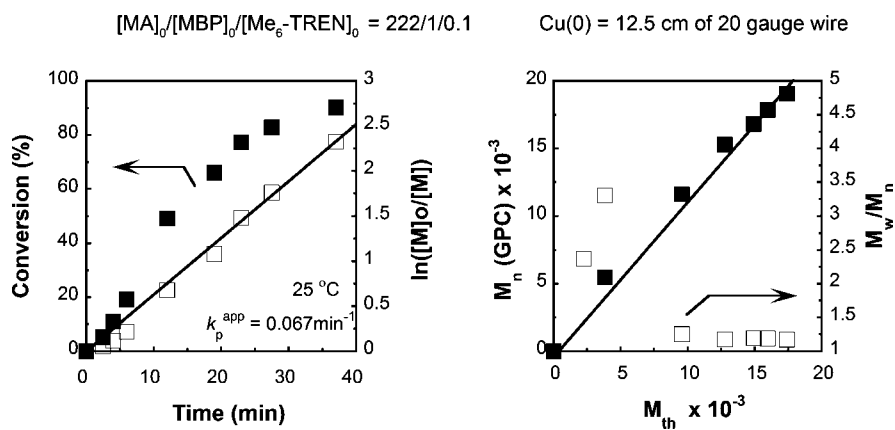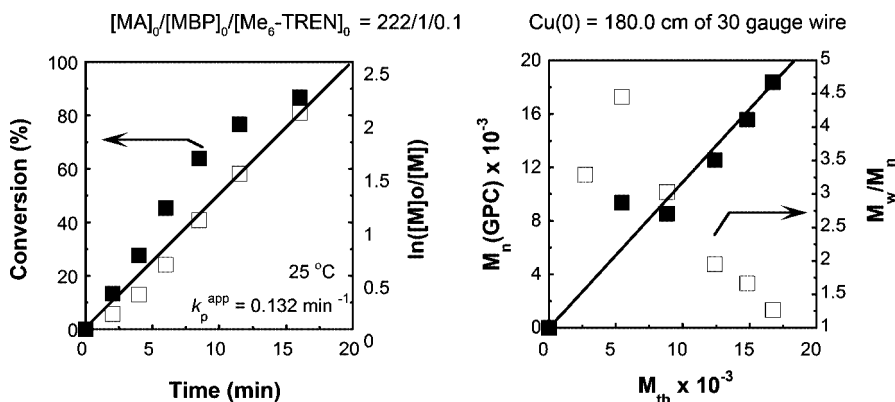**Figure 29.** SET-LRP catalyzed by 180 cm of 30 gauge wire (diameter = 0. 0255 cm). Reprinted with permission from ref 168. Copyright 2009 American Chemical Society.

analogues. Using 12.5 cm of 20 gauge wire (SA = 3.2 cm^2), 90% conversion was achieved in 37 min with $M_w/M_n = 1.17$ (Figure 28). Increasing the total surface area to 14.4 cm^2 via the use of 180 cm of 30 gauge wire results in 87%
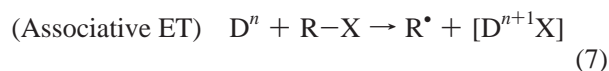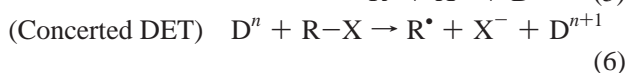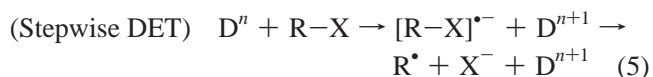
conversion in 16 min with only a small increase in polydispersity $M_w/M_n = 1.27$ (Figure 29). Similar results were achieved when BPE was used as a bifunctional initiator. Observations suggested that there is optimum surface area for maximum regulation of polydispersity. This regulation actually increases with increasing k_p^{app} up until this optimum value and then begins to decrease. The reason for this phenomenon is not clear but is distinct from polydispersity control in ATRP where increasing k_p^{app} is expected to result in decreased ability to mediate the LRP.

It was proposed that nascent Cu^0 produced in situ via disproportionation is the most active species in the SET-LRP activation process. Indeed, DLS experiments have shown a distribution of particles sizes produced via disproportionation.[207] Filtration experiments have shown that Cu^0 produced in this fashion contains, to some degree, extremely small and, therefore, extremely reactive nanoparticles. However, it was also demonstrated that disproportionation in the presence of Cu^0 wire, while not changing the extent of Cu^IX consumed, changes the size distribution of Cu^0 formed. In DMSO with $[Me_6\text{-}TREN]_o/[Cu^IBr]_o = 1$, a bimodal distribution of particle size is formed with a large contribution of suspended colloidal Cu^0, resulting in a turbid solution. In the presence of Cu^0 wire, the disproportionation under the same conditions results in a unimodal distribution of particle sizes and a visibly less turbid suspension. It is, therefore, likely that the Cu^0 wire or powder surfaces used in SET-LRP template the growth of Cu^0 particles and serve as nucleation sites. While these results are only preliminary, they begin to hint at an explanation as to why the initial surface of Cu^0 used in the reaction dictates the kinetics of the reaction. Possible explanations include the following: (1) A large excess of bulk Cu^0 is used relative to nascent Cu^0 produced. (2) The initial surface area dictates the amount of nascent Cu^0 produced via the initiation process. (3) Nascent Cu^0 may in fact partially agglomerate on the bulk Cu^0 surface, removing it from suspension. (4) The surface may regulate the size distribution of Cu^0 formed during disproportionation and, therefore, determine to what extent it contributes to the kinetics.

4.6.3. Activation Step: Electron Transfer

In the previous section, the role of Cu^0 surface area on the kinetics of SET-LRP was explored. The reversible interruption of polymerization by decantation of the reaction mixture from the bulk Cu^0 as well as the predictable correlation of k_p^{app} with surface area provided strong evidence for surface mediated activation by Cu^0.

While the generation of radicals in SET-LRP is likely mediated by the Cu^0 surface, the fundamental mechanism of their generation is a source of debate and speculation. In its simplest formm the activation step of SET-LRP is $D^n + R\text{-}X \rightarrow R^\bullet + (X^- + D^{n+1})$, where D^n is the donor, D, in oxidation state n. A donor, in most cases Cu^0 for SET-LRP and Cu^0 or $SO_2^{-\bullet}$ in the case of SET-DTLRP, oxidatively transfers an electron to an organic halide $R\text{-}X$, resulting in the rupture of the $R\text{-}X$ bond to form organic radical $R^\bullet$ and X^- and D^{n+1}. This seemingly straightforward mechanism can actually proceed through three pathways.[265]

(Stepwise DET) $\quad D^n + R\text{-}X \rightarrow [R\text{-}X]^{\bullet-} + D^{n+1} \rightarrow$
$$R^\bullet + X^- + D^{n+1} \quad (5)$$

(Concerted DET) $\quad D^n + R\text{-}X \rightarrow R^\bullet + X^- + D^{n+1}$
$$\quad (6)$$

(Associative ET) $\quad D^n + R\text{-}X \rightarrow R^\bullet + [D^{n+1}X]$
$$\quad (7)$$

Stepwise dissociative electron-transfer (DET) involves single-electron transfer (SET) from the donor to the organic halide to produce a radical-anion intermediate, which subsequently decomposes to furnish the radical and the halide. Concerted DET involves SET from the donor to the organic halide, mediating direct heterolysis without the intermediacy of a radical anion. Associative electron-transfer (AET) is the abstraction of the halide by the donor without the formation of an ionic intermediate.

Except in donor-free reduction via a glassy carbon electrodes or through solvated electrons, where AET is not applicable, all three processes are valid and continuum of mixed pathways is also possible if not likely.

In systems containing a homogeneous organic or organometallic donor or a heterogeneous metallic donor, any ET process proceeds through the formation of a 1:1 donor/acceptor encounter or precursor complex as described by Mulliken[266] and Hush.[267,268] It is the nature of the encounter complex that most broadly distinguishes the fundamental mechanism of electron transfer. Taube designated electron transfer between two metal centers via a conduit bridging ligand that belongs to the inner-sphere coordination shell of both the donor and the acceptor as an inner-sphere electron transfer (ISET) (Figure 30).[269−271] Electron-transfer reactions that occur through an encounter complex devoid of a bridging inner-sphere ligand were termed outer-sphere electron-transfer (OSET).

While the bridged complex in Taube ISET is often only transient, sometimes a bridging interaction leads to a stable mixed-valence complex. The degree of electron transfer in mixed-valence complexes can increase from complete localization (Robin-Day Class I) to complete delocalization (Robin-Day Class III).[272] ISET and OSET terminology can be generalized to include organic and organometallic donors and acceptors through comparison of the donor−acceptor interaction energies H_{DA}.[273] ET reactions with small values of H_{DA} can be considered OSET, while larger values correspond to ISET. A formal bridging interaction would constitute a large H_{DA} value, and thus, the two definitions for ISET are consistent. An OSET process with low H_{DA} can be readily modeled via potential surface of the self-exchange reactions of donor and acceptor according to Marcus theory.[274]

The $R\text{-}X$ cleavage in SET-LRP and SET-DTLRP can potentially occur via an OSET or an ISET process depending on the degree of interaction between the donor, Cu^0 or $SO_2^{-\bullet}$, and the acceptor $R\text{-}X$ in the encounter complex. In the weakly or noninteracting extreme, an OSET DET process will occur where the electron from the donor is transferred to σ^* $R\text{-}X$ orbital. The resulting destabilization leads to stepwise or concerted bond cleavage to $R^\bullet$ and X^-. Concerted versus stepwise dissociation is largely determined by the stability of the prospective radical-anion intermediate in the
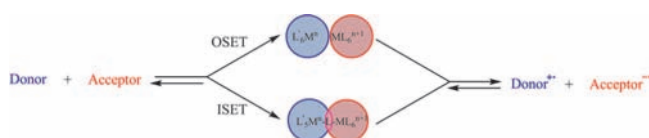

Figure 30. Taube inner-sphere (ISET) and outer-sphere (OSET) electron transfer. Adapted with permission from ref 273. Copyright 2008 American Chemical Society.
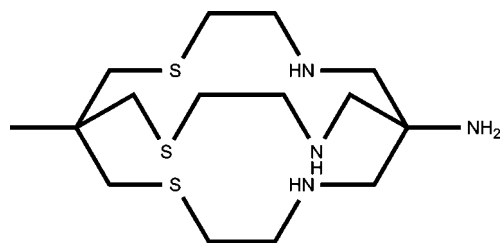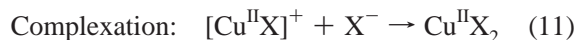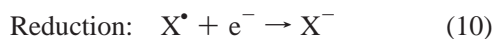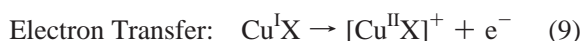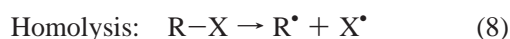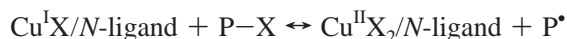
Figure 31. Structure of NH$_2$-capten.

reaction milieu. Stronger interaction between the donor and acceptor molecules can lead to an ISET DET process. Here, the electron transfer to the σ^* orbital proceeds through a more intimate complex of donor and acceptor but ultimately results in the heterolytic cleavage and diffusion of R$^\bullet$ and X$^-$. If a bridging halide interaction does occur in accordance with the Taube ISET model, electron transfer can proceed according to AET, where the halide migrates to the donor, forming a complex and R$^\bullet$.

The continuum between OSET and ISET, DET and AET, and concerted and stepwise depends on the structure of the donor, the acceptor, the electronic environment of the reaction medium, and the temperature, and such classification can be ambiguous. Stepwise OSET DET can be modeled readily via the Marcus–Hush two-state theory. Concerted OSET DET requires modification of the original Marcus theory to include simultaneous bond breaking via a repulsive product curve. ISET DET or AET is not readily modeled by a two-state theory, and the entire donor/acceptor complex needs to be considered.

As a point of reference, ATRP has been dubbed a "homolytic" ISET process, where the equilibrium between dormant species P–X and propagating macroradical is mediated by a complex reaction, composed of four elementary contributing reaction.[130,275]

$$Cu^IX/N\text{-ligand} + P\text{-}X \leftrightarrow Cu^{II}X_2/N\text{-ligand} + P^\bullet$$

$$\text{Homolysis:} \quad R\text{-}X \rightarrow R^\bullet + X^\bullet \qquad (8)$$

$$\text{Electron Transfer:} \quad Cu^IX \rightarrow [Cu^{II}X]^+ + e^- \quad (9)$$

$$\text{Reduction:} \quad X^\bullet + e^- \rightarrow X^- \qquad (10)$$

$$\text{Complexation:} \quad [Cu^{II}X]^+ + X^- \rightarrow Cu^{II}X_2 \quad (11)$$

It was further suggested that the K_{ATRP}, the equilibrium constant of ATRP, is the multiplicative product of the equilibrium constants for all four of these elementary reactions. A series of computational studies were performed on the thermodynamics of homolytic bond dissociation of initiators and dormant species relevant to ATRP.[276–278] While these studies provided useful trends in homolytic bond dissociation energies and obviously the strength of the R–X bond plays a role activation, it is unlikely that the dissection of the ATRP into these elementary steps has any particular relevance. Even if the bond-breaking process resembles homolysis, the interaction between donor and acceptor needs to be incorporated.

Monteiro has reported that the complex of CuBr with NH$_2$-capten (Figure 31) mediates the radical polymerization of Sty initiated with 1-bromoethylbenzene (1-BEB).[214] NH$_2$-capten is a macrobicyclic ligand, and in its complex with Cu$^{I/II}$, the metal should reside in the center of the ligand cavity. In other metal-caged complexes, due to the limited lability of the coordination sites and the steric demands of

the ligand, electron-transfer reactions were found to be outer-sphere.[279–281] Similarly, the formation of an inner-sphere encounter complex between CuBr/NH$_2$-capten and the dormant bromo chain ends of styrene is unlikely, and thus any activation it mediates will occur via OSET. CuBr/NH$_2$-capten mediates LRP of Sty at 60 °C, while CuBr/bpy did not. At 100 °C, CuBr/NH$_2$-capten mediated significantly faster radical polymerization than CuBr/bpy. The polymerization was not living as completely encapsulated CuBr/NH$_2$-capten was unable to mediate significant deactivation. CuBr/NH$_2$-capten was then targeted for use as an activator for the multiblock coupling of α,ω-(dibromo)PSty. Despite CuBr/NH$_2$-capten's remarkable rate acceleration, the radical polymerization of Sty, no multiblock coupling was achieved in toluene. However, in DMSO, a solvent that is known to mediate electron transfer, efficient multiblock coupling could be achieved. It is evident that activation with Cu^{I}Br need not be ISET and that at least comparable if not higher activation rates can be achieved through an OSET process.

The role of DMSO in accelerating Cu^{I}Br/Pr-PMI mediated LRP has been previously discussed.[213] The enhanced polarity of the solvent was suggested to stabilize charge separation in the transition state and induce greater separation of the cuprous halide catalyst resulting in a potentially more reactive Cu$^+$/L active species. Further, it was recognized that DMSO could complex either Cu^{II}, enhancing the activation process, or Cu^I, thereby altering its reactivity. In the context of SET-LRP and perhaps ATRP if it does proceed to some extent through an electron-transfer process, the rate of electron transfer, k_{et}, can be modeled via the Marcus equation.

$$k_{et} = \frac{2\pi}{\hbar}|H_{AB}|^2 \frac{1}{\sqrt{4\pi\lambda k_b T}}\exp\left(\frac{(-\lambda + \Delta G^o)}{4\lambda k_b T}\right) \qquad (12)$$

Here H_{AB} is the donor–acceptor coupling constant also referred to as H_{DA}, λ is the solvent reorganization energy, h is Planck's constant, k_b is Boltzmann's constant, and T is temperature. λ can be broken down according to $\lambda = \lambda_{in} + \lambda_{out}$. Solvation can affect the process in three fundamental ways. First, solvent can affect the outer-sphere reorganization energy λ_{out} as $\lambda_{out} \approx (1/n^2 - 1/\varepsilon_r)$, where n is the index refraction and ε_r is the relative permittivity.[282] This effect of solvent on λ_{in} is not significant for most of the solvents of interest. Second, selective solvation of either products or reactants can affect the ΔG^o of the electron-transfer process. Third, the relative stabilization of charge-transfer complex itself can be affected by solvation. In a radical-abstraction process, as suggested for the "homolytic" ISET process in ATRP, there is limited charge buildup in the transition state/donor–acceptor complex, and as the departing halide is captured by the metal center, Cu^{II} in the case of ATRP, selective solvation of the halide is not expected to be significant. However, the selective solvation of Cu^{II} by coordinating solvents such as DMSO could accelerate ATRP in that media. However, in other polar media that does not selectively solvate Cu^{II}, increasing the solvent polarity or reaction mixture polarity has resulted in decreased reaction k_p^{app}.[283]

SET-LRP is conducted almost exclusively in polar solvent mixtures, as they are generally more apt at mediating disproportionation.[186] It has been demonstrated that the addition of H$_2$O to organic solvents results in a linear increase in the k_p^{app} and a general increase in control. Both the increase in rate and improved control may be partially attributable to improved disproportionation of Cu^{I}X in aqueous media.
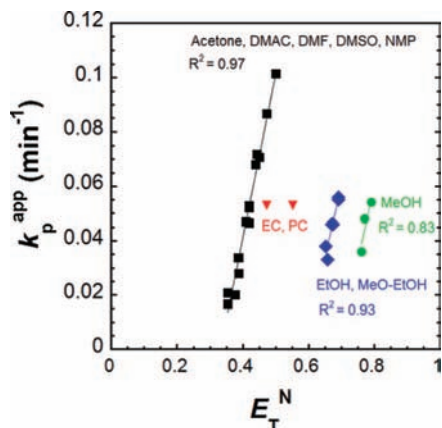
Figure 32. k_p^{app} vs E_T^N for the SET-LRP of MA initiated by MBP in various solvents and binary mixtures of solvents. Reaction conditions: MA = 1.0 mL, solvent 0.5 mL, $[MA]_o$ = 7.4 mol/L, $[MA]_o/[MBP]_o/[Me_6\text{-}TREN]_o$ = 222/1/0.1, Cu^0 = 12.5 cm of 20 gauge wire. Reprinted with permission from ref 186. Copyright 2009 John Wiley & Sons, Inc.

However, it is also evident that the polarity of the solvent itself plays an important role. The transition state in the outer-sphere electron-transfer process of SET-LRP should be a donor−acceptor charge-transfer (CT) complex between the electron donor, Cu^0, and electron-acceptor initiator or dormant propagating species. Solvents that stabilize charge-transfer complexes should also enhance the rate of SET-LRP. DMSO is a very polar organic solvent, and it is no coincidence that it is one of the best solvents for SET-mediated organic reactions[215] and for SET-LRP.[27] The Dimroth−Reichardt parameter (E_T^N),[284−286] is a measure of solvent polarity based on the transition energy of CT band of a pyridinium N-phenolate betaine dye. It is evident that there is a very strong correlation between the E_T^N of the solvent and the k_p^{app} of the reaction (Figure 32). Acetone, DMAC, DMSO, NMP, and their binary mixtures with water can all be fit with a single linear regression. However, EC, PC, EtOH, MeOH, and methoxy ethanol are offset from the main-trend line. Later studies concerning binary mixtures of organic solvents show that, in mixtures of EC−DMSO, EC−DMF, EC−DMAC, and DMSO−acetone, the addition of more polar EC or DMSO serves the same role as H_2O in enhancing the k_p^{app}.[197] For higher proportions of DMSO, DMF, or DMAC, the results fit the trend line observed previously for binary mixtures of organic solvents and H_2O (Figure 33). However, when higher proportions of EC are used in these examples or MeOH in other examples, deviations from the main-trend line are observed. This deviation is likely caused by the fact that alcohols and alkyl carbonates do not stabilize colloidal Cu^0 while DMAC, DMF, and DMSO do. Thus, the kinetics and control of SET-LRP are cooperatively and synergistically controlled by solvent polarity and its ability to stabilize polar transition states and intermediates, as well as the extent of disproportionation in the solvent/ligand mixtures, and its ability to stabilize colloidal Cu^0 and regulate its size distribution.

The rate enhancement afforded by solvents with high Dimroth−Reichardt constants in SET-LRP is likely a combination of its ability to stabilize charge separation in the ET transition state, the cuprous cation, and the halide anion derived via the DET process. Mechanistic studies have suggested a DET mechanism for the oxidative dissolution of Cu^0 by benzyl halides in dipolar aprotic media.[257−260] In their studies, the rate of reaction was not correlated with the
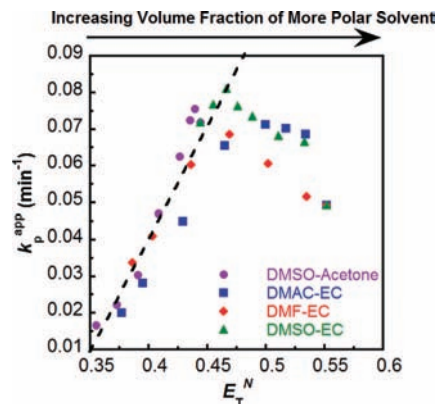

Figure 33. k_p^{app} vs E_T^N for mixtures of DMSO, DMF, and DMAC with acetone and EC. The dashed line corresponds to the trend line observed for binary mixtures of DMSO, DMF, DMAC, acetone, and NMP with water. Reprinted with permission from ref 197. Copyright 2009 John Wiley & Sons, Inc.

Dimroth−Reichardt parameter, though DMSO was still the best solvent. In their case, the $Cu^0 \rightarrow Cu^I$ redox process was occurring without the presence of N-ligand. Thus, they found that specific solvation of in situ generated Cu^I cations with high donor number (DN_{SbCl_5}) solvents was necessary. In SET-LRP, N-ligands such as Me_6-TREN stabilize transient Cu^I and resultant Cu^{II} species, in place of or in conjunction with solvent. Thus, solvent polarity becomes a more prominent effect.

In nontransition-metal catalyzed SET-DTLRP, it was proposed that $SO_2^{\bullet-}$ mediates DET of R−I intermediates. $SO_2^{\bullet-}$ generated via sodium dithionite is well-known for its ability to mediate the perfluoroalkylation or sulfinatodeha-logenation of perfluoroalkyl halides via a radical mechanism, presumably through a heterolytic cleavage of perfluoroalkyl halides.[287] Sulfinatodehalogenation mediated by $SO_2^{-\bullet}$ is presumed to proceed through the SET-mediated cleavage of R_F−X to $R_F^\bullet$ followed by addition of $SO_2/SO_2^{-\bullet}$.[288−290] While the reaction could conceivably proceed through an S_N2 or bromonium abstraction, the presence of $R_F^\bullet$ has been shown in the solution via electron spin resonance (ESR) and chemical trapping studies.[291,292] It is generally believed that this process goes by DET to the σ^* orbital followed by heterolytic cleavage. However, Savéant has noted the significant acceleration of the $SO_2^{\bullet-}$ reduction of CF_3Br versus the corresponding reduction via pure OSET aromatic radical anions in cyclic voltammetry experiments.[293] Savéant invoked either an intimate ISET process or $Br^\bullet$ abstraction as a cause for the rate enhancement and later dubbed $SO_2^{\bullet-}$ an inner-sphere donor. Savéant also suggested that the complexation of SO_2 with Br^- is a driving force for the rate acceleration via an abstraction process. Wakselman has argued against the abstraction mechanism, citing as a chief detractor that, in preparative trifluoromethylations using $SO_2^{\bullet-}$, SO_2Br^- formation was not observed.[288] Regardless of the true nature of the reaction of $SO_2^{\bullet-}$ with CF_3Br, any conclusions drawn for perfluoroalkyl halides is unlikely valid in the case of alkyl halides. In the case of perfluoroalkyl halides, the electron-withdrawing power of the fluoride polarizes the C−X bond, placing a partial positive charge on the halide. Through this partial positive charge, perfluo-roalkyl and perfluoroaromatic halides can complex with Lewis bases and have been used as receptors in crystal, liquid crystal, and polymer organization.[294,295] In alkyl halides, the partial charge on the halide is negative, and thus, an encounter complex between R−X and $SO_2^{\bullet-}$ is expected to

be less intimate and less likely to involve a halide bridge. Thus, even if an inner-sphere encounter complex may be accessible for CF₃Br and other perfluoroalkyl halides, the same cannot be concluded about alkyl halides. Further, in SET-DTLRP, the prospective electron acceptors are alkyl iodides. I⁻ and the reaction is conducted in the aqueous media. The enhanced solvation of I⁻ in aqueous media relative to Br⁻ in polar organic media of Savéant's study[293] further limits the likelihood of a SO₂I⁻ adduct via an associative mechanism.

The likelihood of an SET pathway is often bolstered if the reaction is slowed by the presence of an electron-transfer inhibitor such as dinitrobenzene (DNB). In the Cu⁰/Me₆-TREN catalyzed SET-LRP of MA in toluene/phenol, it was interesting to note that the only phenol additive that did not mediate any polymerization was nitrophenol.[196] Even in the absence of phenol, polymerization proceeded, but with limited conversion and increased polydispersity. While no explanation for the incompatibility of nitrophenol with SET-LRP was given, it is likely that nitrophenol is acting as a competitive electron acceptor. *p*-Nitrophenol is a potent electron acceptor, with $E°$ (DMSO) (vs SCE) of -1.26.[296] Because of the protic nature of nitrophenol, even in aprotic solvents such as DMSO, it undergoes proton-assisted irreversible reduction to *p*-nitrosophenol and a variety of other further reduced adducts. As the reduction potential of nitrophenol is lower or on par with the organic halide initiators and dormant species involved in SET-LRP, it stands to reason that it inhibits the SET process through irreversible reduction, thereby consuming the catalyst.

As DET is the likely mechanism of Cu⁰, Cu₂X, and SO₂⁻· mediated SET-LRP and SET-DTLRP, it is the electron affinity and heterolytic bond dissociation energy that are most relevant to the thermodynamics and kinetics of activation. Accordingly, studies were performed to compute the heterolytic bond dissociation energies (BDEs) of model initiator and dormant halide compounds via DFT (B3LYP) at the 6-31+G* level of theory.[131,27] The trends in heterolytic BDEs were identical to those of homolytic dissociation energies calculated for ATRP, as it is the relative stability of the resulting radical that varies from structure to structure. With an effective electron donor like Cu₂X, Cu⁰, or SO₂·⁻, a mechanism involving heterolytic dissociation via ET is expected to be more rapid than a mechanism that proceeds mostly through homolysis. Further, DFT of the heterolytic dissociation process suggested the possibility of a stepwise pathway via a radical-anion intermediate. Radical anions as transient intermediates are not unfamiliar in organic reactions.[297−301] In all cases except for CH₃CHCl₂, the computed radical-anion intermediate was lower in energy than the completely dissociated radical and anion.[27,166] In the first publication of SET-LRP,[27] which contained a more limited set of computations, this radical-anion intermediate was referred to as a "radical-anion cluster", which may be caged with the resulting Cu^{I}X/L⁺ salt[27] (Figure 34). However, when the study was expanded to include a greater diversity of initiator and dormant-species model compounds, the intermediate was referred to specifically as a radical anion.[166] This distinction will be addressed (vida infra).

The relative energies of the radical-anion intermediates to the neutral organic halide provide a trend for the electron affinities of the model initiators and dormant halides. In all cases, the electron affinity decreased according to I > Br > Cl. However, the stability of the radical-anion intermediates
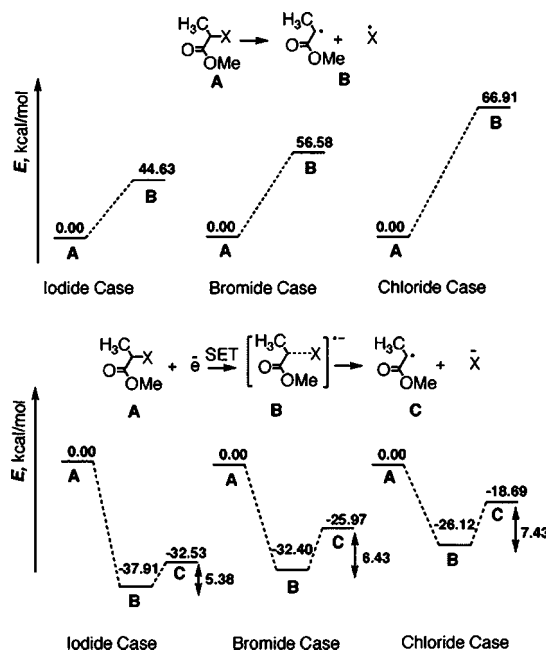

Figure 34. Comparison of homolytic and heterolytic dissociation processes for methyl acrylate model compounds. Reprinted with permission from ref 27. Copyright 2006 American Chemical Society.

decreased according to I < Br < Cl. MMA-dormant chains were found to be more effective electron acceptors than MA dormant chains, which were better acceptors than VC or vinyl acetate (VAc) chain ends. Notably, arenesulfonyl halides were found to have the highest electron affinities of all species, which falls in line with their enhanced rate of initiation (vida supra). The variation of heterolytic BDE between organic chlorides, bromides, and iodides was much less significant than differences between the homolytic BDEs. A later study evaluated the thermodynamics of bond dissociation through G3(MP2)-RAD(+) ab initio methods. This higher level of theory study addressed the obvious point that the negative entropy of dissociation, the oxidation potential of the catalyst, and the solvation will somewhat mitigate the benefits of the heterolytic OSET process and perhaps favor a concerted rather than stepwise process where radical anions are at most transient species.[166] Organic halides with high electron affinities are expected to react with Cu⁰ via an electron-transfer mechanism. The relatively small difference in heterolytic BDEs is corroborated by less than an order of magnitude differences in k_p^{app} for iodo chain ends vs chloro chain ends. These observations are in accord with other outer-sphere heterolytic dissociative electron-transfer processes.[28] These can be contrasted to the difference in 10^3-10^4 differences in k_{act} for ATRP, which bear greater accord with results from reactivity trends in other inner-sphere processes.[29]

Later re-examination of the computational studies on heterolytic BDEs and electron affinities revealed three related oversights.[165] (1) Most but not all stable radical-anion intermediates are somewhat higher in energy than the neutral compound and significantly higher in energy than the dissociated product, as is the case for the decomposition of aryl halides. (2) In most cases, the R−X bond distances found were too long to be considered a radical anion. (3) The only case where the supposed radical-anion intermediate was higher in energy than the dissociated radical and anion was CH₃CHCl₂. In this case, the R−X bond distance was much
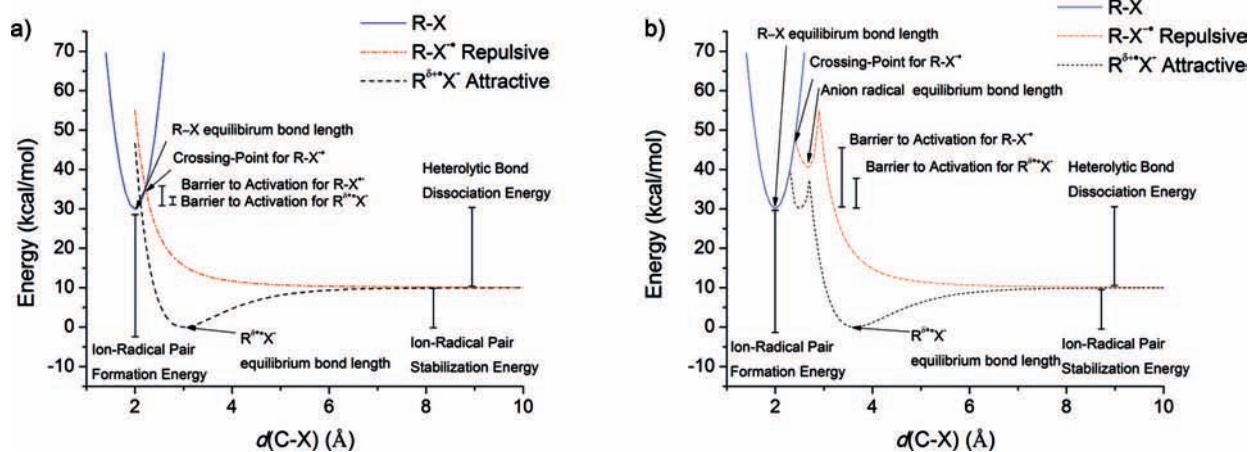
Figure 35. Energy profiles for the intrinsic self-exchange of R−X/{R•X⁻} in (a) concerted and (b) stepwise sticky dissociation. Reprinted with permission from ref 165 Copyright 2008 John Wiley & Sons.

Table 9. Representative Examples of Dormant Chain-End BDEs Modeled at the B3LYP/6-31+G* level[165]

compound	BDE$_{homolytic}$(kcal/mol)	BDE$_{hetrolytic}$(kcal/mol)	electron affinity (kcal/mol)	{R•X⁻} stabilization energy (kcal/mol)
MA−Cl	66.9	−18.7	−27.5	7.5
MA−Br	56.6	−26.0	−33.7	7.0
MA−I	45.2	−32.6	−39.3	6.6
MMA−Cl	63.9	−21.7	−31.8	10.1
MMA−Br	53.1	−29.5	−37.4	8.0
MMA−I	40.6	−37.2	−43.4	6.2
VC−Cl	73.7	−12.0	−20.7	8.7
VC−Br	62.2	−20.4	−28.11	7.7
VC−I	49.7	−28.0	−34.5	6.4

shorter than the other cases and was more consistent with a radical anion.

Savéant also made careful study of the electrode-catalyzed dissociative electron transfer to organic halides largely via cyclic voltammetry and computational modeling.[302] He has observed significant accelerations in electron transfer to organic halides bearing strong electron-withdrawing groups, including perfluoroalkyl halides,[302,303] carbon tetrahalides,[304] haloacetonitriles,[305] and α-haloacyl[306] and related compounds. This rate acceleration has been attributed to the largely Coulombic attraction of relatively electropositive organic radicals, made so via the pendant electron-withdrawing group, and anions. This ion−dipole interaction modulates the activation barrier via a correction to the Marcus−Hush relationship. As the stabilization term is in the quadratic Gibbs free-energy portion of the equation (eq 12), very small stabilization energies can have a dramatic effect. Thus, even in polar media that attenuate ion-dipole clustering, the small residual interaction still results in notable rate acceleration. This mechanism of DET has been termed sticky dissociation (Figure 35).[305] It should be noted that, while sticky dissociation has been confirmed experimentally, theoretically according to the Marcus equation, and in gas-phase ab initio studies, similar ab initio studies using continuum dielectric models have routinely failed to find a minimum corresponding to the anion-radical pair. This has been regarded as a failing not of the theory but of the state of solvation modeling in traditional quantum mechanics packages. It should also be noted that, while this form of dissociation does result in an intermediate, bond breaking is concerted with electron transfer.

The effect of sticky dissociation can be best visualized through potential energy profiles. The presence of an ion-dipole in sticky dissociation and the formation of a caged anion-radical pair results in a transition from purely dissociative curve to a Morse potential, lowering the energy of the intersection point (diabatic transition state or intrinsic self-exchange energy for R−X/{R• + X⁻}). This effect can also be observed in cases where a true radical anion may precede the formation of the anion-radical pair (Figure 35).[307]

The computational studies reported previously were repeated, this time adding to them an examination of the potential energy surfaces of homolytic and heterolytic dissociation. While the trends of the previous study were replicated (Table 9), there were some new findings. First, the potential energy profiles in almost all of the SET-LRP relevant compounds investigated (organic halides with electron-withdrawing functionality) were akin to those reported for other systems found to undergo sticky dissociation. Specifically, a minimum was observed at large C−X bond distances corresponding to a Coulombic ion-dipole attraction. An example is shown for MMA−Cl (Figure 36). In these cases, the charge was almost entirely localized on the halide and conversely the spin was largely concentrated on the carbon center. Second, while the electron affinity and stabilization trends from the original study were by and large replicated, some corrections were made as a lower energy minima was found at a different bond distance than what was reported previously. Most notably in the case of the CH_2Cl_2 anomaly, a lower energy sticky anion-radical pair was found at larger distance, bringing it in line with the other compounds. However, it is possible that, in the DET of CH_2Cl_2, a true radical-anion intermediate may precede the anion-radical pair, providing for a stepwise DET pathway. This intersection of the homolytic and heterolytic dissociation curves allowed for the crude approximation of the intrinsic self-exchange barrier for the organic halides being investigated. The values reported are uncorrected energies calcu-
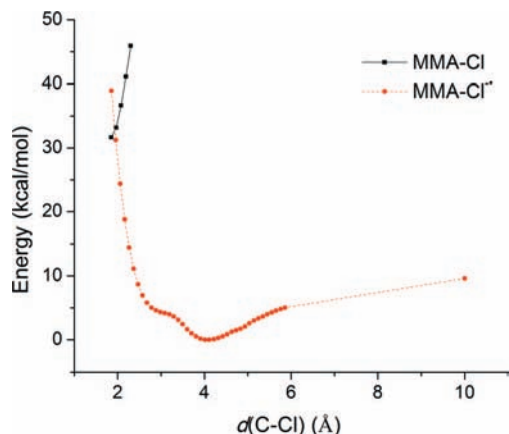
Figure 36. Example of self-exchange energy profile for MMA−Cl. Reprinted with permission from ref 165. Copyright 2008 John Wiley & Sons, Inc.

lated at a relatively low level of theory. However, it is not the quantitative nature of this exercise that is important, but rather the implied trends. Specifically, we were interested in what monomers and initiators that have not currently been investigated experimentally might be compatible with SET-LRP. It was found that acrylonitrile, methyl acrylonitrile, styrene, α-methylstyrene, vinyl bromide, vinyl fluoride, vinyl acetate, and 2-chloropropene all have electron affinities and anion-radical pair stabilization energies comparable with monomers already shown to be compatible with SET-LRP. Thus, under suitable conditions, their SET-LRP is expected.

Further, it was found that, while clearly less favored than activation of other organic halides, the activation of certain organic fluorides, such as head-to-head and head-to-tail poly(vinylidene fluoride) (PVDF), may be possible. It has been reported that $CuCl/Me_6$-TREN can mediate the graft polymerization of MMA and oxyethylene acrylate in NMP initiated with poly(vinylidene fluoride).[308] This polymerization was originally reported as an ATRP process. The solvent/ligand combination of NMP and Me_6-TREN has been reported to mediate the disproportionation of Cu^IX, and thus, an SET-LRP mechanism is more likely.[27] Additionally, the Cu^0-wire/Me_6-TREN SET-LRP of MA in NMP has been reported.[186] This is supported by the compatibility with near room temperature conditions, despite the homolytically inert C−F bond. Further, the use of Me_6-TREN as ligand resulted in a huge rate increase relative to 4,4′-dimethyl-2,2′-dipyridyl (DMDP, a bpy analogue). This can be attributed to faster disproportionation via Me_6-TREN providing for a Cu^0 rather than a Cu^I catalyzed process more readily than it can be attributed to the enhanced reactivity of Cu^ICl/Me_6-TREN versus $Cu^ICl/DMDP$,[111,309] in direct analogy to the way in which Cu^0 regardless of ligand choice provides for reactivation of the stable dormant geminal-dihalides in VC polymerization, while Cu^IX catalysts uniformly fail. Additionally, it had been concluded that, for all intents and purposes, reaction control was lost in Cu^ICl/Me_6-TREN MMA polymerizations relative to Cu^ICl/bpy polymerization.[309] In the Cu^ICl/Me_6-TREN catalyzed extension polymerization of MMA initiated with PVDF, switching from a bpy analogue to Me_6-TREN as a ligand increased the reaction rate without diminishing the control of molecular weight distribution. In fact, for the reported conversion, the control was better. In a Cu^I mediated activation of PVDF, a Cu^I fluoride complex will result. It is not clear how well this product will mediate deactivation to form the dormant chloride chain end.
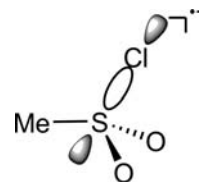

Figure 37. Radical anion formed during the outer-sphere heterolytic dissociation of $MeSO_2Cl$.

However, as disproportionation is occurring in Me_6-TREN, Cu^IICl_2/Me_6-TREN deactivator is being produced without going through the fluoride complex. Thus, Cu^0/Me_6-TREN likely provides rate acceleration via enhanced k_{act}, while disproportionation provides control, thus SET-LRP.

4.6.4. Experimental Evidence of Radical Anions and Consequences for ET

Of note, phenylsulfonyl halides were one of the species examined through energy profile modeling to reveal a single radical-anion-like intermediate.[165] Here, the bond distances of the intermediate were only increased by 0.5−0.7 Å and charge and spin were more delocalized. Recently, it has been shown through pulse radiolysis studies that the heterolytic dissociation of $MeSO_2Cl$ does indeed proceed through a radical-anion intermediate.[62] In aqueous media, a single solvated electron adds to the $σ^*$ S−Cl orbital to form a quasi-trigonal bipyramidal intermediate (Figure 37).

DFT energy profile modeling of $MeSO_2Cl$ reveals values for bond electron affinity, radical-anion stabilization energy, and heterolytic bond dissociation energy that are within 1 kcal/mol of the values obtained for $PhSO_2Cl$. Also the bond elongation in the radical anion and $PhSO_2Cl$ reveals slightly greater if any difference in charge and spin delocalization. Thus, $PhSO_2Cl$ and $MeSO_2Cl$ are expected to behave similarly in ET processes. Cu^0 and Cu_2X LRP initiated with sulfonyl halides exhibited several orders of magnitude faster initiation than propagation. This suggests that greater electron affinity and stability of the radical-anion intermediate may dramatically enhance ET, even more so than in the case of alkyl halides with electron-withdrawing groups. The existence of radical anions in DET reactions has also been suggested by Wakselman.[288] NaI and CF_3Br in the presence of $SO_2^{•-}$ results in the formation of CF_3I. It was suggested that $SO_2^{•-}$ mediates the production of $CF_3^{•-}$, which colligates with I^- to form a radical anion, which is subsequently oxidized.

The only dormant chain-end mimetic that exhibited similar behavior to sulfonyl halides in computational studies was methyl cyanoacrylate. However, what could be seen in all cases was that increasing the electron-withdrawing character of the side groups on the initiator or monomer decreased both homolytic and heterolytic bond dissociation energies and increased both the electron affinity of the organic halide and the stability of the radical pair. At the extremes of electron-withdrawing character, a true radical-anion intermediate may be formed via ET. Thus, a continuum between concerted and stepwise dissociative electron transfer may exist in SET-LRP (Figure 38).

4.6.5. Deactivation Step via $Cu^{II}X_2/N$-Ligand

Other than the propagation step, which is expected to be identical with all radical polymerizations, the only other expected commonality with ATRP is the deactivation step. In both ATRP and SET-LRP, the propagating macroradical
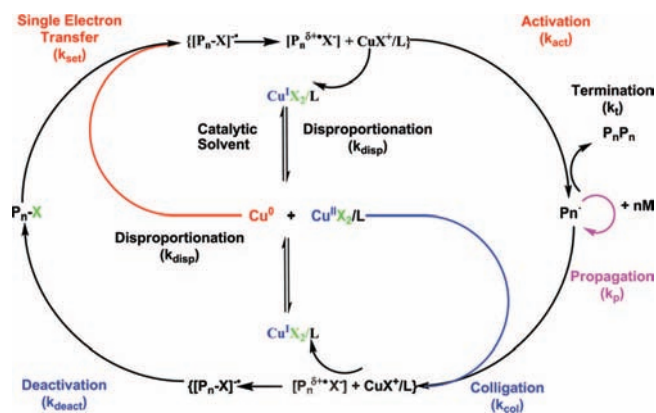
Figure 38. Mechanism of SET-LRP that incorporates a continuum between stepwise and concerted DET. Reprinted with permission from ref 165. Copyright 2008 John Wiley & Sons, Inc.

$P_n^\bullet$ is assumed to be converted to the dormant species P_n-X via $Cu^{II}X_2/N$-ligand. A few subtle differences are expected. First, the use of polar solvents is expected to solvate the halide and produce deactivators with the structure $[Cu^{II}X/L]^+$ as opposed to neutral $Cu^{II}X_2$. This may affect the fundamental mechanism of deactivation. It is possible in this case that deactivation proceeds through the formation of a $C-Cu^{III}X$ complex that rapidly decomposes to $C-X$ and a cuprous species. Alternatively, an electron-transfer mechanism via radical and halide colligation followed by Cu^{II}-mediated oxidation could be envisioned as suggested by Wakselman for the reaction of NaI and perfluoromethyl radicals.[288] Such a reaction either requires an unlikely ternary collision of Cu^{II}, radical, and halide or through the intermediate formation of stabilized anion-radical pairs or radical anions. It has been difficult to probe such a reaction through cyclic voltammetry because polarimetric reductions of electron-withdrawn organic halides result in irreversible two-electron reduction to the anion. There has been some ESR observation of perfluoroalkyl halide radical anions and sulfonyl halide radical anions by ESR, hinting at a discernible lifetime of such species in solution.

From the standpoint of kinetic experiments, calculation of the external rate order of polymerization in $[Cu^{II}X_2/Me_6$-TREN$]_o$ provides some interesting insight. In the original report of SET-LRP, most experiments were performed without the addition of CuBr2. A series of experiments was performed where the $CuBr_2/Me_6$-TREN to Cu^0 ratio was increased from 0.1 to 2.0 in the SET-LRP of MA initiated with MBP. Here evaluation of the semilogarithmic plot of $\ln[Cu^{II}Br_2]_0$ versus $\ln(k_p^{app})$ demonstrated an external rate order in $[Cu^{II}Br_2/Me_6$-TREN$]_0$ of -0.92.[27] Another series of experiments was performed where the $Cu^{II}Cl_2/Me_6$-TREN to Cu^0 ratio was increased from 0.2 to 0.6 in the SET-LRP of MA initiated with MCP. Here, evaluation of the semi-logarithmic plot of $\ln[Cu^{II}Cl_2]_0$ versus $\ln(k_p^{app})$ demonstrated an external rate order in $[Cu^{II}Cl_2/Me_6$-TREN$]_0$ of -0.80.[177] However, one more series of experiments was conducted where the $Cu^{II}Br_2/Me_6$-TREN to Cu^0 ratio was increased from 0.05 to 0.2 in the SET-LRP of MA initiated with MBP. Though not described in the report, evaluation of the semilogarithmic plot of $\ln[Cu^{II}Br_2]_0$ versus $\ln(k_p^{app})$ demonstrated an external rate order in $[Cu^{II}Br_2/Me_6$-TREN$]_0$ of -0.16.[179] It is apparent that the external rate order of deactivator varies depending upon the domain of equivalency. At very low loading levels, for instance, 0.05 deactivator to initiator, a significant improvement in the
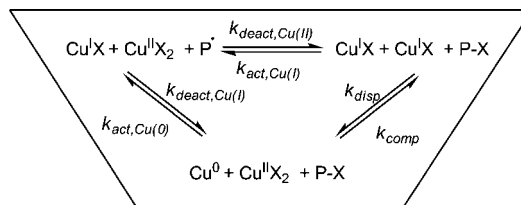

Figure 39. Simple Onsager triangle analysis of SET-LRP. Adapted with permission from ref 172. Copyright 2007 American Chemical Society.

control of molecular weight evolution and distribution can be achieved without altering the k_p^{app}. Here, deactivation at the early stages of polymerization is provided by external addition of deactivator, while initiation and disproportion are still building up needed loading levels, but its effect is diminished through eventual entrance into the disproportionation cycle. At higher external loading levels of $Cu^{II}Br_2$, deactivation and disproportionation do not significantly diminish the $Cu^{II}Br_2$ loading levels, and thus, the amount of deactivator present in solution is externally rather than internally controlled.

4.6.6. Regarding Microscopic Reversibility of SET-LRP

It has been suggested that the mechanism of SET-LRP violates the principle of microscopic reversibility.[172] A typical Onsager triangle network analysis[310] was applied to the analysis of the SET-LRP (Figure 39).

In the Onsager triangle network analysis, the product of the rate constants of the forward cycle should equal the product of the rate constants of the reverse cycle. If these were the only and correct contributing reactions in SET-LRP, an inverse relationship between K_{disp} and the rate constant of Cu^0 catalyzed activation would be correct as stated:[172]

$$\frac{k_{act,Cu(0)}}{k_{act,Cu(I)}} = \frac{k_{deact,Cu(I)}}{k_{deact,Cu(II)}} \frac{1}{K_{disp}} \qquad (13)$$

Such analysis would suggest that any system where disproportionation is strongly favored would also mean that Cu^0 is a less active catalyst in that system. A constant challenge for those pursuing the development of SET-LRP is that the mechanism is not so simple (Figure 40).

This disproportionation and activation/deactivation cycle is not an isolated homogeneous system as described in the simpler Onsager triangle. Rather, activation from Cu^0 is a heterogeneous process, while deactivation and disproportionation are homogeneous processes. This heterogeneous process occurs both via Cu^0 supplied in bulk and the nascent Cu^0 derived via disproportionation, two distinct catalysts. While some details are emerging regarding the formation and agglomeration of nascent Cu^0,[207] the kinetics and thermodynamics of the agglomeration process are not understood fully at the present time. Additionally, the disproportionation process and the activation processes must incorporate the change binding state of the ligand. Finally, the propagation of active radicals in the homogeneous phase and the corresponding exothermic driving force must also be considered. As mentioned in a recent essay on microscopic reversibility,[311] exothermic interface crossing reactions can drive reactions in unilateral directions. While complex mechanism and "special circumstances" should not be invoked to simply attempt to dodge the logic of the fundamental principle of microscopic reversibility, it is just
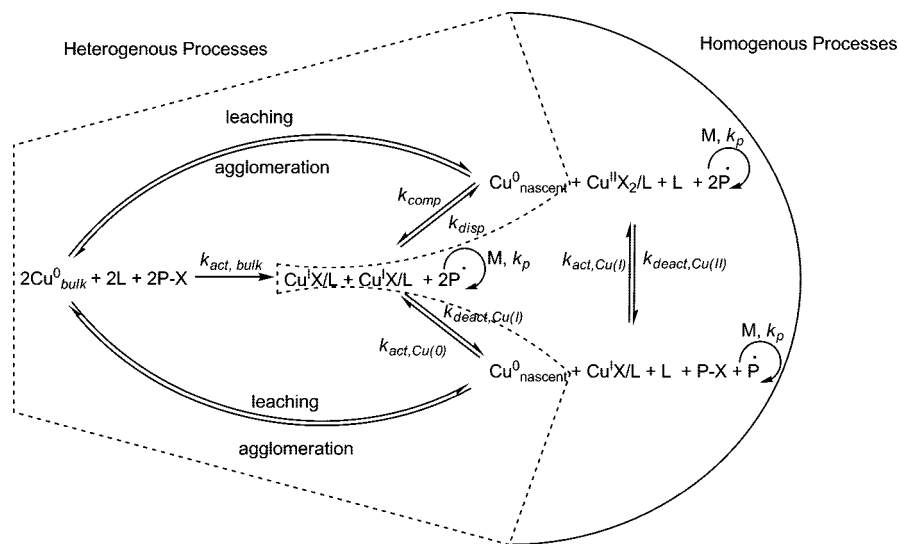
Figure 40. Full mechanism of SET-LRP involving all heterogeneous and homogeneous processes.
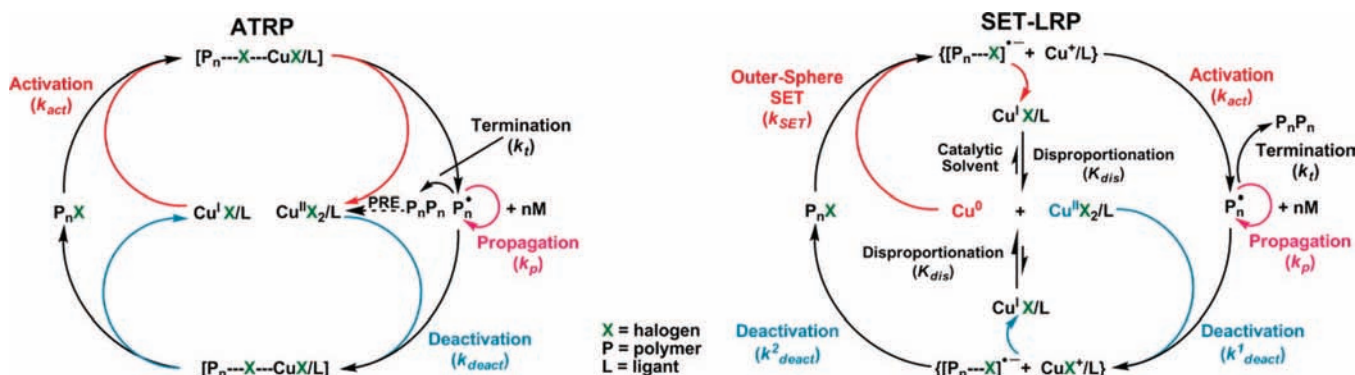

Figure 41. Comparison of ATRP (left) and SET-LRP (right) mechanisms. Reprinted with permission from ref 166. Copyright 2007 John Wiley & Sons, Inc.

as important to incorporate all processes into the network and apply the principles in a sensible way.

4.6.7. Mechanistic Overview and Perspective

The mechanism of SET-LRP, like most metal-mediated polymerizations, is multifaceted and requires further investigation. In spite of the many unknowns, a few details are clear. The observed rate acceleration compared to Cu^IX catalyzed LRP even at room temperature or below as well as the fact that k_p^{app} is roughly equivalent for chloro-, bromo-, and iodo-initiated polymerizations strongly suggest an OSET activation process.[27] The rate acceleration in SET-LRP is likely due to the enhanced reactivity of bulk and nascent Cu^0. This enhanced reactivity is evidenced by the ability of Cu^0 to mediate the LRP of unreactive monomers such as VC. Additionally, results to be published soon indicate that Cu^0 nanoparticles prepared via disproportionation are significantly more active for polymerization than bulk Cu^0, commercially available powders, or Cu^IX. An example of polymerization with target MW of 20 000 g/mol ([MA]$_o$/ [MBP]$_o$/[Cu^0]$_o$/[Me$_6$-TREN]$_o$ = 222/1/0.1/0.1) utilizing these highly active nanoparticles achieved k_p^{app} = 0.330 min^{-1} while maintaining a relatively narrow polydispersity, M_W/ M_n = 1.21. These mimics of "nascent" Cu^0 suggest that smaller Cu^0 species generated in situ via disproportionation will be even more reactive. The direct dependence of k_p^{app} on Cu^0 surface area suggests a heterogeneous (i.e., surface-mediated) process. The dependence of k_p^{app} on external Cu^{II}

concentration is not as significant as expected in a process dominated by a Cu^I activation/Cu^{II} deactivation equilibrium. Disproportionation is mediated by the cooperative and synergistic use of appropriate N-ligand, N-ligand concentration, and solvent. Without disproportionation, poor predictability of molecular weight evolution and distribution, as well as poor retention of chain-end functionality, is observed. Computational studies have suggested that SET to the initiator and dormant propagating macroradical can proceed through a continuum of stepwise DET via a radical anion or through concerted DET to form an anion-radical pair. While both processes can lead to enhanced k_{act} relative to the proposed homolytic ISET process of ATRP, the preparative implications for the two processes are not clear, though it has been shown that enhanced solvent polarity increases the rate of polymerization, presumably through the stabilization of the polar intermediates and transitions states of the SET process.

SET-LRP (Figure 41 right) can be mediated by the use of bulk Cu^0, Cu^0 derived from initiation/activation with Cu_2X (X = Te, Se, S, O), or Cu^0 produced in situ via the disproportionation of Cu^IX. SET-LRP at its core involves electron transfer followed by heterolytic bond dissociation. Cu^IX mediated ATRP (Figure 41 left) in its modern formulation is proposed to involve homolytic bond dissociation and electron transfer to the resulting halide. Like SET-LRP, ATRP can be accessed from a variety of Cu oxidation states including Cu^IX (normal ATRP) or $Cu^{II}X_2$ (inverse
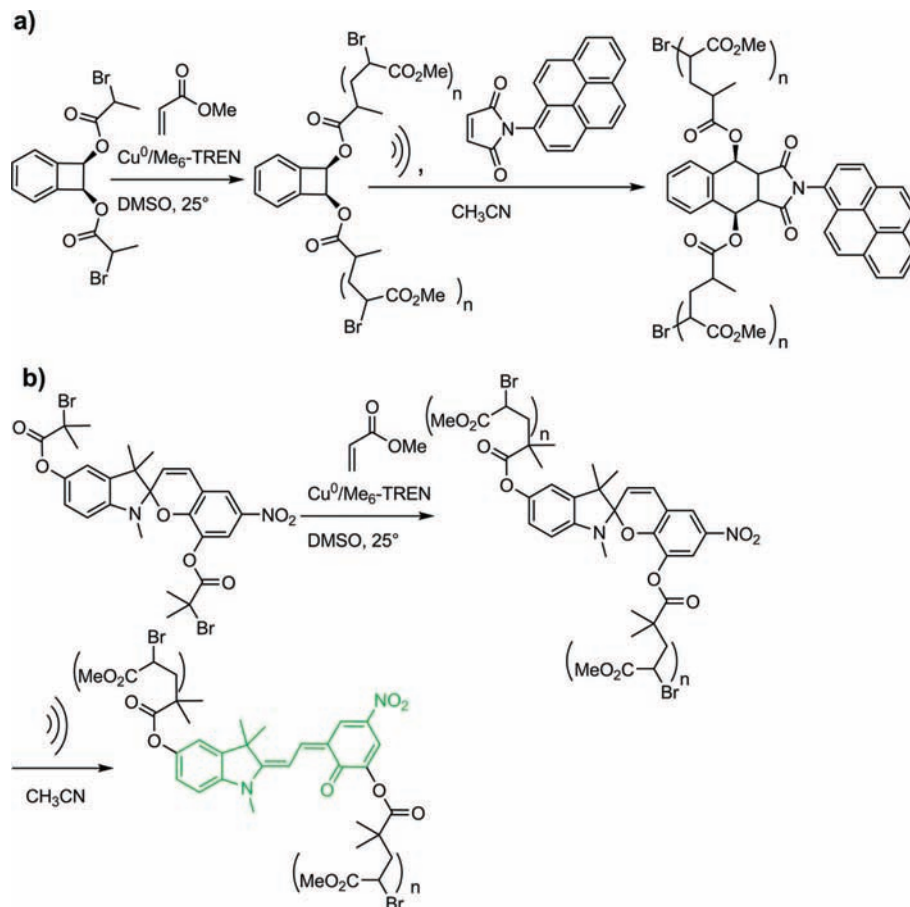
Figure 42. Mechanophore-linked addition polymers via SET-LRP. (a) Benzocyclobutene mechanophore can be activated with ultrasound to a reactive *ortho*-quinodimethide and trapped with *N*-(1-pyrene)maleimide (b) Spiropyran mechanophore can be activated with ultrasound. Block-copolymers via sequential SET-LRP and ATRP. Adapted with permission from ref . Copyright 2007 American Chemical Society.

ATRP, A(R)GET-ATRP), and zerovalent Cu^0 may be useful in some cases for modulating equilibrium constant via redox reactions. While proponents of ATRP may be apt to lump SET-LRP into a category of "modified" or ARGET-ATRP, there is clear evidence that this is not the case. Further, it should be noted that reducing conditions used in AGET and ARGET ATRP such as hydrazine[312] may in fact produce Cu^0 as opposed to Cu^IX, or at minimum a mixture of the two, and experimental conditions such as aqueous, other protic, and dipolar aprotic media, used in the various ATRP strategies, in many cases mediate disproportionation of Cu^IX. Therefore, many so-called ATRP reactions may be mediated in part or in full by Cu^0 processes and be in fact SET-LRP.

The mechanism of SET-LRP can most certainly be characterized as a complex system.[32,33] Dissecting any single component of the mechanism while providing insight into the underlying processes does not fully describe the interaction of the system as whole. SET-LRP combines heterogeneous and homogeneous chemistry as well as electron-transfer and radical addition reactions and is self-regulated through disproportionation. SET-LRP responds to environmental conditions such as solvent polarity, ligand type and concentration, extent of disproportionation in the ligand/solvent mixture, and its ability to stabilize colloidal Cu^0 and self-regulate its size distribution. While the complexity of the system may be daunting, it should indeed be a source of new inspiration for discovery.

4.7. Applications of SET-LRP

SET-LRP, at least in name, was only recently developed. As such, it is still in its infancy by way of specific application. In spite of this, in the short time SET-LRP has been available, there have been a few noteworthy implementations.

4.7.1. Mechanophore-Linked Polymers

Moore and Sottos have reported on the synthesis of mechanophore-linked addition polymers[313–316] wherein SET-LRP was utilized to create tailored polymeric handles for mechanical activation. In one case (Figure 42, part a)[313–315] a bifunctional benzocyclobutene (BCB) containing initiator was polymerized via SET-LRP to form a PMA–BCB–PMA polymer. Mechanical stress via ultrasound causes the BCB unit to be cleaved ring-opened via a Woodward–Hoffmann[317] rules-violating mechanism to form a reactive *ortho*-quinodimethide intermediate, which was trapped for analysis with *N*-(1-pyrene)maleimide. In a second example (Figure 42, part b),[313,316] a bifunctional spiropyran containing initiator was polymerized via SET-LRP to form a PMA–SP–PMA polymer. Mechanical stress induces the fragmentation of the weak C–O bond, inducing a molecular rearrangement to a UV-active mesocyanine moiety. The mesocyanine unit creates a green pigmentation to the polymer, allowing both qualitative and quantitative assessment of fatigue in the polymer system. In both cases, SET-LRP provided a reliable way to tailor the mechanical handles of the mechanophore-containing polymer, from low to high molecular weight.

Scheme 8. Double Hydrophilic Graft Copolymers for Au-Nanoparticle Formation and Stabilization (Adapted with Permission from Ref 190; Copyright 2009 John Wiley & Sons, Inc.)
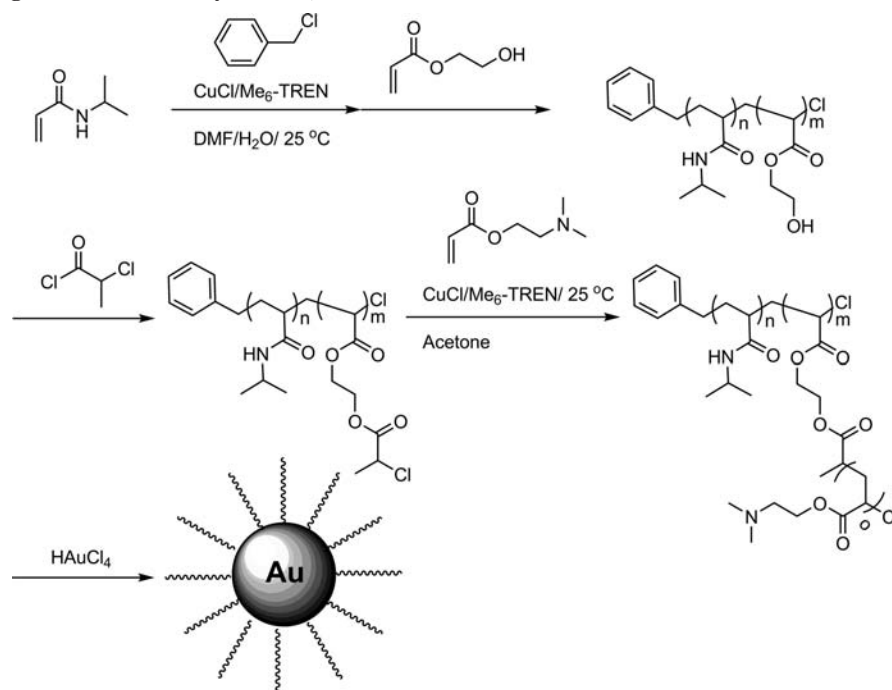
4.7.2. Double Hydrophilic Graft-Copolymers for Gold Nanoparticle Stabilization

Huang had previously developed a technique for the Cu^{I}Cl/Me$_6$-TREN catalyzed block-copolymerization of hydrophilic monomers, NIPAM, PEGMEA, and 2-EHA in DMF/H$_2$O and THF/H$_2$O.[187−190] Recently, it was discovered that the process, previously thought to be ATRP, was undergoing SET-LRP via rapid disproportionation of Cu^{I}Cl/Me$_6$-TREN in aqueous media.[190] Using a combination of SET-LRP and ATRP, they were able to develop double hydrophilic graft-copolymers that were able to mediate the formation of gold nanoparticles of controlled size from HAuCl$_4$ in aqueous solution without external reducing agent. The first stage of the process consists of the Cu^{I}Cl/Me$_6$-TREN catalyzed SET-LRP block-copolymerization of NIPAM and 2-EHA initiated with benzyl chloride in DMF/H$_2$O at 25 °C. The PEHA block of PNIPAM-b-PEHA is converted to a graft initiator via acylation with 2-chloropropionyl chloride. Cu^{I}Cl/Me$_6$-TREN catalyzed ATRP of 2-(dimethylamino)ethyl acrylate (DMAEA) initiated with PNIPAM-b-PEHA−Cl in acetone at 40 °C produce PNIPAM-b-(PEA-g-PDMAEA). PNIPAM-b-(PEA-g-PDMAEA) in the presence of aqueous HAuCl$_4$ produced Au-nanoparticles stabilized by the PDMAEA graft block without the addition of a reducing agent.

4.7.3. Micellar and Vesicular Structures

Monteiro has utilized SET-LRP for the synthesis of micellar and vesicular structures.[185] Cu^0/Me$_6$-TREN-catalyzed SET-LRP of solketal acrylate (SA) initiated with MBP or 4-armed star initiator 4BrPr in DMSO at 25 °C, produced linear Br−PMA−Br and 4-armed star [Br−(PMA)−O−CH$_2$]$_4$C macroinitiators, respectively. Chain extension SET-LRP of SA initiated with the linear or branched macroinitiators and catalyzed by Cu^0/Me$_6$-TREN in DMSO at 25 °C resulted in PMA-b-PSA and 4-armed star [(PSA-b-PMA)−O−CH$_2$]$_4$C with molecular weight in accord with theory and excellent control of molecular weight distribution

(M_w/M_n = 1.14 linear and M_w/M_n = 1.10 4-armed star). Treatment of the linear and 4-armed star block-copolymers with 6N HCl in THF provided near quantitative deprotection of the solketal side chains to glycerol. Self-assembly of the linear PMA-b-PGA in water provided micellar structures with the typical core−shell topology as indicated by analysis via DLS, attenuated field-flow fractionation (AFFF), and transmission electron microscopy (TEM). Self-assembly of the 4-armed star [(PGA-b-PMA)−O−CH$_2$]$_4$C in water produced vesicular structures. The water-stable vesicular structures provided by the 4-armed star polymer are of interest in drug-delivery applications, as acrylate homopolymers and block copolymers have been found to be biocompatible.[318]

Using the same approach as described in the preceding section, Hung has also grafted poly(2-acryoyloxyethyl ferrocenecarboxylate) (PAEFC) from (PNIPAM-b-PEA) (Scheme 10).[262] Here as before, the (PNIPAM-b-PEA) main chain was prepared via CuCl/Me$_6$-TREN catalyzed SET-LRP, while the grafting was performed with CuCl/PMDETA catalyzed ATRP. PNIPAM-b-(PEA-g-PAEFC) prepared in this fashion formed micelles in aqueous media as visualized by TEM. The morphology of the micelles was determined by the length of the PAEFC side chain. These materials may be of use in redox-controlled drug-delivery or as nanoreactors.

In addition to graft-copolymers that form micelles and vesicles, SET-LRP has been used to prepare other micelle-forming structures. Tang recently reported the synthesis of AB$_2$-Type amphiphillic block copolymers (Scheme 11).[212] Y-shaped PEG-b-(PNIPAM)$_2$ and PEG-b-PNIPAM were prepared through CuCl/Me$_6$-TREN catalyzed SET-LRP of NIPAM initiated with PEG acylated with 2,2-dichloro-acetyl chloride or 2-bromoisobutyryl bromide, respectively. It was found above the lower critical solution temperature (LCST) that Y-shaped PEG-b-(PNIPAM)$_2$ underwent a phase transition from dissolved chains to what is likely PNIPAM cored micelles. Solution-phase differential scanning calorimetry (DSC) revealed that, while this transition temperature was similar for Y-shaped PEG$_{44}$-b-(PNIPAM$_{55}$)$_2$ and similar

Scheme 9. Synthesis of Amphiphillic Linear and Star Block-Copolymers via SET-LRP (Reprinted with Permission from Ref 185; Copyright 2008 John Wiley & Sons, Inc.)
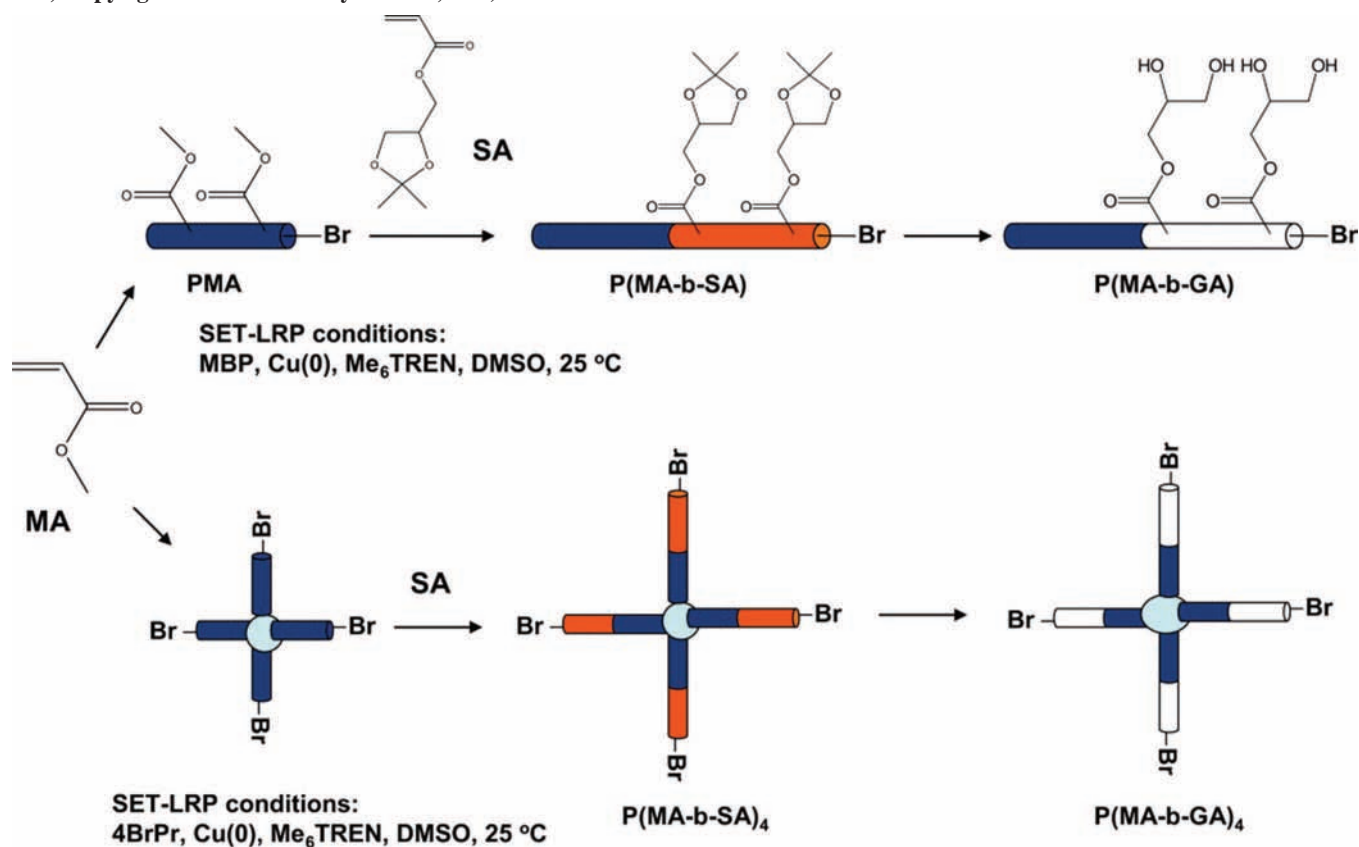
Scheme 10. Synthesis of Micelle-Forming PNIPAM-*b*-(PEA-*g*-PAEFC)
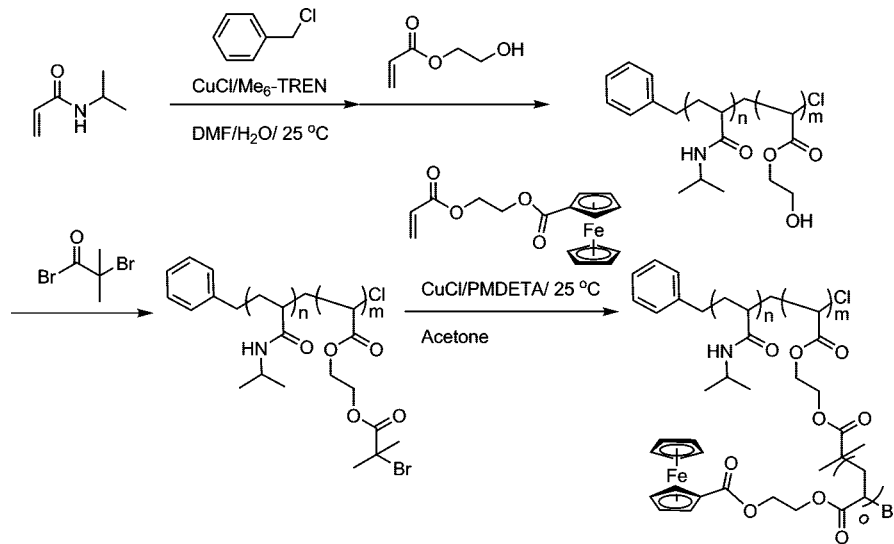
weight linear PEG$_{44}$-*b*-PNIPAM$_{110}$, the transition enthalpy was much lower for the AB$_2$ molecule.

4.7.4. Synthesis of Telechelics, Stars, and Block-Copolymers Based on PVC

SET-DTLRP has provided access to a variety of previously inaccessible block- and star-copolymers based on PVC and telechelic PVC (Figure 8). SET-LRP of VC initiated with bromide initiators provides even greater control of molecular weight evolution and distributions. Therefore, the same diversity of structures accessible for SET-DTLRP is available only with greater precision.

4.7.5. SET-LRP for Other Reactions

SET-RAFT[195] provided the first example of the use of the SET activation mechanism of SET-LRP to generate radicals useful for other organic reactions. In that case, the purpose was similar to that of SET-LRP, to produce a polymer. Polystyrene was prepared via SET initiation, followed by a mixture of SET-LRP and RAFT polymerization. As suggested by the mechanistic diagram (Figure 43) for SET-RAFT, it is not known to what extent SET-LRP and RAFT contribute to the polymerization. A recent report by a different group has suggested that Cu^0/PMDETA catalyzed SET-LRP of MMA can be conducted using 2-cyanoprop-

Scheme 11. Synthesis of AB₂ PEG-*b*-(PNIPAM)₂ and PEG-*b*-PNIPAM by SET-LRP
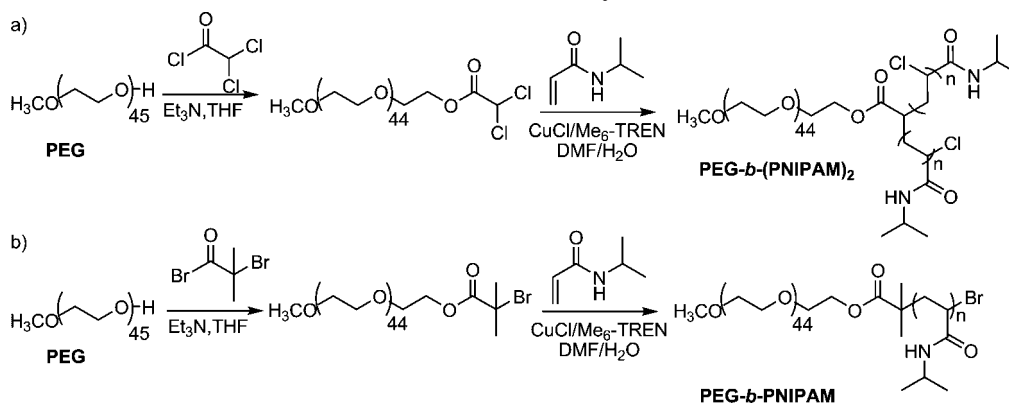
2-yl 1-dithionaphthalate (CPDN), a common RAFT reagent, as an initiator. Here, the absence of the halide initiator eliminates the possibility of the deactivation via $Cu^{II}X_2/N$-ligand, as is the case in SET-LRP processes. NMR and reinitiation studies of the resulting polymers suggest incorporation of the CPDN at both chain ends. On the basis of these results, SET-RAFT may in fact be similar to SET-DTLRP, wherein initiation and to a greater or lesser extent of activation is mediated by Cu^0, which competes with degenerative chain transfer with the RAFT agent.

In 1998, Matyjaszewski demonstrated that the radicals generated via ATRP could be trapped with 2,2,6,6-tetramethylpiperidinyloxyl (TEMPO).[319] Later, Haung took this meth-

Figure 43. Proposed Mechanism of SET-RAFT. Reprinted with permission from ref 195. Copyright 2008 American Chemical Society.

Figure 44. GPC traces indicate efficient coupling of PS−Br and TEMPO−PEO to form PS-*b*-PEO. Reprinted with permission from ref 322. Copyright 2009 American Chemical Society.

Scheme 12. Mechanism of SET-NRC and the Substrates Tested[322]

$$P_n\text{-}X \xrightarrow{\text{Cu(0)/PMDETA}} P_n^\bullet + \text{Cu(I)X/PMDETA}$$

P_n = PMA, P*t*BA, PMMA, PS
P_m = PEO, PCL
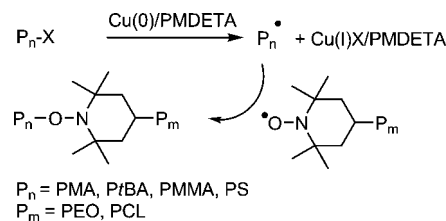
odology a step further by using ATRP to generate radicals from P*t*BA−Br or PS−Br, which could be *grafted-onto* poly(4-glycidyloxy-2,2,6,6-tetramethylpiperidine-1-xoyl-*co*-ethylene oxide).[320] This technique termed atom-transfer nitroxide radical coupling (ATNRC), was also utilized in the preparation of 3-miktoarmed star terpolymers, where one arm was attached via CuAAC click chemistry and the other arm was installed via ATNRC.[321] In the original publication on TEMPO trapping of ATRP-generated radicals, Cu^0 was used as an additive to, according to the proposed mechanism, reduce $Cu^{II}X_2$ back to Cu^IX. In ATNRC, radicals are generated by Cu^IBr/PMDETA at relatively high temperature, which can lead to deleterious side reactions. Recently, Huang was able to combine the ambient-temperature radical generation provided by SET-LRP with trapping with TEMPO-capped polymer to efficiently produce diblocks connected with an alkoxamine linkage (Scheme 12).[322] In this technique, termed single-electron transfer nitroxide radical coupling (SET-NRC), Cu^0/PMDETA mediates the generation of radicals from bromide terminated poly(acrylate)s, PMMA and PS, which is rapidly and efficiently trapped with a TEMPO capped poly(ethylene oxide) (PEO) or poly(ε-caprolactone) (PCL) (Figure 44). While disproportionating solvents such as EtOH and MeOH were effective for SET-NRC, nondisproportionating solvents such as THF were also effective. The mechanism of SET-NRC, unlike SET-LRP, does not require disproportion (Scheme 12).

By analogy with the impact of MADIX on the field of synthesis via radical methodology,[323] it is expected that SET-LRP will also provide mild reactions and higher efficiency in radical-mediated small-molecule synthesis.[324]

4.7.6. Accelerated Methods for TERMINI

SET-LRP provides access to more rapid and efficient methods for TERMINI (vida supra). The perfect chain-end functionality of polymers prepared via SET-LRP was readily demonstrated through ^{1}H NMR and reinitiation experiments. However, rigorous determination of chain-end functionality
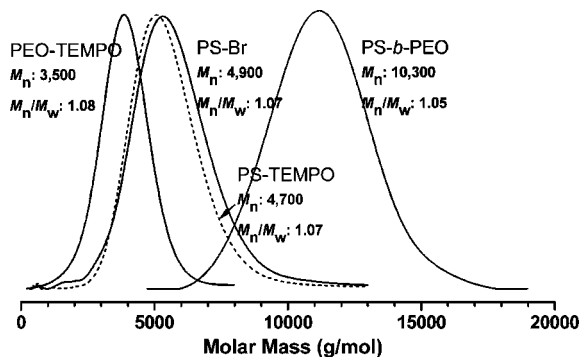
Scheme 13. Two-Step Synthesis Utilizing the "Thio-Bromo" Click Reaction Used to Provide PTP Dendrimers (Reprinted with Permission from Ref 325; Copyright 2009 John Wiley & Sons, Inc.)
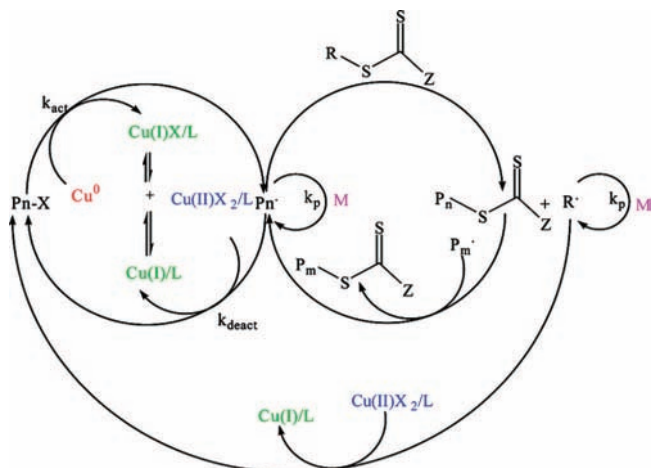

Scheme 14. Synthesis of G1–G4 PTP Dendrimers/Macroinitiators[a] (Reprinted with Permission from Ref 325; Copyright 2009 John Wiley & Sons, Inc.)
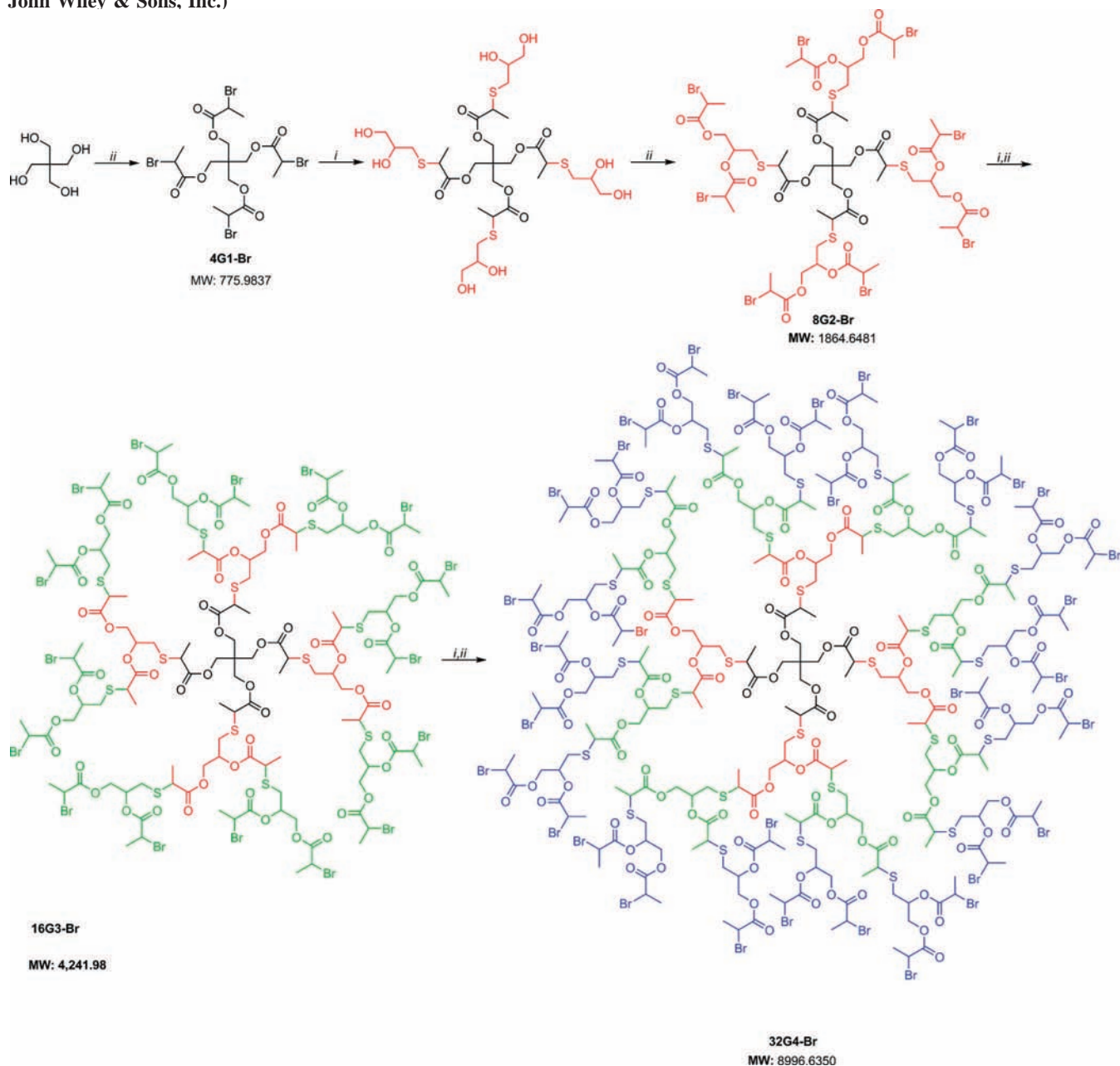
[a] Reagents and conditions: (i) thioglycerol, Et₃N, CH₃CN, 25 °C; (ii) 2-bromopropionyl bromide, pyridine, THF or CH₂CL₂, 0 °C.

by MALDI-TOF is complicated by a number of factors. For PMA, the mru has a mass of 86.04 g/mol, and the bromine end-group itself has an atomic weight of 79.9 g/mol. With such a small difference between end-group and mru, loss of chain-end functionality via proton abstraction or bimolecular termination cannot be detected. For higher MW monomers, chain-end functionality can be underestimated by MALDI-TOF via loss of HBr during analysis. In order to overcome these challenges, there was devel-

oped a method of polymer end-capping bromide-terminated using thiols, in the presence of carbonate base.[173,174] Here, the thiol acts as a nucleophile to displace the α-bromo end group via an S_N2 mechanism. End-capping with thiophenol provided a sufficient shift of polymer MW to distinguish between those polymers containing bromide chain ends and those without. This chain-end-capping reaction requires click-chemistry characteristics, specifically quantitative and rapid conversion.

Scheme 15. Three-Step Branch and Grow Strategy Employing Sequential Thio-Bromo Click Chemistry and SET-LRP (Reprinted with Permission from Ref 326; Copyright 2009 John Wiley & Sons, Inc.)
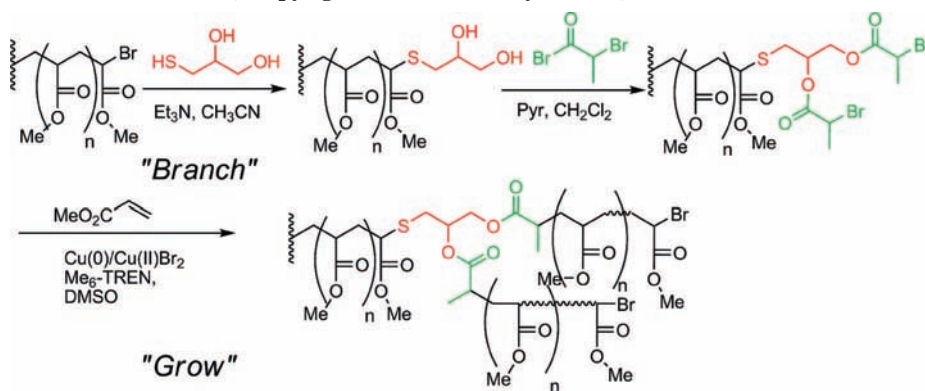
Percec has adapted this "thio-bromo click chemistry" to prepare poly(thioglycerol-2-propionate) (PTP) dendrimers[325] as well as dendritic macromolecules via a "Branch and Grow" strategy.[326] Among the library of thiols compatible

Scheme 16. Synthesis of G1−G5 Dendritic Macromolecules (Reprinted with Permission from Ref 326; Copyright 2009 John Wiley & Sons, Inc.)
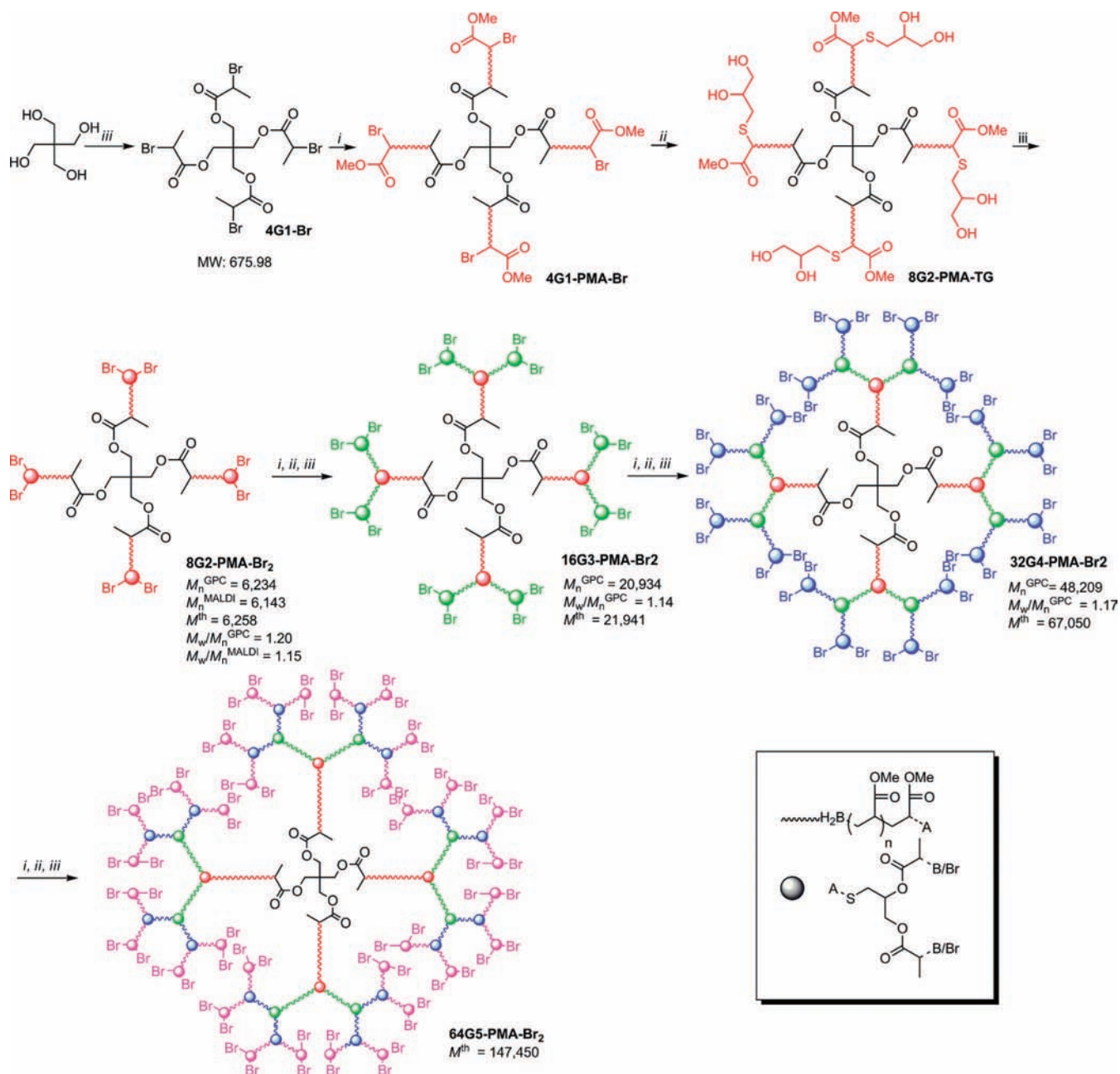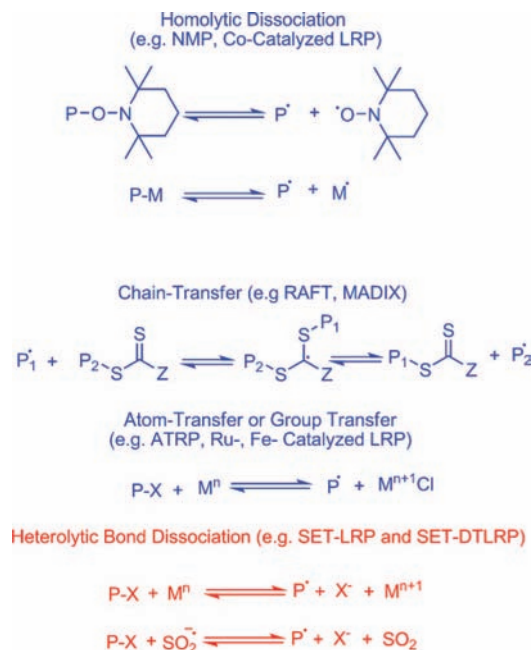
Figure 45. SET-LRP and SET-DTLRP in context of other LRP techniques.

with this S_N2 displacement, thioglycerol (3-mercaptopropane-1,2-diol) is a convenient commercial available for the introduction of a branching point. In addition to commercially available thioglycerol, (2-mercaptomethyl)-2-methylpropane-1,3-diol has been shown to be a novel alternative branching unit. In the presence of Et_3N or Hünig's base and acetonitrile as solvent, the four α-bromides of Pentaerythritol(tetrakis 2-bromopropionate) (4G1-Br) can be quantitatively thioetherified with thioglycerol (Scheme 13). This thioetherification is completely selective over the competive O-etherification reaction. The two new hydroxyl groups on each arm can be acylated with 2-bromopropionyl bromide in the presence of pyridine as base and THF or CH_2Cl_2 as solvent to provide two new sites per arm for subsequent branching (Scheme 13). Iterative use of this two-step synthesis provided G1–G4 hydroxy or α-bromo ester-terminated PTP dendrimers (Schemes 13 and 14).[325] The α-bromo ester-terminated PTP dendrimers are suitable as 4, 8, 16, and 32-armed initiators for star polymers using SET-LRP.

In addition to the synthesis of PTP dendrimers, the thiobromo click chemistry can be utilized in sequence with SET-LRP to provide dendritic macromolecules.[326] Here, a three-step Branch and Grow strategy is employed (Scheme 15). As with the synthesis of PTP dendrimers, 4G1–Br was employed as a starting material. However, instead of using the α-bromo esters sites to directly introduce a branching point, 4G1–Br was used as a 4-armed star initiator for SET-LRP. The resulting 4-armed star polymer was subjected to thioetherification with thioglycerol, and the hydroxyl groups acylated with 2-bromopropionyl bromide. The Branch and Grow process of SET-LRP, thioetherification, and acylation was repeated to produce G1–G5 dendritic macromolecules (Scheme 16). By the third generation, significant deviation of the M_n^{GPC} from the Mth is observed indicative of the dendritic effect on the hydrodynamic volume. This approach is complementary to the TERMINI concept (vida supra). While TERMINI introduces the branching point and terminates the polymerization in one step, it requires multistep synthesis of the TERMINI molecule. The Branch and Grow strategy utilizes efficient click reactions to install the branch-

ing point via commercially available materials. It is expected that the Branch and Grow strategy will provide access to a variety of unique dendritic macromolecules, through variation of branching patterns and thiols.

5. Conclusion

As summarized by Otsu[20] in regard to LRP provided by reversible homolytic dissociation: "In order to find a system of living radical polymerization in homogeneous solution, one must try to form propagating polymer chain ends which may dissociate into a polymer with a radical chain end and a small radical, which must be stable enough not to initiate a new polymer chain."

Many polymerization techniques including some metal-catalyzed techniques such as ATRP and co-mediated LRP rely on this model (Figure 45). Other approaches rely exclusively on degenerative chain transfer (e.g., RAFT, MADIX, TERP, SBRP) (Figure 45). However, SET-LRP and SET-DTLRP have provided an alternative model. Here, through heterolytic dissociation, there is no concern about reinitiation from the anionic fragment.

The developments of SET-DTLRP and more recently SET-LRP are a powerful set of tools for the synthesis of vinyl polymers. Both techniques provide for the ultrafast synthesis of ultrahigh molecular weight polymers while maintaining excellent control of molecular weight evolution and distribution and perfect retention of chain-end functionality. The use of simple Cu^0 wire and powder in SET-LRP and the option of nontransition metal catalysts in SET-DTLRP, the compatibility of both techniques with commercial-grade starting materials without prior purification, and the limited purification need of the resulting polymers make them a suitable option for the synthesis of tailored polymers, block-copolymers, star block-copolymers, and polymers with complex architecture.

Finally, it is a well-established notion that reactions developed for organic chemistry can be applied to the synthesis of polymers. ATRA and Cu^ICl/bpy radical cyclization[36] were applied to polymer synthesis resulting in ATRP. Xanthate chemistry[17] was adapted in the development of MADIX.[18] There is no reason why this paradigm cannot be reversed, where a method developed for polymerization is applied to small-molecule organic synthesis. There is still significant interest in the development of free-radical reactions in organic chemistry.[327,328] Perhaps the mild conditions for radical generation offered by SET-LRP can be applied to organic synthesis triggered by the heterolytic cleavage of activated R−X bonds.

6. Glossary

2EHA	2-ethylhexyl acrylate
AET	associative electron transfer
AN	acrylonitrile
ARGET	activators regenerated via electron transfer
ATRA	atom-transfer radical addition
ATRP	atom-transfer radical polymerization
BA	n-butyl acrylate
BMA	n-butyl methacrylate
bmimPF_6	1-butyl-3-methylimidazolium hexafluorophosphate
BPE	bis(2-bromopropyionyloxy)ethane
BPN	2-bromopropionitrile
bpy	2,2′-bipyridyl
DCAP	2,2-dichlroacetophenone

DET	dissociative electron transfer
DFT	density functional theory
DMAEA	2-(dimethylamino)ethyl acrylate
DN_{SbCl5}	donor number, or the enthalpy of formation of a 1:1 complex between a Lewis base and $SbCl_5$
DT	degenerative transfer
EA	ethyl acrylate
E_a	electron affinity
EBiB	ethyl 2-bromoisobutyrate
ESR	electron spin resonance
ET	electron transfer
GPC	gel permeation chromatography
GTP	group-transfer polymerization
H_{DA}	donor−acceptor interaction energy
HFIP	hexafluoroisopropanol
HMTETA	1,1,4,7,10,10-hexamethyltriethylenetetraamine
iBA	isobutyl acrylate
I_{eff}	initiator efficiency
ISET	inner-sphere electron transfer
k_{act}	rate constant of activation
k_{deact}	rate constant of deactivation
K_{dis}	equilibrium constant of disproportionation
k_p^{app}	apparent rate constant of polymerization
k_p	rate constant of polymerization
k_t	rate constant of bimolecular termination
LA	lauryl acrylate
LCST	lower critical solution temperature
LRP	living radical polymerization
MA	methyl acrylate
MADIX	macromolecular design via the interchange of xanthates
MALDI-TOF	matrix-assisted laser desorpton/ionization−time-of-flight mass spectroscopy
MBP	methyl 2-bromopropionate
MBSC	p-methoxybenzenesulfonyl chloride
MCP	methyl 2-chloropropionate
MEHQ	4-methoxyphenol
Me_6-TREN	tris(2-(dimethylamino)ethyl)amine
MMA	methyl methacrylate
M_n	number-average molecular weight
M_n^{GPC}	number-average molecular weight determined via gel permeation chromatography
MRU	monomer repeat unit
M^{th}	theoretical molecular weight for a given conversion
M_w	weight-average molecular weight
M_w/M_n	polydispersity index or molecular weight distribution
NIPAM	N-isopropylacrylamide
NMP	nitroxide-mediated polymerization or N-methyl pyrollidinone
OSET	outer-sphere electron transfer
PAN	poly(acrylonitrile)
PBA	poly(butyl acrylate)
PBMA	poly(butyl methacrylate)
PDMAEA	poly[2-(dimethylamino)ethyl acrylate]
PDSC	phenoxybenzene-2,2′-disulfonyl chloride
PEGMEA	poly(ethylene glycol) methyl ether acrylate
PEHA	poly(2-ethylhexylacrylate)
PEI	polyethyleneimine
PMA	poly(methyl acrylate)
PMDETA	N,N,N',N',N-pentamethyldiethylenetriamine
PMMA	poly(methyl methacrylate)
PNIPAM	poly(N-isopropylacrylamide)
PRE	persistent radical effect
Pr-PMI	N-(n-propyl)-2-pyridiyl(methaninimine) or Haddleton's ligand
PS	polystyrene
PSA	poly(solketal acrylate)
PVC	poly(vinyl chloride)
PVDF	poly(vinylidene fluoride)

PtBA	poly($tert$-butyl acrylate)
PTC	phase-transfer catalyzed or phase-transfer catalyst
RAFT	reversible addition/fragmentation transfer polymerization
ROMP	ring-opening metathesis polymerization
ROP	ring-opening polymerization
SA	solketal acrylate or surface area
SA/V	surface area-to-volume ratio
SBRP	organostibine-mediated LRP
SET	single-electron transfer
SET-DTLRP	single-electron transfer degenerative chain transfer living radical polymerization
SET-LRP	single-electron transfer living radical polymerization
Sty	styrene
tBA	$tert$-butyl acrylate
TBDMSCl	$tert$-butylchlorodimethylsilane
TEMPO	2,2,6,6-tetramethylpiperidinyloxyl
TERMINI	terminator multifunctional initiator
TERP	organotelluride-mediated LRP
TREN	tris(2-aminoethyl)amine
UHMW	ultrahigh molecular weight
VC	vinyl chloride

7. Acknowledgments

8. Note Added in Proof

During the review of the proof of this manuscript, Monteiro et al. reported an accelerated method to single-electron transfer nitroxide radical coupling (SET-NRC).[329] In this improved methodology, Cu^0 generated in situ by the disproportionation of Cu^IBr in the presence of Me_6-TREN and DMSO provided for the quantitative and rapid formation of macroradicals from the halide terminated polymers, which could be trapped with diversely functionalized TEMPO derivatives and nearly diffusion-controlled rates. This approach was utilized directly to produce linear block and three-arm star polymers, as well as in a tandem "Click" sequence incorporating SET-NRC and Cu-catalyzed azide−alkyne cycloaddition.

9. Note Added after ASAP Publication

After publication of this manuscript online, an important article appeared in print detailing the synthesis of high molecular weight polyacrylates with dumbbell topology.[330] In order to prepare these dumbbell polymers, a telechelic dibromo-(PBA-r-PtBA) was first used as a macroinitiator for the polymerization of 2-hydroxyethyl acrylate (HEA) to form the ABA triblock copolymer, PHEA-b-(PBA-r-PtBA)-b-PHEA. The hydroxyl groups of the short PHEA blocks were acylated with 2-bromo-2-methylpropanoyl bromide. Subsequent copolymerization of BA and tBA using acylated PHEA-b-(PBA-r-PtBA)-b-PHEA as a grafting-from macroinitiator provided polyacrylates with an overall dumbbell-like shape. It is interesting to note that, for the synthesis of high molecular weight telechelic dibromo-PBA-r-PtBA and PHEA-b-(PBA-r-PtBA)-b-PHEA macroinitiators, a combination of Cu^0, Cu^IBr, and PMDETA in acetone was required.

High molecular macroinitiators could not be produced in the absence of Cu^0 nanopowder additive. A SET-LRP mechanism was provided as one of the possible explanations for the improved performance of the polymerization in the presence of Cu^0 nanopowder. Recent studies have indicated the enhanced reactivity of Cu^0 nanopowders[167] in the SET-LRP of acrylates vs conventional Cu^0 powder and wire catalysts. Additionally, the solvent employed in this study, acetone, has also been recently demonstrated to be a very effective solvent for the SET-LRP of acrylates.[168]

In addition, it was observed that some of the early studies from our laboratory related to $Cu^I X$ and Cu^0/Me_6-TREN in DMSO were omitted from this manuscript. Following the discovery of $Cu^0/TREN$ as an effective catalyst for the SET-DTLRP of VC initiated with CHI_3 in THF/H_2O,[131] efforts were focused on the development of methods for the synthesis of ABA triblock copolymers containing PVC as the B-block. It was first demonstrated that PVC prepared via SET-DTLRP initiated with CHI_3 exhibited high chain-end functionality and, therefore, could be employed as a macroinitiator for the $Cu^I Cl/bpy$ catalyzed polymerization of MMA in Ph_2O at 90 °C to produce PMMA-b-PVC-b-PMMA with $M_w/M_n = 1.2$.[163] This was not a trivial result since the $Cu^{II} I_2$ generated during this process is known to be unstable. In a later study, the synthesis of PMMA-b-PVC-b-PMMA was optimized by screening various $Cu^I X$ and Cu^0 catalysts, N-ligands, and solvents capable of dissolving telechelic diiodo–PVC macroninitiator including Ph_2O, DMSO, cyclohexanone, and ethylene carbonate.[331] A nearly 3-fold acceleration in rate could be achieved by utilizing $Cu^I Cl/Me_6$-TREN in DMSO at 90 °C for the polymerization of MMA initiated by telechelic diiodo-PVC as compared to $Cu^I Cl/bpy$ in Ph_2O at 90 °C. In the same study, Cu^0/Me_6-TREN in DMSO at 90 °C was also demonstrated to be a competent catalyst for the LRP of MMA initiated with telechelic diiodo-PVC.[331] A second screen of N-ligands revealed that, in fact, Me_6-TREN and to a lesser extent TREN provided for the most rapid LRP of MMA initiated with telechelic diiodo-PVC in DMSO, yielding high conversion to PMMA-b-PVC-b-PMMA in 15 min at 90 °C or 60−100 min at 25 °C.[332] Additionally, it was shown that increasing the concentration of DMSO as solvent enhanced both the rate of the reaction and the initiator efficiency.[332] The "catalytic effect" of DMSO on the $Cu^I X$ and Cu^0/N-ligand catalyzed LRP of MMA was evaluated through the use CH_3CHCII, CH_2I_2, CHI_3, and $F(CF_2)_8I$ as small-molecule models for the geminal chloroiodo chain ends of telechelic diiodo-PVC.[333] Amongst all catalysts, ligands, and solvents surveyed, the highest rates of polymerization and initiator efficiencies were found for Cu^0/M_6-TREN-catalyzed LRP of MMA initiated with CH_3CHCII at 25 °C in DMSO. Upon lowering the reaction temperature to 0 °C, the reaction still proceeded, but with lower rate and initiator efficiency.[333] In the range of concentrations studied for toluene/DMSO mixtures, an external order of reaction of nearly 1 for DMSO was observed.[333] In addition to PMMA-b-PVC-b-PMMA,[332] PMA-b-PVC-b-PMA was prepared through the Cu^0/Me_6-TREN catalyzed LRP of MA in DMSO at 25–90 °C.[334] At the time these experiments were performed, it was not clear if these results were providing a departure from SET-DTLRP since only iodo-containing dormant species were used. The observations regarding the catalytic effect of DMSO with $Cu^I Cl$ or Cu^0 as catalysts were later attributed in the first publication of SET-LRP[27] to the disproportionation of $Cu^I X/$

Me_6-TREN in DMSO, and in a later study, also to its high polarity and corresponding ability to accelerate electron transfer via the stabilization of polar intermediates.[168]

10. References

(1) Nelson, D. L.; Cox, M. M. *Lehninger Principles of Biochemistry*, 4th ed.; W. H. Freeman: New York, 2004.
(2) Maskarinec, S. A.; Tirrel, D. A. *Curr. Opin. Biotechnol.* **2005**, *16*, 422, and references therein.
(3) Moad, G.; Solomon, D. H. *The Chemistry of Free Radical Polymerization*; Elsevier: New York, 1995.
(4) *Catalysis in Precision Polymerization*; Kobayashi, S., Ed.; John Wiley & Sons: New York 1997.
(5) Webster, O. W. *Science* **1991**, *251*, 887.
(6) Szwarc, M. *Nature* **1956**, *178*, 1168.
(7) Szwarc, M. *J. Polym. Sci., Part A: Polym. Chem.* **1998**, *56*, ix.
(8) Kennedy, J. P. *J. Polym. Sci., Part A: Polym. Chem.* **1999**, *37*, 2285.
(9) *Ring-Opening Polymerization: Mechanisms, Catalysis Structure, Utility*; Brunelle, D. J., Ed.; Hanser Publishers: New York, 1993.
(10) Bielawski, C. W.; Grubbs, R. H. *Prog. Polym. Sci.* **2007**, *32*, 1.
(11) Webster, O. W.; Hertler, W. R.; Sogah, D. Y.; Farnham, W. B.; RajanBabu, T. V. *Polym. Prepr. (Am. Chem. Soc., Div. Polym. Chem.)* **1983**, *24* (2), 52.
(12) Webster, O. W. *J. Polym. Sci., Part A: Polym. Chem.* **2000**, *38*, 2855.
(13) Otsu, T.; Yoshida, M.; Tazaki, T. *Makromol. Chem. Rapid Commun.* **1982**, *3*, 133.
(14) Solomon, D. H.; Rizzardo, E.; Cacioli, P. Eur. Pat. Appl. 135280, 1985.
(15) Hawker, C. J.; Bosman, A. W.; Harth, E. *Chem. Rev.* **2001**, *101*, 3661.
(16) Chiefari, J.; Chong, Y. K.; Ercole, F.; Krstina, J.; Jeffrey, J.; Le, T. P. T.; Mayadunne, R. T. A.; Meijs, G. F.; Moad, C. L.; Moad, G.; Rizzardo, E.; Thang, S. H. *Macromolecules* **1998**, *31*, 5559.
(17) Zard, S. Z. *Angew. Chem., Int. Ed.* **1997**, *36*, 672.
(18) Perrier, S.; Takolpuckdee, P. *J. Polym. Sci., Part A: Polym. Chem.* **2005**, *43*, 5347.
(19) Yamago, S. *J. Polym. Sci., Part A: Polym. Chem.* **2006**, *44*, 1.
(20) Otsu, T. *J. Polym. Sci., Part A: Polym. Chem.* **2000**, *38*, 2121.
(21) Kamaigato, M.; Ando, T.; Sawamoto, M. *Chem. Rev.* **2001**, *101*, 3689.
(22) Otsu, T.; Tazaki, T.; Yoshioka, M. *Chem. Exp.* **1990**, *10*, 801.
(23) Wayland, B. B.; Poszmik, G.; Mukerjee, S. L.; Fryd, M. *J. Am. Chem. Soc.* **1994**, *116*, 7943.
(24) Wayland, B. B.; Basickes, L.; Mukerjee, S.; Wei, M.; Fryd, M. *Macromolecules* **1997**, *30*, 8109.
(25) Matyjaszewski, K.; Xia, J. *Chem. Rev.* **2001**, *101*, 2921.
(26) Percec, V.; Popov, A. V.; Ramirez-Castillo, E.; Weichold, O. *J. Polym. Sci., Part A: Polym. Chem.* **2003**, *41*, 3283.
(27) Percec, V.; Guliashvili, T.; Ladislaw, J. S.; Wistrand, A.; Stjerndahl, A.; Sienkowska, M. J.; Monteiro, M. J.; Sahoo, S. *J. Am. Chem. Soc.* **2006**, *128*, 14156.
(28) Marzilli, L. G.; Marzilli, P. A.; Halpern, J. *J. Am. Chem. Soc.* **1970**, *92*, 5752.
(29) Howes, K. R.; Bakac, A.; Espenson, J. H. *Inorg. Chem.* **1988**, *27*, 3147.
(30) Fischer, H. *J. Polym. Sci., Part A: Polym. Chem.* **1999**, *37*, 1885.
(31) Fischer, H. *Chem. Rev.* **2001**, *101*, 3581.
(32) Ottino, J. M. *AIChE J.* **2003**, *49*, 292.
(33) Ottino, J. M. *Nature* **2004**, *427*, 399.
(34) Kato, M.; Kamigaito, M.; Sawamoto, M.; Higashimura, T. *Polym. Prepr. Jpn.* **1994**, *43*, 1792.
(35) Kato, M.; Kamigaito, M.; Sawamoto, M.; Higashimura, T. *Macromolecules* **1995**, *28*, 1721.
(36) Nagashima, H.; Ozaki, N.; Seki, K.; Ishii, M.; Itoh, K. *J. Org. Chem.* **1989**, *54*, 4497.
(37) Wang, J.-S.; Matyjaszeski, K. *J. Am. Chem. Soc.* **1995**, *117*, 5614.
(38) Matsumoto, H.; Nakano, T.; Nikaido, T.; Nagai, Y. *Chem. Lett.* **1978**, 115.
(39) Lee, G. M.; Weinreb, S. M. *J. Org. Chem.* **1990**, *55*, 1281.
(40) Nagashima, H.; Seki, K.; Oxaki, N.; Wakamtsu, H.; Itoh, K.; Tomo, Y.; Tsuji, J. *J. Org. Chem.* **1990**, *55*, 985.
(41) Percec, V.; Barboiu, B. *Macromolecules* **1995**, *28*, 7970.
(42) Asscher, M.; Vofsi, D. *J. Chem. Soc.* **1964**, 4962.
(43) Orochov, A.; Asscher, M.; Vofsi, D. *J. Chem. Soc. B* **1969**, 255.
(44) Sinnreich, J.; Asscher, M. *J. Chem Soc., Perkin Trans. 1* **1972**, 1543.
(45) Orochov, A.; Asscher, M.; Vofsi, D. *J. Chem Soc., Perkin Trans. 2* **1973**, 1200.
(46) Kamigata, N.; Sawada, H.; Kobayashi, M. *J. Org. Chem.* **1983**, *48*, 3793.
(47) Percec, V.; Barboiu, B.; Neumann, A.; Ronda, J. C.; Zhao, M. *Macromolecules* **1996**, *29*, 3665.

(48) Percec, V.; Kim, H.- J.; Barboiu, B. *Macromolecules* **1997**, *30*, 6702.

(49) Percec, V.; Barboiu, B.; Hill, D. H. *Abstracts of the 36th IUPAC International Symposium on Macromolecules*, Seoul, Korea, Aug 4−9, 1996; p 68.

(50) Percec, V.; Barboiu, B. *Polym. Prepr. (Am. Chem. Soc., Div. Polym Chem.)* **1997**, *38* (1), 733.

(51) Percec, V.; Barboiu, B.; Kim, H.-J. *J. Am. Chem. Soc.* **1998**, *120*, 305.

(52) Percec, V.; Kim, H. -J.; Barboiu, B. *Macromolecules* **1997**, *30*, 8526.

(53) Minisci, F. *Acc. Chem. Res.* **1975**, *8*, 165.

(54) The phenomena reported by Minisci were later observed in attempts to perform the Cu(0) catalyzed living radical copolymerization tetrafluoroethyle (TFE) and hexafluoropropylene (HFP) initiated with perfluoroalkylsulfonyl halides in steel reactors. Feiring, A. E.; Wonchoba, E. R.; Davidson, F.; Percec, V.; Barboiu, B. *J. Polym. Sci., Part. A.: Polym. Chem.* **2000**, *38*, 3313.

(55) Hájek, M.; Silhavy, P; Málek, J. *Tetrahedron Lett.* **1974**, *36*, 3193. (b) Hájek, M.; Silhavy, P. *Collect. Czech. Chem. Commun.* **1983**, *48*, 1710.

(56) Hájek, M.; Silhavy, P.; Málek, J. *Collect. Czech. Chem. Commun.* **1980**, *45*, 3488.

(57) Hájek, M.; Silhavy, P.; Málek, J. *Collect. Czech. Chem. Commun.* **1980**, *45*, 3502.

(58) Hájek, M.; Silhavy, P.; Spirková, B. *Collect. Czech. Chem. Commun.* **1990**, *55*, 2949.

(59) Percec, V.; Barboiu, B.; van der Sluis, M. *Macromolecules* **1998**, *31*, 4053.

(60) Van der Sluis, M.; Barboiu, B.; Pesa, N.; Percec, V. *Macromolecules* **1998**, *31*, 9409.

(61) Matyjaszewski, K.; Coca, S.; Gaynor, S. G.; Wei, M.; Woodworth, B. E. *Macromolecules* **1997**, *30*, 7348.

(62) Tamba, M.; Dajka, K.; Ferrerri, C.; Asmus, K.-D.; Chatgiliaoglu, C. *J. Am. Chem. Soc.* **2007**, *129*, 8716.

(63) Kórösy, F. *Nature* **1947**, *160*, 21.

(64) Tributsch, H.; Bennet, J. C. *Ber. Bunsen-Ges. Phys. Chem.* **1976**, *80*, 321.

(65) Timofeev, S. V.; Smirnova, A. L.; Blyumberg, E. A. *Kinet. Katal.* **1991**, *32*, 1176.

(66) Smirnova, A. L.; Tavadyan, L. A.; Blyumberg, E. A. *Kinet. Katal.* **1988**, *29*, 1098.

(67) Percec, V.; Asandei, A. D.; Asgarzadeh, F.; Bera, T. K.; Barboiu, B. *J. Polym. Sci., Part A: Polym. Chem.* **2000**, *38*, 3839.

(68) Percec, V.; Asandei, A. D.; Asgarzadeh, F.; Barboiu, B.; Holerca, M. N.; Grigoras, C. *J. Polym. Sci., Part A: Polym. Chem.* **2000**, *38*, 4353.

(69) Poshkus, A. C.; Herweh, J. E.; Magnotta, F. A. *J. Org. Chem.* **1963**, *28*, 2766.

(70) Litvinenko, L. M.; Dadali, V. A.; Savelova, V. A.; Krichvtsova, T. I. *J. Gen. Chem. USSR* **1964**, *34*, 3780.

(71) Gilbert, E. E. *Synthesis* **1969**, *1*, 3.

(72) Siggia, S.; Eddsberg, R. L. *Ind. Eng. Chem., Anal. Ed.* **1948**, *20*, 938.

(73) Grigoras, C.; Percec, V. *J. Polym. Sci., Part A: Polym. Chem.* **2005**, *43*, 319.

(74) Percec, V.; Grigoras, C. *J. Polym. Sci., Part A: Polym. Chem.* **2005**, *43*, 3920.

(75) Percec, V.; Grigoras, C. *J. Polym. Sci. Part A: Polym Chem.* **2005**, *43*, 5283.

(76) Percec, V.; Barboiu, B. *Abstracts of the 36th IUPAC International Symposium on Macromolecules*, Seoul, Korea, Aug 4−9, 1996; p 672.

(77) Barbiou, B.; Percec, V. *Macromolecules* **2001**, *34*, 8626.

(78) Percec, V.; Cho, W. D.; Ungar, G.; Yeardley, D. J. P. *J. Am. Chem. Soc.* **2001**, *123*, 1302.

(79) Percec, V.; Holerca, M. N.; Numelin, S.; Morrison, J. J.; Glodde, M.; Smidrkal, J.; Peterca, M.; Rosen, B. M.; Uchida, S.; Balagurusamy, V. S. K.; Sienkowska, M. J.; Heiney, P. A. *Chem.−Eur. J.* **2006**, *12*, 6216.

(80) Percec, V.; Peterca, M.; Sienkowska, M. J.; Ilies, M. A.; Aqad, E.; Smidrkal, J.; Heiney, P. A. *J. Am. Chem. Soc.* **2006**, *128*, 3324.

(81) Percec, V.; Dulcey, A. E.; Balagurusamy, V. S. K.; Miura, Y.; Smidrkal, J.; Peterca, M.; Numelin, S.; Edlund, U.; Hudson, S. D.; Heiney, P. A.; Duan, H.; Magonov, S. N.; Vinogradov, S. A. *Nature* **2004**, *430*, 764.

(82) Percec, V.; Glodde, M.; Bera, T. K.; Miura, Y.; Shiyanovskaya, I.; Singer, K. D.; Balagurusamy, V. S. K.; Heiney, P. A.; Schnell, I.; Rapp, A.; Spiess, H.-W; Hudson, S. D.; Duan, H. *Nature* **2002**, *419*, 384.

(83) Rosen, B. M.; Wilson, C. J.; Wilson, D. A.; Peterca, M.; Imam, M. R.; Percec, V. *Chem. Rev.* **2009**, *109*, (cr-2009-00157).

(84) Percec, V.; Bera, T. K.; De, B. B.; Sanai, Y.; Smith, J.; Holerca, M. N.; Barboiu, B.; Grubbs, R. B.; Fréchet, J. M. J. *J. Org. Chem.* **2001**, *66*, 2104.

(85) Percec, V.; Grigoras, C.; Bera, T. K.; Barboiu, B.; Bissel, P. *J. Polym. Sci., Part A: Polym. Chem.* **2005**, *43*, 4894.

(86) Percec, V.; Barboiu, B.; Grigoras, C.; Bera, T. K. *J. Am. Chem. Soc.* **2003**, *125*, 6503.

(87) Percec, V.; Grigoras, C.; Kim, H.-J. *J. Polym. Sci., Part A: Polym. Chem.* **2004**, *42*, 505.

(88) Starnes, W. H., Jr. *Prog. Polym. Sci.* **2002**, *27*, 2133.

(89) Starnes, W. H., Jr.; Zaikov, V. G.; Chung, H. T.; Wojciechowski, B. J.; Tran, H. V.; Saylor, K.; Benedikt, G. M. *Macromolecules* **1998**, *3*, 1508.

(90) Starnes, W. H., Jr. *J. Vinyl Addit. Technol.* **1996**, *2*, 277.

(91) Starnes, W. H., Jr.; Chung, H.; Wojciechowski, B. J.; Skillicorn, D. E.; Benedikt, G. M. *Adv. Chem. Ser.* **1996**, *249*, 3.

(92) Park, G. S.; Saleem, M. *Polym. Bull.* **1979**, *1*, 409.

(93) Valko, L.; Tvaroska, I.; Kovarik, P. *Eur. Polym. J.* **1975**, *11*, 411.

(94) Valko, L.; Tvaroska, I. *Angew. Makromol. Chem.* **1972**, *23*, 173.

(95) Enomoto, S. *J. Polym. Sci., Part A: Polym. Chem.* **1969**, *7*, 1255.

(96) Ahrens, W.; Brandstetter, F.; Hildenbrand, P.; Simak, P. *J. Macromol. Sci., Chem.* **1982**, *17*, 1093.

(97) Abdel-Alim, A. H.; Hamielec, A. E. *J. Appl. Polym. Sci.* **1972**, *16*, 783.

(98) Vidotto, G.; Crosato-Arnaldi, A.; Talamini, G. *Makromol. Chem.* **1968**, *114*, 217.

(99) Starnes, W. H., Jr.; Wojciechowski, B. J.; Velazquez, A.; Benedikt, G. M. *Macromolecules* **1992**, *25*, 3638.

(100) Starnes, W. H., Jr.; Wojciechowski, B. J. *Makromol. Chem. Macromol. Symp.* **1993**, *70−71*, 1.

(101) Starnes, W. H., Jr.; Schilling, F. C.; Plitz, I. M.; Cais, R. E.; Freed, D. J.; Hartless, R. L.; Bovey, F. A. *Macromolecules* **1983**, *16*, 790.

(102) Park, G. S.; Saleem, M. *Polym. Bull.* **1979**, *1*, 409.

(103) Rigo, A.; Palma, G.; Talamini, G. *Makromol. Chem.* **1972**, *153*, 219.

(104) Carenza, M.; Palma, G.; Tavan, M. *J. Polym. Sci., Polym. Symp.* **1973**, *42*, 1031.

(105) Pike, R. D.; Starnes, W. H., Jr.; Jeng, J. P.; Bryant, W. S.; Kourtesis, P.; Adams, C. W.; Bunge, S. D.; Kang, Y. M.; Kim, A. S.; Kim, J. H.; Macko, J. A.; O'Brien, C. P. *Macromolecules* **1997**, *30*, 6957.

(106) Hjertberg, T.; Sorvik, E. M. In *Degradation and Stabilization of PVC*; Owen, E. D., Ed.; Elsevier: New York, 1984; Chapter 2, pp 21−79.

(107) Rogestedt, M.; Hjertberg, T. *Macromolecules* **1993**, *26*, 60.

(108) Starnes, W. H., Jr.; Plitz, I. M.; Schiling, F. C.; Villacorta, G. M.; Park, G. S.; Saremi, A. H. *Macromolecules* **1984**, *17*, 2507.

(109) Benedikt, G. M.; Cozens, R. J.; Goodall, B. L.; Rhodes, L. F.; Bell, M. N.; Kemball, A. C.; Starnes, W. H. *Macromolecules* **1997**, *30*, 10.

(110) Purmova, J.; Pauwels, K. F. D.; van Zoelen, W.; Vorenkamp, E. J.; Schouten, A. J.; Coote, M. L. *Macromolecules* **2005**, *38*, 6352.

(111) Queffelec, J.; Gaynor, S. G.; Matyjaszewski, K. *Macromolecules* **2000**, *33*, 8629.

(112) Asandei, A. D.; Percec, V. *J. Polym. Sci., Part A: Polym. Chem.* **2001**, *39*, 3392.

(113) Fischer, H. *J. Am. Chem. Soc.* **1986**, *108*, 3925.

(114) Fischer, H. *Macromolecules* **1997**, *30*, 5666.

(115) Souaille, M.; Fischer, H. *Macromolecules* **2000**, *33*, 7378.

(116) Rueegge, D.; Fischer, H. *Int. J. Chem. Kinet.* **1989**, *21*, 703.

(117) Kother, T.; Marque, S.; Martschke, R.; Popov, M.; Fischer, H. *J. Chem. Soc., Perkins Trans. 2* **1998**, 1553.

(118) Souaille, M.; Fischer, H. *Macromolecules* **2001**, *34*, 2830.

(119) Marque, S.; LeMercier, C.; Tordo, P.; Fischer, H. *Macromolecules* **2000**, *33*, 4403.

(120) Sobek, J.; Martschke, R.; Fischer, H. *J. Am. Chem. Soc.* **2001**, *123*, 2849.

(121) *Polymer Handbook*; Brandrup, J., Immergut, E. H., Grulke, E. A., Eds.; Wiley: New York 1999; pp II−100.

(122) Fenwick, F. *J. Am. Chem. Soc.* **1926**, *48*, 860.

(123) Heinerth, E. *Z. Elektrochem.* **1931**, *37*, 61.

(124) Malyszko, J.; Duda, L. *Monatsh. Chem.* **1975**, *106*, 633.

(125) Ciavatta, L.; Ferri, D.; Polbari, R. *J. Inorg. Nucl. Chem.* **1980**, *42*, 593.

(126) Endicott, J. F.; Taube, H. *Inorg. Chem.* **1965**, *4*, 437.

(127) Ahrland, S.; Rowsthorne, J. *Acta Chem. Scand.* **1970**, *24*, 157.

(128) Tindall, G. W.; Bruckenstein, S. *Anal. Chem.* **1968**, *40*, 1402.

(129) Desmarquest, J. P.; Trinh-Dinh, C.; Bloch, O. *J. Electroanal. Chem.* **1970**, *27*, 101.

(130) Tsarevsky, N. V.; Braunecker, W. A.; Matyjaszewski, K. *J. Organomet. Chem.* **2007**, *692*, 3212.

(131) Percec, V.; Popov, A. V.; Ramirez-Castillo, E.; Monteiro, M.; Barboiu, B.; Weichold, O.; Asandei, A. D.; Mitchell, C. M. *J. Am. Chem. Soc.* **2002**, *124*, 4940.

(132) Guarrotxena, N.; Martinez, G.; Millán, J. *J. Polym. Sci., Part A: Polym. Chem.* **1996**, *34*, 2387.

(133) Bovey, F. A.; Hood, F. P.; Anderson, E. W.; Kornegay, R. L. *J. Phys. Chem.* **1967**, *71*, 312.

(134) Talamani, G.; Vidotto, G. *Makromol. Chem.* **1967**, *100*, 48.

(135) Cavalli, L.; Borsini, G. C.; Carrano, G.; Confalonieri, G. *J. Polym Sci., Part A: Polym. Chem.* **1970**, *8*, 801.

(136) Huang, W.-Y.; Wu, F.-H *Isr. J. Chem.* **1999**, *39*, 167.

(137) Feiring, A. E.; Wonchoba, E. R. *J. Fluorine Chem.* **2000**, *105*, 129.

(138) Dolbier, W. R., Jr.; Médebielle, M.; Ait-Mohand, S. *Tetrahedron Lett.* **2001**, *42*, 4811.

(139) Percec, V.; Popov, A. V.; Ramierez-Castillo, E.; Coelho, J. F. J.; Hinojosa-Falcon, L. A. *J. Polym. Sci., Part A: Polym. Chem.* **2004**, *42*, 6267.

(140) Percec, V.; Popov, A. V.; Ramirez-Castillo, E.; Weichold, O. *J. Polym. Sci., Part A: Polym. Chem.* **2004**, *42*, 6364.

(141) Coelho, J. F. J.; Simões, P. N.; Mendonça, P. V.; Fonseca, A. C.; Gil, M. H. *J. Appl. Polym. Sci.* **2008**, *109*, 2729.

(142) Lamberth, D. O.; Palmer, G. *J. Biol. Chem.* **1973**, *248*, 6095.

(143) Ji, B.-s.; Ji, H.; Liu, G.-q. *Acta Pharmacol. Sin* **2004**, *25*, 297.

(144) Ascenzi, P.; Bertollini, A.; Colletta, M.; Lucacchini, A. *Biotechnol. Appl. Biochem.* **1999**, *30*, 185.

(145) Burgess, R. H. In *Manufacture and Processing of PVC*; Burgess, R. H., Ed.; MacMillan: New York, 1982; pp 16−17.

(146) Anselmi, E.; Blazejewski, J. -C.; Tordeaux, M.; Wakselman, C. *J. Fluorine Chem.* **2000**, *105*, 41.

(147) Marvel, C. S.; Glavis, F. J. *J. Am. Chem. Soc.* **1938**, *60*, 2622.

(148) Ivin, K. *J. Polym. Sci., Part A: Polym. Chem.* **1998**, *38*, 2137.

(149) Percec, V.; Ramirez-Castillo, E.; Hinojosa-Falcon, L. A.; Popov, A. V. *J. Polym. Sci., Part A: Polym. Chem.* **2005**, *43*, 2185.

(150) Coelho, J. F. J.; Mendonça, P. V.; Popov, A. V.; Percec, V.; Gonçalves, P. M. O. F.; Gil, M. H. *J. Polym. Sci., Part A: Polym. Chem.* 2009. in press.

(151) Coelho, J. F. J.; Carbalho, E. Y.; Marques, D. S.; Popov, A. V.; Percec, V.; Gonçalves, P. M. F. O.; Gil, M. H. *J. Polym. Sci., Part A: Polym. Chem.* **2008**, *46*, 421.

(152) Coelho, J. F. J.; Silva, A. M. F. P.; Popov, A. V.; Percec, V.; Abreu, M. V.; Gonçalves, P. M. O. F.; Gil, M. H. *J. Polym. Sci., Part A: Polym. Chem.* **2006**, *44*, 2809.

(153) Coelho, J. F. J.; Carvalho, E. Y.; Marques, D. S.; Popov, A. V.; Percec, V.; Gil, M. H. *J. Polym. Sci., Part A.: Polym. Chem.* **2008**, *46*, 6542.

(154) Percec, V.; Ramierez-Castillo, E.; Popov, A. V.; Hinojosa-Falcon, L. A.; Guliashvili, T. *J. Polym. Sci., Part A: Polym. Chem.* **2005**, *43*, 2178.

(155) Coelho, J. F. J.; Carvalho, E. Y.; Marques, D. S.; Popov, A. V.; Goncalves, P. M.; Gil, M. H. *Macromol. Chem. Phys.* **2007**, *208*, 128.

(156) Coelho, J. F. J.; Gois, J.; Fonseca, A. C.; Carvalho, R. A.; Popov, A. V.; Percec, V.; Gil, M. H. *J. Polym. Sci., Part A: Polym. Chem.* **2009**, *47*, 4454.

(157) Percec, V.; Popov, A. V.; Ramierez-Castillo, E.; Coelho, J. F. J. *J. Polym. Sci., Part A: Polym. Chem.* **2005**, *43*, 773.

(158) Sienkowska, M. J.; Percec, V. *J. Polym. Sci., Part A: Poylm. Chem.* **2009**, *47*, 635.

(159) Coelho, J. F. J.; Silva, A. M. F. P.; Popov, A. V.; Percec, V.; Abreu, M. V.; Gonçalves, P. M. O. F.; Gil, M. H. *J. Polym. Sci., Part A: Polym. Chem.* **2006**, *44*, 3001.

(160) Coelho, J. F. J.; Carreira, M.; Gonçalves, P. M. O. F.; Popov, A. V.; Gil, M. H. *J. Vinyl Addit. Technol.* **2006**, *12*, 156.

(161) Coelho, J. F. J.; Carreira, M.; Popov, A. V.; Gonçalves, P. M. O. F.; Gil, M. H. *Eur. Polym. J.* **2006**, *42*, 2313.

(162) Percec, V.; Sienkowska, M. J. *J. Polym. Sci., Part A: Polym. Chem.* **2009**, *47*, 628.

(163) Percec, V.; Guliashvili, T.; Popov, A. V.; Ramirez-Castillo, E. *J. Polym. Sci., Part A: Polym. Chem.* **2005**, *43*, 1478.

(164) Ladislaw, J. S. Ph.D.Thesis, University of Pennsylvania, Philadelphia, PA, 2008.

(165) Rosen, B. M.; Percec, V. *J. Polym. Sci., Part A: Polym. Chem.* **2008**, *46*, 5663.

(166) Guliashvili, T.; Percec, V. *J. Polym. Sci., Part A: Polym. Chem.* **2007**, *45*, 1607.

(167) Lligadas, G.; Rosen, B. M.; Bell, C. A.; Monteiro, M. J.; Percec, V. *Macromolecules* **2008**, *41*, 8365.

(168) Nguyen, N. H.; Rosen, B. M.; Lligadas, G.; Percec, V. *Macromolecules* **2009**, *42*, 2379.

(169) Xue, L.; Agarwal, U. S.; Lemstra, P. J. *Macromolecules* **2002**, *35*, 8650.

(170) Ciampolini, M.; Nardi, N. *Inorg. Chem.* **1966**, *5*, 41.

(171) Willoughby, I.; Haddleton, D. M.; Levere, M. Online Monitoring of Single Electron Transfer Living Radical Polymerizations using PL-PMC; Varian Application Note SI-01202; http://www.varianinc.com.

(172) Matyjaszewski, K.; Tsarevsky, N. V.; Braunecker, W. A.; Dong, H.; Huang, J.; Jakubowski, W.; Kwak, Y.; Nicolay, R.; Tang, W.; Yoon, A. E. *Macromolecules* **2007**, *40*, 7795.

(173) Lligadas, G.; Percec, V. *J. Polym. Sci., Part A: Polym. Chem.* **2007**, *45*, 4684.

(174) Lligadas,; Ladislaw, J. S.; Guliashvili, T.; Percec, V. *J. Polym. Sci., Part A: Polym. Chem.* **2008**, *46*, 278.

(175) Lligadas, G.; Percec, V. *J. Polym. Sci., Part A: Polym. Chem.* **2008**, *46*, 6880.

(176) Lligadas, G.; Rosen, B. M.; Monteiro, M. J.; Percec, V. *Macromolecules* **2008**, *41*, 8360.

(177) Lligadas, G.; Percec, V. *J. Polym. Sci., Part A: Polym. Chem.* **2008**, *46*, 4917.

(178) Lligadas, G.; Percec, V. *J. Polym. Sci., Part A: Polym. Chem.* **2008**, *46*, 3174.

(179) Lligadas, G.; Percec, V. *J. Polym. Sci., Part A: Polym. Chem.* **2008**, *46*, 2745.

(180) Hillenkamp, F.; Karas, M. In *MALDI MS: A Practical Guide to Instrumentation, Methods, and Applications*; Hillenkamp, F., Peter-Katalini, J., Eds. Wiley-VCH: Weinheim, Germany, 2007; pp14−15.

(181) Matyjaszewski, K.; Pintauer, T.; Gaynor, S. *Macromolecules* **2000**, *33*, 1476.

(182) Ydens, I.; Moins, S.; Botteman, F.; Degee, P.; Dubois, P. *e-Polym.* **2004**, *39*.

(183) Faucher, S.; Okrutny, P.; Zhu, S. *Macromolecules* **2006**, *39*, 3.

(184) Percec group. Unpublished results, 2009.

(185) Whittaker, M. R.; Urbani, C. N.; Monteiro, M. J. *J. Polym. Sci., Part A: Polym. Chem.* **2008**, *46*, 6346.

(186) Nguyen, N. H.; Rosen, B. M.; Jiang, X.; Fleischmann, S.; Percec, V. *J. Polym. Sci., Part A: Polym. Chem.* **2009**, *47*, 5577.

(187) Gu, L.; Shen, Z.; Feng, C.; Li, Y.; Lu, G.; Huang, X. *J. Polym. Sci., Part A: Polym. Chem.* **2008**, *46*, 4056.

(188) Feng, C.; Shen, Z.; Gu, L.; Zhang, S.; Li, L.; Lu, G.; Huang, X. *J. Polym. Sci., Part A: Polym. Chem.* **2008**, *46*, 5638.

(189) Masci, G.; Giacomelli, L.; Crescenzi, V. *Macromol. Rapid Commun.* **2004**, *25*, 559.

(190) Feng, C.; Shen, Z.; Li, Y.; Gu, L.; Zhang, Y.; Lu, G.; Huang, X. *J. Polym. Sci., Part A: Polym. Chem.* **2009**, *47*, 1811.

(191) Percec, V.; Grigoras, C. *J. Polym. Sci., Part A: Polym. Chem.* **2005**, *43*, 5609.

(192) Zhang, Z.; Wang, W.; Xia, H.; Zhu, J.; Zhang, W.; Zhu, X. *Macromolecules* 2009, *42*DOI: 10.1021/ma901064h.

(193) Wang, W.; Zhang, Z.; Zhu, J.; Zhou, N.; Zhu, X. *J. Polym. Sci., Part A: Polym. Chem.* **2009**, *47*, DOI: 10.1002/pola.23674.

(194) Sienkowska, M. J.; Rosen, B. M.; Percec, V. *J. Polym. Sci., Part A: Polym. Chem.* **2009**, *47*, 4130.

(195) Subramanian, S. H.; Babu, R. P.; Dhamodharan, R. *Macromolecules* **2008**, *41*, 262.

(196) Wright, P. M.; Mantovani, G.; Haddleton, D. M. *J. Polym. Sci., Part A: Polym. Chem.* **2008**, *46*, 7376.

(197) Xiang, J.; Fleischmann, S.; Nguyen, N. H.; Rosen, B. M.; Percec, V. *J. Polym. Sci., Part A: Polym Chem.* **2009**, *47*, 5591.

(198) Percec, V.; Heck, J.; Tomazos, D.; Ungar, G. *J. Chem. Soc., Perkins Trans.* **1993**, *2*, 2381.

(199) Kwon, Y. K.; Chvalun, S.; Schnedier, A. I.; Blackwell, J.; Percec, V.; Heck, J. A. *Macromolecules* **1994**, *27*, 6129.

(200) Kwon, Y. K.; Chvalun, S. N.; Blackwell, J.; Percec, V.; Heck, J. A. *Macromolecules* **1995**, *28*, 1552.

(201) Percec, V.; Schlueter, D.; Ronda, J. C.; Johansson, G.; Ungar, G.; Zhou, J. P. *Macromolecules* **1996**, *29*, 1464.

(202) Percec, V.; Schlueter, D. *Macromolecules* **1997**, *30*, 5783.

(203) Percec, V.; Schlueter, D.; Ungar, G.; Cheng, S. Z. D.; Zhang, A. *Macromolecules* **1998**, *31*, 1745.

(204) Percec, B.; Ahn, C. H.; Ungar, G.; Yeardley, D. J. P.; Möller, M.; Sheiko, S. S. *Nature* **1998**, *391*, 161.

(205) Percec, V.; Ahn, C. H.; Cho, W.-D.; Jameson, A. M.; Kim, J.; Leman, T.; Schmidt, M.; Gerle, M.; Möller, M.; Prokhorova, S. A.; Sheiko, S. S.; Cheng, S. Z. D.; Zhang, A.; Ungar, G.; Yeardley, D. J. P. *J. Am. Chem. Soc.* **1998**, *120*, 8619.

(206) Shcherbina, M. A.; Chvalun, S. N.; Percec, V. *Polym. Sci., Ser. A* **2008**, *50*, 166.

(207) Rosen, B. M.; Jiang, X.; Wilson, C. J.; Nguyen, N. H.; Monteiro, M. J.; Percec, V. *J. Polym. Sci., Part A: Polym. Chem.* **2009**, *47*, 5606.

(208) Matyjaszewski, K.; Paik, H. J.; Zhou, P.; Diamanti, S. J. *Macromolecules* **2001**, *34*, 5125.

(209) Boyle, R. E. *J. Org. Chem.* **1966**, *31*, 3880.

(210) Gurr, P. A.; Mill, M. F.; Qiao, G. G.; Solomon, D. H. *Polymer* **2005**, *46*, 2097.

(211) Plessis, C.; Arzamendi, G.; Alberdi, J. M.; van Herk, A. M.; Leiza, J. R.; Asua, J. M. *Macromol. Rapid Commun.* **2003**, *24*, 173.

(212) Tang, X.; Liang, X.; Yang, Q.; Fan, X.; Shen, Z.; Zhou, Q. *J. Polym. Sci., Part A: Polym. Chem.* **2009**, *47*, 4420.

(213) Monge, S.; Darcos, V.; Haddleton, D. M. *J. Polym. Sci., Part A: Polym. Chem.* **2004**, *42*, 6299.

(214) Bell, C. A.; Whittaker, M. R.; Gahan, L. R.; Monteiro, M. J. *J. Polym. Sci., Part A: Polym. Chem.* **2008**, *46*, 146.

(215) Bunnet, J. F.; Scamehorn, R. G.; Traber, R. P. *J. Org. Chem.* **1976**, *41*, 3677.

(216) Malyszko, J.; Scendo, M. *Monatsh. Chem.* **1987**, *118*, 435.

(217) Malyszko, J.; Scendo, M. *J. Electroanal. Chem.* **1989**, *269*, 113.

(218) Yanov, L. A.; Molodov, A. I. *Elektrokhimiya* **1975**, *11*, 1112.

(219) Singh, P.; MacLeod, I. D.; Parker, A. J. *J. Solution Chem.* **1982**, *11*, 495.

(220) Carmichael, A. J.; Haddleton, D. M.; Bon, S. A. F.; Seddon, K. R. *Chem. Commun.* **2000**, 1237.

(221) Bierdron, T.; Kubisa, P. *Macromol. Rapid Commun.* **2001**, *22*, 1237.

(222) Bierdron, T.; Kubisa, P. *J. Polym. Sci., Part A: Polym. Chem.* **2002**, *40*, 2799.

(223) Bierdron, T.; Kubisa, P. *Polym. Int.* **2003**, *52*, 1584.

(224) Sarbu, T.; Matyjaszewski, K. *Macromol. Chem. Phys.* **2001**, *202*, 3379.

(225) Perrier, S.; Davies, T. P; Carmichael, A. J.; Haddleton, D. M. *Chem. Commun.* **2002**, 2226.

(226) Perrier, S.; Davies, T. P.; Carmichael, A. J.; Haddleton, D. M. *Eur. Polym. J.* **2003**, *32*, 417.

(227) Ryan, J.; Aldabbagh, F.; Zetturland, P. B.; Yamada, B. *Macromol. Rapid Commun.* **2004**, *25*, 930.

(228) Zhang, H.; Hong, K.; Mays, J. W. *Polym. Bull.* **2004**, *52*, 9.

(229) Percec, V.; Wang, J. H.; Clough, R. S. *Makromol. Chem. Macromol. Symp.* **1992**, *54/55*, 275.

(230) Percec, V.; Clough, R. S.; Grigoras, M.; Rinaldi, P. L.; Litman, V. E. *Macromolecules* **1993**, *26*, 3650.

(231) Percec, V.; Clough, R. S.; Rinaldi, P. L.; Litman, V. E. *Macromolecules* **1991**, *24*, 5889.

(232) Randles, J. E. B. *J. Chem. Soc.* **1941**, 802.

(233) Ahrland, S.; Bläuenstein, P.; Tagesson, B.; Tuhtar, D. *Acta Chem. Scand. A* **1980**, *34*, 265.

(234) Foll, A.; Le Demezet, M.; Courtot-Coupez, J. *J. Electroanal. Chem.* **1972**, *35*, 41.

(235) Coetzee, J. F.; Siao, W. S. *Inorg. Chem.* **1963**, *2*, 14.

(236) Datta, D.; Indian, J. *Chem.* **1987**, *26*, 605.

(237) Lewandowski, A.; Malinska, J. *Electrochim. Acta* **1989**, *34*, 333.

(238) Cotton, F. A.; Wilkinson, G. *Advanced Inorganic Chemistry*, 3rd ed.; John Wiley & Sons: New York, 1970; p 905.

(239) Haddleton, D. M.; Jasieczek, C. B.; Hannon, M. J.; Shooter, A. J. *Macromolecules* **1997**, *30*, 2190.

(240) Haddleton, D. M. personal communication.

(241) Mamardashvili, G. M.; Berezin, B. D. *Russ. J. Coord. Chem.* **2006**, *32*, 276.

(242) Rosen, B. M.; Percec, V. *J. Polym. Sci., Part A: Polym. Chem.* **2007**, *45*, 4950.

(243) Tang, W.; Kwak, Y.; Braunecker, W.; Tsarevsky, N. V.; Coote, M. L.; Matyjaszewski, K. *J. Am. Chem. Soc.* **2008**, *130*, 10702.

(244) Gaynor, S.; Qiu, J.; Matyjaszewski, K. *Macromolecules* **1998**, *31*, 5951.

(245) Jousset, S.; Qiu, J.; Matyjaszewski, K. *Macromolecules* **2001**, *34*, 6641.

(246) Wang, X.-S.; Jackson, R. A.; Armes, S. P. *Macromolecules* **2000**, *33*, 255.

(247) McDonald, S.; Rannard, S. P. *Macromolecules* **2001**, *34*, 8600.

(248) Micheva, R.; Paneva, D.; Mespouille, L.; Manolova, N.; Rashkov, I.; Dubois, P. *J. Polym. Sci., Part A: Polym. Chem.* **2009**, *47*, 1108.

(249) Monteiro, M. J.; Guliashvili, T.; Percec, V. *J. Polym. Sci., Part A: Polym. Chem.* **2007**, *45*, 1835.

(250) Nguyen, N. H.; Jiang, X.; Fleischmann, S.; Rosen, B. M.; Percec, V. *J. Polym. Sci., Part A: Polym. Chem.* 2009, *47*, 5629.

(251) Thomas, J. M.; Thomas, W. J. *Heterogeneous Catalysis*; Wiley-VCH: Weinheim, Germany, 1997.

(252) Ye, J.; Narain, R. *J. Phys. Chem. B* **2009**, *113*, 676.

(253) Lin, J.-L.; Bent, B. E. *J. Phys. Chem.* **1992**, *96*, 8529.

(254) Lin, J.-L.; Bent, B. E. *J. Phys. Chem.* **1993**, *97*, 9713.

(255) Lin, J. L.; Bent, B. E. *J. Phys. Chem.* **1996**, *100*, 10721.

(256) Armentrout, D. D.; Grassian, V. H. *Langmuir* **1994**, *10*, 2071.

(257) Egorov, A. M.; Mayukhova, S. A.; Anisimov, A. V. *Int. J. Chem. Kinet.* **2005**, *37*, 496.

(258) Egorov, A. M.; Matyukhova, S. A.; Anisimov, A. V. *Russ. J. Gen. Chem.* **2005**, *75*, 1131.

(259) Egorov, A. M.; Matyukhova, S. A.; Anisimov, A. V. *Int. J. Chem. Kinet.* **2005**, *37*, 296.

(260) Egorov, A. M.; Matyukhova, S. A. *Int. J. Chem. Kinet.* **2007**, *39*, 547.

(261) Liou, Y. H.; Lo, S. L.; Lin, C. J. *Water Res.* **2007**, *41*, 1705.

(262) Feng, C.; Shen, Z.; Yang, D.; Li, Y.; Hu, J.; Lu, G.; Huang, X. *J. Polym. Sci., Part A: Polym. Chem.* **2009**, *47*, 4346.

(263) Powder Metallurgy. In *Tool and Manufacturing Engineers Handbook*, 4th ed.; Bakerjian, R., Cubberly, W. H., Eds.; Society of Manufacturing Engineers: Dearborn, MI, 1988; p17-I.

(264) ASTM Standard B 258-02; ASTM International: West Conshohocken, PA, 2002.

(265) Wakselman, C. *J. Fluorine Chem.* **1992**, *59*, 367.

(266) Mulliken, R. S. *J. Am. Chem. Soc.* **1952**, *74*, 811.

(267) Hush, N. S. *Trans. Faraday Soc.* **1961**, *57*, 557.

(268) Hush, N. S. *Prog. Inorg. Chem.* **1967**, *8*, 391.

(269) Taube, H. *Electron-transfer Reactions of Complex Ions in Solution*; Academic Press: New York, 1970.

(270) Taube, H.; Myers, H. J.; Rich, R. L. *J. Am. Chem. Soc.* **1953**, *75*, 4118.

(271) Taube, H. *Angew. Chem., Int. Ed. Engl.* **1984**, *23*, 329.

(272) Robin, M. B.; Day, P. *Adv. Inorg. Chem. Radiochem.* **1967**, *10*, 247.

(273) Rosokha, S. V.; Kochi, J. K. *Acc. Chem. Res.* **2008**, *41*, 641, and references therein.

(274) Marcus, R. A. *J. Chem. Phys.* **1956**, *24*, 966.

(275) Pintauer, T.; McKenzie, B.; Matyjaszewski, K. *ACS Symp. Ser.* **2003**, *33*, 5825.

(276) Gillies, M. B.; Matyjaszewski, K.; Norrby, P.-O.; Pintauer, T.; Poli, R.; Richard, P. *Macromolecules* **2003**, *36*, 8551.

(277) Matyjaszewski, K.; Poli, R. *Macromolecules* **2005**, *38*, 8093.

(278) Lin, C. Y.; Coote, M.; Gennaro, A.; Matyjaszewski, K. *J. Am. Chem. Soc.* **2008**, *130*, 12762.

(279) Creaser, I. I.; Sargeson, A. M.; Zanella, A. W. *Inorg. Chem.* **1983**, *22*, 4022.

(280) Bernhard, P.; Sargeson, A. M. *Inorg. Chem.* **1987**, *26*, 4122.

(281) Dubs, R. V.; Gahan, L. R.; Sargeson, A. M. *Inorg. Chem.* **1983**, *22*, 2523.

(282) Sutin, N. *Acc. Chem. Res.* **1982**, *15*, 275.

(283) Iovu, M.; Maithufi, N.; Mapolie, S. *Macromol. Symp.* **2003**, *193*, 209.

(284) Dimroth, K.; Reichardt, C.; Siepmann, T.; Bohlmann, F. *Liebigs Ann. Chem.* **1963**, *661*, 1.

(285) Reichardt, C.; Harbusch-Görnert, E. *Liebigs Ann. Chem.* **1983**, 721.

(286) Reichardt, C. In *Solvents and Solvent Effects in Organic Chemistry*; Wiley-VCH: Weinheim, Germany, 2003; Chapter *7*, pp 411−425.

(287) Huang, W.-Y. *J. Flourine Chem.* **1992**, *58*, 1.

(288) Wakselman, C. *J. Flourine Chem.* **1992**, *59*, 367.

(289) Chen, Q.-Y. *Isr. J. Chem.* **1999**, *39*, 179.

(290) Dolbier, W. R. *Chem. Rev.* **1996**, *96*, 1557.

(291) Feiring, A. E. *J. Org. Chem.* **1985**, *50*, 3269.

(292) Feiring, A. E. *J. Fluorine Chem.* **1984**, *24*, 191.

(293) Andrieux, C. P.; Gellis, L.; Savéant, J. M. *J. Am. Chem. Soc.* **1990**, *112*, 786.

(294) Metrangolo, P.; Resnati, G. *Chem.−Eur. J.* **2001**, *7*, 2511.

(295) Metrangolo, P.; Resnati, G.; Pilati, T.; Liantonio, R.; Meyer, F. *J. Polym. Sci., Part A: Polym. Chem.* **2006**, *45*, 1.

(296) Amatore, C.; Capobianco, G.; Farnia, G.; Sandonà, G.; Savéant, J. M.; Saverin, M. G.; Vianello, E. *J. Am. Chem. Soc.* **1985**, *107*, 1815.

(297) Kornblum, N. *Angew. Chem., Int. Ed. Engl.* **1975**, *14*, 734.

(298) Bunnet, J. F. *Acc. Chem. Res.* **1992**, *25*, 2.

(299) Curran, D. P.; Fevig, T. L.; Jasperse, C. P.; Totleben, M. J. *Synlett* **1992**, 943.

(300) Molander, G. A.; Harris, C. R. *Chem. Rev.* **1996**, *96*, 307.

(301) Rossi, R. A.; Pierini, A. B.; Penenory, A. B. *Chem. Rev.* **2003**, *103*, 71.

(302) Andrieux, C. P.; Gélis, L.; Medebielle, M.; Pinson, J.; Savéant, J. M. *J. Am. Chem. Soc.* **1990**, *112*, 3509.

(303) Bertran, J.; Gallardo, I.; Moreno, M.; Savéant, J. M. *J. Am. Chem. Soc.* **1992**, *114*, 9576.

(304) Pause, L.; Robert, M.; Savéant, J. M. *J. Am. Chem. Soc.* **2000**, *122*, 9829.

(305) Cardinale, A.; Isse, A. A.; Gennaro, A.; Robert, M.; Savéant, J. M. *J. Am. Chem. Soc.* **2002**, *124*, 13533.

(306) Costentin, C.; Louault, C.; Robert, M.; Teillout, A.-L. *J. Phys. Chem A* **2005**, *109*, 2984.

(307) Costetin, C.; Robert, M.; Savéant, J. M. *J. Am. Chem. Soc.* **2004**, *126*, 16834.

(308) Inceolglu, S.; Olugebefola, S. C.; Acar, M. H.; Mayes, A. M. *Des. Monomers Polym.* **2004**, *7*, 181.

(309) Tang, W.; Matyjaszewski, K. *Macromolecules* **2006**, *39*, 4953.

(310) Onsager, L. *Phys. Rev.* **1931**, *37*, 405.

(311) Blackmond, D. G. *Angew. Chem., Int. Ed.* **2009**, *48*, 2648.

(312) Wu, S.-H.; Chen, D.-H. *J. Colloid Interface Sci.* **2004**, *273*, 165.

(313) Potisek, S. L.; Davis, D. A.; Sottos, N. R.; White, S. R.; Moore, J. S. *J. Am. Chem. Soc.* **2007**, *129*, 13808.

(314) Hickenboth, C. R.; Moore, J. S.; White, S. R.; Sottos, N. R.; Baudry, J.; Wilson, S. R. *Nature* **2007**, *446*, 423.

(315) Rosen, B. M.; Percec, V. *Nature* **2007**, *446*, 381.

(316) Davis, D. A.; Hamilton, A.; Yang, J. Y.; Cremar, L. D.; Gough, D. V.; Potisek, S. L.; Ong, M. T.; Braun, P. V.; Martinez, T. J.; White, S. R.; Moore, J. S.; Sottos, N. R. *Nature* **2009**, *459*, 68.

(317) Woodward, R.; Hoffmann, R. *The Conservation of Orbital Symmetry*; Academic Press: New York, 1970.

(318) Ma, Y.; Tang, Y.; Billingham, N. C.; Armes, S. P.; Lewis, A. L.; Lloyd, A. W.; Salvage, J. P. *Macromolecules* **2003**, *36*, 3475.
(319) Matyjaszewski, k.; Woodworth, B. E.; Zhang, X.; Gaynor, S. G.; Metzner, Z. *Macromolecules* **1998**, *31*, 5955.
(320) Fu, Q.; Lin, W.; Huang, J. *Macromolecules* **2008**, *41*, 2381.
(321) Fu, Q.; Wang, G.; Huang, J. *J. Polym. Sci., Part A: Polym Chem.* **2008**, *47*, 986.
(322) Fu, Q.; Zhang, Z.; Lin, W.; Huang, J. *Macromolecules* **2009**, *42*, 4381.
(323) Zard, S. Z. *Top. Curr. Chem.* **2006**, *264*, 201.
(324) Clark, A. J. *Chem. Soc. Rev.* **2002**, *31*, 1.
(325) Rosen, B. M.; Lligadas, G.; Hahn, C.; Percec, V. *J. Polym. Sci., Part A: Polym. Chem.* **2009**, *47*, 3931.
(326) Rosen, B. M.; Lligadas, G.; Hahn, C.; Percec, V. *J. Polym. Sci., Part A: Polym. Chem.* **2009**, *47*, 3940.
(327) Curran, D. P. *Synthesis* **1988**, 489.
(328) Iqbal, J.; Bhatia, B.; Nayyar, K. *Chem. Rev.* **1994**, *94*, 519.

(329) Kulis, J.; Bell, C. A.; Micallef, A. S.; Jia, Z.; Monteiro, M. J. *Macromolecules* **2009**, DOI: 10.1021/ma9014565.
(330) Dimitrov, P.; Iyer, P.; Bharadwaj, R.; Mallya, P.; Hogen-Esch, T. E. *Macromolecules* **2009**, *42*, 6873.
(331) Percec, V.; Guliashvili, T.; Popov, A. V.; Ramirez-Castillo, E.; Coelho, J. F. J.; Hinojosa-Flacon, L. A. *J. Polym. Sci., Part A: Polym. Chem.* **2005**, *43*, 1649.
(332) Percec, V.; Guliashvili, T.; Popov, A. V.; Ramirez-Castillo, E.; Hinojosa-Flacon, L. A. *J. Polym. Sci., Part A: Polym. Chem.* **2005**, *43*, 1660.
(333) Percec, V.; Guliashvili, T.; Popov, A. V.; Ramirez-Castillo, E. *J. Polym. Sci., Part A: Polym. Chem.* **2005**, *43*, 1935.
(334) Percec, V.; Guliashvili, T.; Popov, A. V. *J. Polym. Sci., Part A: Polym. Chem.* **2005**, *43*, 1948.